Heterogeneity in apoplastic barrier deposition, respiration and ion accumulation in the roots of diverse barley seedlings

Muhammad Khairul Hisyam Ahmad Sohaimi

Thesis submitted as part of the requirements for the degree of

Doctor of Philosophy

School of Agriculture, Food and Wine
Faculty of Sciences
The University of Adelaide

December 2020

Table of Contents

Abstract

The formation of both root endodermal and exodermal barriers can contribute to plant tolerance to saline, water and O_2-limited environments. Previous studies have suggested that cultivated barley (*Hordeum vulgare*) does not form an exodermal layer, whereas wild *Hordeum* grasses can form an inducible exodermal barrier in response to abiotic stress. Here a diverse barley collection was used as a resource for experiments to assess genetic diversity in root apoplastic barriers. Barke and seven wild barley accessions with the greatest diversity in root barrier formation were selected from the collection and the relationships between the formation of barriers and trends in the following properties were assessed: (i) Root and shoot growth, (ii) Na^+ and K^+ accumulation and (iii) Root O_2 consumption, and (iv) Response to phytohormone treatments. The lines with the most substantial exodermal barriers tended to have lower rates of root respiration relative to the other lines, revealing the possibility that the lines differed in their partitioning of energy for cell wall formation relative to other processes.

Investigation of the regulation of root barrier formation by phytohormones revealed that treatments with abscisic acid enhanced root suberisation in barley, similar to observations reported previously for Arabidopsis. Treatments with the ethylene precursor 1-Aminocyclopropane-1-carboxylic acid had no effect on barrier formation, differing from trends in Arabidopsis. This indicates that the mechanisms regulating changes in cell wall barriers differ in barley relative to Arabidopsis.

A wild barley line, HID138, was identified which had a strong exodermal barrier, and had higher K^+ retention relative to commercial Barke, raising the possibility that the exodermal barrier could have had a role in preventing K^+ loss from the roots. To further evaluate the relationship between the exodermal barrier and ion accumulation, a subset of progeny lines from the Barke x HID138 NAM population (HEB13s) were phenotyped. The findings did not

reveal a strong relationship between the differences in K^+ retention and the variation in exodermal barrier deposition, indicating further research is needed to clarify the role of the exodermis.

Both cell wall barriers and variation in ion transport mechanisms can contribute to differences in ion content. To explore potential variation in ion transport mechanisms the transcript abundance and the sequences of the Na^+ transporter *HvHKT1;5* were analysed in lines of interest. This revealed differences in *HKT1;5* sequences in the lines. Barke contains a non-functional *HvHKT1;5* which codes for a proline at position 189, whereas *HvHKT1;5* in the wild barley lines coded for leucine (L) at position 189. The analysis of transcript abundance revealed that *HvHKT1;5* was not expressed at the early seedling stage, excluding a contribution of this transporter to the observed differences in tissue ion content at the stage tested.

The diversity in apoplastic barriers in the diverse collection is likely to be a useful resource for studying the role of these barriers in abiotic stress tolerance.

Thesis Declaration

I certify that this work contains no material which has been accepted for the award of any other degree or diploma in my name, in any university or other tertiary institution and, to the best of my knowledge and belief, contains no material previously published or written by another person, except where due reference has been made in the text. In addition, I certify that no part of this work will, in the future, be used in a submission in my name, for any other degree or diploma in any university or other tertiary institution without the prior approval of the University of Adelaide and where applicable, any partner institution responsible for the joint-award of this degree.

I acknowledge that copyright of published works contained within this thesis resides with the copyright holder(s) of those works.

I also give permission for the digital version of my thesis to be made available on the web, via the University's digital research repository, the Library Search and also through web search engines, unless permission has been granted by the University to restrict access for a period of time.

Muhammad Khairul Hisyam Ahmad Sohaimi

Signature:____ _____ **Date:** 31/12/2020

Acknowledgements

I would like to thank Grains Research and Development Corporation (GRDC) and Australian Centre of Excellence Plant Energy Biology (ARC PEB) for the Rana Munns Scholarship funding for this project. Firstly, I would to express my sincere gratitude to my supervisory team, my principal supervisor, Dr. Stefanie Wege and co-supervisors, Dr. Caitlin Byrt and Dr. Rhiannon Schilling. Thank you for your continuous support in my PhD journey, your motivation and patience, and your immense knowledge and ideas that you shared. This PhD journey would not be possible without all of your support.

I also would like thank my postgraduate coordinator Associate Professor Ken Chalmers, Professor Stephen Tyerman and Associate Professor Stuart Roy for the advice and support. Special thanks to all people that involved in making this journey possible, especially Jodie Kretschmer and Dr. Daniel Menadue for the technical assistance, Dr. Gwen Mayo for the microscopy support.

I am so blessed to be surrounded by amazing people in Professor Matthew Gilliham Lab. Thank you for all your help and for being good companions during my PhD program.

Finally, I would like to thank my parents for their unconditional love and moral support for me to complete this doctorate program.

List of abbreviations

ABA	Abscisic acid
ACC	1-Aminocyclopropane-1-carboxylic acid
ANOVA	Analysis of variance
ARC	Australian Research Council
ATP	Adenosine triphosphate
BC_1	Progeny of F1 after back-crossing with Barke
BC_1S_3	Progeny of BC_1 after three rounds of selfing
Bp	Base pair
cDNA	Complementary DNA
Cl^-	Chloride ion
cm	Centimetre
cv.	Cultivar
d	Days
DM	Dry mass
DNA	Deoxyribonucleic acid
DW	Dryweight
EDTA	Ethylene diamine tetra acetic acid
RNA	Ribonucleic acid
F1	First generation after initial crosses
FSH	Full strength Hoagland
FTIR	Fourier transform infrared spectrometry
FW	Freshweight
g	Grams
GC-MS	Gas chromatography-mass spectrometry
GRDC	Grain Research and Development Corporation
h	Hour (s)
HCl	Hydrochloric acid
HEB25	Halle Exotic Barley 25

HID	*Hordeum* identity
HKT	High-affinity potassium (K^+) transporter
K^+	Potassium ion
MIFE	Micro-electrode Ion Efflux Estimation
min	Minute
ml	Millilitre
mM	Millimolar
MW	Molecular weight
n	sample size
Na^+	Sodium ion
NaCl	Sodium chloride
NAM	Nested association mapping
NHX	Sodium hydrogen exchanger
NILs	Near isogenic lines
M/S	Murashige and Skoog
µl	Microliter
µM	Micromolar
PCA	Principal component analysis
PEG	Polyethylene Glycol
PM	Plasma membrane
R_{DARK}	Rate respiration/O_2 consumption in the dark
RILs	Recombinant Inbred Lines
ROS	Reactive Oxygen Species
s	Seconds
sgn3	*schengen3*
SUB	SUBERMAN
V	Volt
v/v	volume per volume

Nomenclature and terminology

Hordeum marinum is ‘sea barley grass’

Hordeum vulgare is ‘barley’ (strictly *Hordeum vulgare* ssp *vulgare*); cultivars (=cultivated variety).

Hordeum spontaneum, is ‘wild barley’ (strictly *Hordeum vulgare* ssp *spontaneum*). Wild species have the gene for brittle rachis so the seed is shed when ripe for the purpose of seed dispersal; to turn this into a cultivatable plant means finding a natural mutation in the gene for brittle rachis, so seed can be harvested without loss.

The 25 HIDs are accessions, i.e. seed collected and deposited in a seed collection without being genotyped or having a pedigree. Lines usually means a breeding line; the HEBs are lines (descended from two parents). This is the terminology used by Maurer et al. (2015).

List of figures

Chapter 1: **Literature Review**

Chapter 2: **Diversity in root apoplastic barrier deposition in salt treated wild and domesticated barley seedlings**

List of tables

Chapter 2: **Diversity in root apoplastic barrier deposition in salt treated wild and domesticated barley seedlings**

Chapter 4: *HvHKT1;5* SNPs within diverse barley accessions and expression analysis during early development

List of appendices

Chapter 1:

Literature review

1.0 Introduction

Salinity is a major environmental and agricultural problem impacting the performance of crops worldwide. Almost seven percent of the Earth's land mass is salt-affected (Munns and Tester, 2008). In general, when soil salinity exceeds 40 mM NaCl, the root growth of most domesticated cereals is reduced (Munns, 2005). In salt-affected soils roots are in direct contact with the saline environment and root function in these circumstances plays an important part in whether or not the plant is able to reach its yield potential.

Barley (*Hordeum vulgare* L.) is the fourth most important crop by productivity worldwide. Barley is also considered to be one of the most salt tolerant cereal crops (Munns and Tester, 2008). However, salinity still prevents barley from reaching its genetic yield potential (Harris et al., 2010). Unlike modern domesticated cereals, many wild grasses can maintain growth in saline and dry soils (Islam et al., 2007). For example, a wild barley relative, *Hordeum marinum*, known as sea barley-grass, inhabits salt marshes and is considered more salt tolerant compared to modern domesticated barley (Garthwaite et al., 2005; Islam et al., 2007). However, it is unclear which of the many traits that enable the wild grasses to better tolerate saline and dry environments relative to commercial varieties are useful for improving modern cereals.

One of the major differences between wild barley grasses and modern cultivars is the deposition pattern of root apoplastic barriers, which might contribute to enabling them to tolerate abiotic stresses, such as saline soils (Ranathunge et al., 2017; Kreszies et al., 2019b) (Figure 1). In general, there are two types of apoplastic barriers in roots of vascular plants: an endodermis, surrounding the stele, and an exodermis (hypodermis) below the root epidermis. Almost all vascular plants develop an endodermis, whereas not all plants develop an exodermis. Cereals such as maize (*Zea mays* L.) and rice (*Oryza sativa* L.), in many wild grasses such as *H.marinum*, and in other dicot plants such as cotton (*Gossypium hirsutum* L.), an exodermis is

formed (Figure 2). Unlike wild barley grasses, commercial barley has been reported to lack an exodermis (Figure 1) (Ranathunge et al., 2017; Kreszies et al., 2019b).

The formation of exodermal barriers has been reported to be an advantage in plants in relation to tolerating saline, water and oxygen-limited conditions (Figure 2) (Zimmermann and Steudle, 1998; Kotula et al., 2009b; Kotula et al., 2009c; Ranathunge et al., 2011a). However, the enhanced cell wall material for these additional barriers requires energy and resources, but it could be a good investment relative to the investment required to adapt to challenging conditions without the advantage of an exodermis. The development of exodermal barriers can be constitutive, as observed in the roots of plants such as mangroves (*Avicennia officinalis*), or stress inducible, such as in rice and *H. marinum* (Garthwaite et al., 2008; Ranathunge et al., 2011a; Krishnamurthy et al., 2014).

FIGURE 1 Spatial suberin deposition in commercial and wild barley. The root cross sections of commercial barley, *Hordeum vulgare* (a & b), replicated from Ranathunge et al. (2017) and (Kreszies

et al., 2018), respectively; and wild barley (c & d), as shown in Kreszies et al. (2019b) and Kotula et al. (2014), respectively. The root cross sections were made at 100 mm (a), basal part (c), 50 mm (d) from the root apex. Root sections were stained with Fluorol Yellow 088 and counterstained with aniline blue. The presence of suberin is indicated in yellow. The endodermal suberin is shown by the arrows and the exodermal suberin indicated by the arrowheads. Abbreviation: en, endodermis, ex, exodermis. Scale bars = 50 µm (A & C), 200 µm (b & d).

FIGURE 2 Suberin deposition in the roots across species. (a) rice (Ranathunge et al., 2011a), (b) maize (Liska et al., 2016), (c) Arabidopsis (Ranathunge and Schreiber, 2011), and (d) cotton (Reinhardt and Rost, 1995), under different abiotic stresses, such as exposure to waterlogging (a), drought (b), and salinity (d). The sections were stained with Fluorol Yellow 088 (a, b, & d) and lipophilic dye Sudan red 7B (c) for suberin. In (a), the section was counterstained with aniline blue. Suberin lamellae were developed at 30mm (a), 70 mm (b), 40 mm (c) and 150 mm (d) from the root apex. Abbreviation: en, endodermis; ex, exodermis. Scale bars = 50 µm (a), 200 µm (b), 25 µm (c) and 264 µm (d).

At the beginning of this research project in 2017, there was limited information about apoplastic barrier deposition in barley. The available literature at that time indicated that cultivated barley did not form an exodermis, and that a wild barley relative, *H. marinum* did form an exodermis in response to water limited environments (Garthwaite et al., 2008; Kotula et al., 2014; Ranathunge et al., 2017). Since then, notable progress has been made with the most recent findings revealing the effect of osmotic stress on apoplastic barrier deposition in a collection of commercial and wild barley (*H. vulgare* spp. *spontaneum*) accessions (Kreszies et al., 2019a; Kreszies et al., 2019b). These findings provide key insights into the development of apoplastic barriers in diverse barley accessions. The authors reported that all of the commercial barley lines tested did not form an exodermis and within the wild barley accessions only one known as ICB181466, from Jordan, was identified to form an exodermis in response to osmotic stress (Kreszies et al., 2019b). However, it is important to note that different growth conditions and treatments could impact the development of apoplastic barriers, particularly exodermal barriers, as reported in previous studies in maize (Zimmermann and Steudle, 1998; Shen et al., 2015). The information on the effect of salt stress on apoplastic barrier development in barley is still limited, and it is not known whether salt stress would have the same or different effects on apoplastic barriers as has been reported in previous studies. In this project, the effect of saline conditions on apoplastic barriers in a diverse barley collection was investigated to better understand the genetic variation in apoplastic barrier depostion; and to explore the potential for variation in barrier deposition to be linked with variation in ion transport or root respiration characteristics.

1.1 Transport pathways

In roots, radial transport refers to the flow of water and solutes from external sources, such as the soil or a hydroponic solution, through the epidermis, and the cortex before reaching the

vascular system. Solute and water movement can also take place *vice versa*, from the stele into the media. This radial movement of solutes and water across the root tissues can occur in three different ways (Steudle and Peterson, 1998; Steudle, 2000; Barberon, 2017; Byrt et al., 2018): (1) Apoplastic, this bypass pathway occurs across the fibrils of cell walls in the intercellular space; (2) symplastic, this pathway involves solute uptake across the cell membrane into the cytoplasm and subsequently flow through plasmodesmata; (3) transcellular, this pathway occurs across membrane layers, in and out of the cell through aquaporins and other membrane transporters (Figure 3).

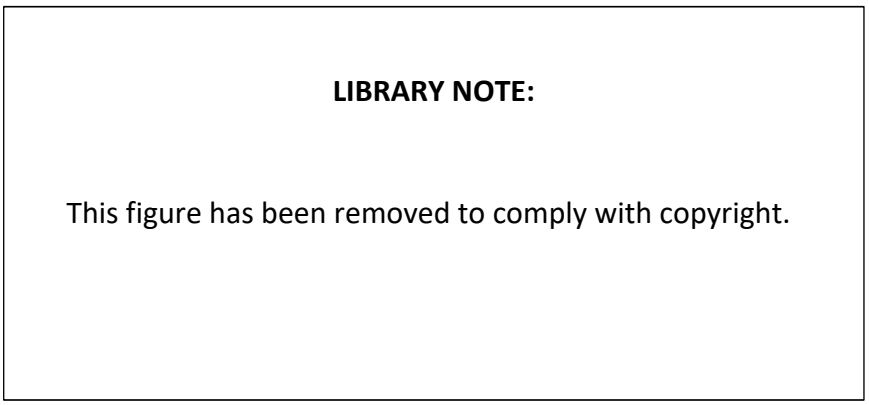

FIGURE 3 Radial transport in a model plant. Schematic view of three radial transport pathways of water and solutes from the soil across the epidermis and cortical cell layers into the vascular system; apoplastic, symplastic and coupled transcellular pathways. This figure was replicated from (Barberon, 2017).

1.2 Apoplastic root barriers

1.2.1 The characteristics of apoplastic barrier material

There are two key compounds associated with apoplastic barriers; lignin and suberin. Both lignin and suberin are hydrophobic. Lignin deposition in the root cell wall is an irreversible process while suberin deposition is reversible (Zhao and Dixon, 2011; Barberon et al., 2016).

1.2.2 Stages of endodermal and exodermal differentiation

The endodermis is the innermost cortex cell layer, which surrounds the vascular tissues (Andersen et al., 2015). All vascular plants except *Lycopodium* develop an endodermis in their

roots (Damus et al., 1997; Enstone et al., 2002). It plays a crucial role as the last checkpoint for nutrients and water intake from the cortex into the stele before they are distributed to the aerial parts of the plants (Barberon, 2017). The development of the endodermal cells can be grouped into three stages. The first stage is characterised by the formation of Casparian strips, a ring-like, lignified and hydrophobic structure that is deposited in the anticlinal walls of endodermal cells (Naseer et al., 2012). At this stage, free apoplastic diffusion into the stele is blocked, but most water and solutes diffusion can still occur via symplastic and transcellular pathways. The second stage is the complete suberisation of the entire endodermal cells and these deposits are known as suberin lamellae. Suberin lamellae form at the inner surface of primary cell walls. They form between the primary cell wall and the plasma membrane, covering the entire endodermal cells. At this stage, direct uptake of nutrients and water into the endodermal cells through the plasma membrane might be greatly reduced; and indirect uptake of nutrients and water through plasmodesmata of adjacent cells occurs symplastically (Clarkson et al., 1987; Barberon et al., 2016) (Figure 4). Some cells remain at the first stage of endodermal development, and these are known as passage cells. For example, Ranathunge et al. (2017) demonstrated that in a fully developed lamellae ring at 100 mm from the apex of the seminar root of hydroponically treated, 16- to 20-day-old barley plants ten percent of the endodermal cells did not become suberized. The third stage is the thickening of the cell wall through the deposition of cellulose in the endodermal cells, generally in the basal part of the roots (Enstone et al., 2002). The cellulose thickening of the cell wall is thicker in the area facing the stele than the area facing the cortex (Enstone et al., 2002; Geldner, 2013). The effects of this cell wall thickening on the solute and water transport have not yet been investigated.

FIGURE 4 Development of endodermis. The transition during Casparian strip development from stage I (left) into stage II in the endodermal cell wall composition (right), characterised by suberin deposition. This figure was replicated from Barberon et al. (2016).

In addition to the endodermis, the exodermis provides hydrophobic interface between the external environments and the cortex (Kotula et al., 2009b; Kotula et al., 2014; Landgraf et al., 2014; Kreszies et al., 2019b). The exodermis develops in outer cortical cells below the epidermis. In relation to terminology, the exodermis is also known as a hypodermis with Casparian strips in its anticlinal walls (Peterson and Perumalla, 1990). In this case, this cell layer with enhanced cell wall material is simply know as an exodermis. The exodermis, in many plants is a single layer (uniseriate), but in some plants it can also be multiple layer (multiseriate) (Peterson and Perumalla, 1990; Seago et al., 1999). In general, less is known about the exodermis, but the structure and function seem to resemble the endodermis but with some distinct differences. For example, the development of exodermal Casparian strips and suberin lamellae can occur simultaneously and the amount of lignin and suberin is generally less than in endodermal cells (Schreiber et al., 1999; Enstone et al., 2002). There is also non-suberized exodermal cells and in some studies these cells are known as hypodermal passage

cells (HPC) (Liu et al., 2019). The passage cell in the exodermis can lack in suberin lamellae but it can still have intact Casparian strips in its anticlinal walls. In this case, these unsuberised exodermal cells are simply known as exodermal passage cells. Similar to endodermal passage cells, the exodermal passage cells could also play a role as key sites where the direct uptake of water and solutes into the roots occurs (Peterson and Enstone, 1996; Enstone et al., 2002). The exodermal passage cell has also been reported to contain a dense cytoplasm rich in mitochondria, a feature of highly active cells (Wilson and Robards, 1980; Peterson and Enstone, 1996). In contrast to the information in the literature about endodermal passage cells, there is little information about exodermal passage cells.

1.3 The plasticity of apoplastic barriers

1.3.1 Environmental factors influence the development of root apoplastic barriers

The Casparian strip and suberin lamellae development in endo- and exodermal cells can be modulated by the plant in response to the external environment. Any changes in external environment would first be registered by exodermal cells before the endodermal cells due to the location of exodermal cells in the outer cortex. Generally, exodermal barriers develop closer to the root tips in response to salt stress; these barriers can be altered by changes in the availability of some nutrients, water and oxygen (Reinhardt and Rost, 1995; Karahara et al., 2004; Krishnamurthy et al., 2014; Shen et al., 2015; Barberon et al., 2016). For instance, two studies found that, in the primary roots of maize, salt stress affects the development and morphology of radial barriers: Casparian strips were much wider and they developed closer to the tips in salt stressed maize roots relative to roots that were not salt stressed (Karahara et al., 2004; Tylova et al., 2017). In addition, a previous study discovered that salinity accelerated the maturity of endodermal cell walls and induced exodermis formation in cotton seedling roots (Reinhardt and Rost, 1995). The plasticity of these barriers in response to abiotic stresses

demonstrates a plant strategy to reduce the intake of salt and/or to prevent the leakage of water, oxygen or important ions such as K^+ needed for growth.

1.3.2 The regulation of suberisation by phytohormones

Suberisation in the root is reversible in *Arabidopsis thaliana*; it is controlled by the antagonistic action of abscisic acid (ABA) and ethylene, and is influenced by external nutrient availability (Barberon, 2017). For example, salt stress and K^+ deficiency trigger an increase in ABA signalling, whereas manganese-, zinc- and iron- deficiencies trigger an increase in ethylene signalling (Barberon et al., 2016). ABA signalling leads to enhanced suberisation while ethylene leads to either reduced suberisation in the younger part of the root or suberin breakdown in the older part of the root (Barberon et al., 2016). A decrease in non-suberized endodermal cells (passage cells) when roots were treated with increasing ABA treatment has also been reported (Andersen et al., 2018). Repression of ABA for 29 h led to disappearance of suberin indicating a de-repression of ABA signalling and interference in suberin maintenance (Andersen et al., 2018). The effect of these hormones on the suberin deposition in the roots of plant species other than Arabidopsis is unknown.

1.3.3 Cell wall suberisation can change in response to abiotic stress

Salt stress and osmotic stress can have differing effects on the regulation of cell wall suberisation. Therefore, these stresses may influence water and solute transport, root anatomy and architecture differently. For example, a study comparing the effect of osmotic (20% polyethylene Glycol, PEG) and salt stress (200 mM NaCl) on maize seedling roots grown in hydroculture showed distinct cell wall modifications in the response to each stress (Shen et al., 2015). They reported that salt stress induced the suberisation of the exodermis before suberisation of the endodermis. In contrast, osmotic stress induced the suberisation in both the endodermis and exodermis almost simultaneously. They also found that salt stress induced a multiseriate suberisation pattern, which ranged in size from a few layers to the entire cortex

region, whereas osmotic stress only induced a limited layer of suberised cells, three or four cells thick in the outermost cortical cells, just below the epidermis (Shen et al., 2015). This reveals that depending on what environment plants are exposed to the suberisation of their root cell wall is likely to differ, and this is expected to be associated with consequences for root solute and water permeability.

1.3.4 Salt stress can influence lignification in the roots

Previous studies have assessed whether salt stress enhances lignification in roots of different plant species (Neves et al., 2010; Byrt et al., 2018). For example, a histochemical analysis of salt-stressed wheat seedlings revealed that a salt-tolerant variety had greater root lignification compared to a salt-sensitive variety (Jbir et al., 2001). A study in soybean also reported that 24 hours of a NaCl treatment induced secondary lignin development in the root cell walls of three-day-old seedlings (Neves et al., 2010). In rice reduced lignification was observed in an *rss3* mutant; *rss3* is a nuclear factor gene that normally regulates cell wall properties, and the mutant was more sensitive to salt than wild type plants, as evidenced by reduced root growth under salt treatment compared to the wildtype (Toda et al., 2013). Enhanced lignification caused by salt stress has been associated with reduced root growth and biomass (Neves et al., 2010), and lignin deposition in the cell walls also reduces the permeability of water and solutes. However, the extent of variation in the amounts of lignin, spatial lignin deposition, and the effect on growth and ion fluxes in barley is not well understood.

1.4 Functions of root apoplatic barriers (Casparian strips and suberin lamellae)

1.4.1 Can root barriers limit Na^+ permeability?

In most studies the accelerated formation of Casparian strip and suberisation in both endodermal and exodermal cells are linked to low leaf Na^+ accumulation. For example, Krishnamurthy et al. (2009) demonstrated that Pokkali, a salt-tolerant rice variety with extensive root suberisation had lower leaf Na^+ compared to salt-sensitive IR29, which had less

suberized roots, under 200 mM salt stress after two days. The authors suggested that the hydrophobic barriers reduced Na^+ bypass flow in the roots (Krishnamurthy et al., 2011). Since it has been suggested that apoplastic flow in rice is an important pathway of Na^+ entry into the shoots, reinforcing root apoplastic barriers might be one of the factors contributing to the observed salt tolerance phenotype in these two studies (Yeo et al., 1987; Anil et al., 2005; Gong et al., 2006). However, differences in membrane transporter function may also influence this trait. Membrane transporters, for example High Affinity Potassium (K^+) Transporters (HKT1;5s), have been identified in many cereal plants such as wheat, rice and barley (Ren et al., 2005; Byrt et al., 2007; James et al., 2011; Munns et al., 2012; Byrt et al., 2014). Transcript levels of OsHKT1;5 were reported to be more abundant in the roots of salt-tolerant Pokkali relative to salt-sensitive IR29 (Walia et al., 2007). HKT1;5 is actually a Na^+ transporter, and *HKT1;5* is expressed in the xylem parenchyma cells where the protein retrieves Na^+ from the xylem, contributing to limiting root-to-shoot Na^+ transport and enabling retention of Na^+ in the roots (Cotsaftis et al., 2012; Munns et al., 2012; Byrt et al., 2014; Kobayashi et al., 2017; Al Nayef et al., 2020). Therefore, it is reasonable to surmise that there may be relationships between the function of ion transport proteins and changes in root anatomy and cell wall composition under saline conditions.

Previous studies focussed on maize, Castor bean (*Ricinus communis L.*), and mangrove have reported that these plants reinforce their root barriers in response to salt stress (Karahara et al., 2004; Schreiber et al., 2005a; Krishnamurthy et al., 2014). These plants accelerated the maturity of endodermal cells; and in addition to having earlier endodermis development, maize, Castor bean and mangrove also developed an exodermis (Karahara et al., 2004; Schreiber et al., 2005a; Krishnamurthy et al., 2014). Overall, these findings highlight a link between diffusion barrier development and limited radial Na^+ flow in the roots that warrants further

investigation particularly in cereal crops where optimising these traits may contribute to improving productivity in saline soils.

A study by Ranathunge and Schreiber (2011) compared previously known Arabidopsis *horst* mutants with reduced suberin deposition (Hofer et al., 2008), and *esb1* mutants with enhanced suberin deposition (Baxter et al., 2009) and reported results indicating the complexity in the link between suberin deposition and solute permeability. Arabidopsis *horst* mutants had almost 33% less suberin monomer accumulation than the wildtype, had relatively higher water and NaCl permeability compared to the wildtype (Ranathunge and Schreiber, 2011). In contrast, *esb1* mutants with twice the suberin content of the wildtype did not differ in water and salt permeability into the roots (Ranathunge and Schreiber, 2011). Other studies investigating the *esb1* mutants suggested that elevated suberin caused changes in the shoot ionome (Baxter et al., 2009). These conflicting findings may be related to differences in the growth conditions and methods used in the studies (Ranathunge and Schreiber, 2011). Additionally, *casp1-casp3* mutants had a similar phenotype to *esb1* mutants since there is reciprocal requirement of both Enhanced Suberin 1 (ESB1) and Casparian strip domain proteins (CASPs) for correct localisation of Casparian strip domain to the plasma membrane (Baxter et al., 2009; Hosmani et al., 2013); and their expression is governed by the transcription factor MYB36 (Kamiya et al., 2015). The loss of MYB36 resulted in incorrect localization of Casparian strips (Kamiya et al., 2015). Disrupted Casparian strip formation can result in reduced shoot calcium accumulation (Li et al., 2017), which would influence the shoot ionome; hence there is complexity in the relationships between Casparian strip formation, suberin deposition and shoot ion accumulation (Wang et al., 2019).

Research has revealed that *esb1*, *casp1*; *casp3* and *myb36* mutants show an increase in leaf Na^+ but a significant decrease in leaf Ca^{2+} (Baxter et al., 2009; Hosmani et al., 2013; Kamiya et al., 2015). Interestingly, *esb1* mutants, have a 40% increase in leaf Na^+ and 50%

reduction of leaf Ca^{2+} under low external Na^{+}, compared to wildtype (Baxter et al., 2009). These results indicate that Na^{+} and Ca^{2+} might have different pathways into the roots and to the shoot. In contrary, an increase in suberin deposition in the roots has been associated with reduced leaf Na^{+} in rice (Yadav et al., 1996; Krishnamurthy et al., 2009). However, it is important to highlight that, unlike rice, Arabidopsis does not develop an exodermis (Figure 2c). The exodermis layer might provide an additional barrier to limit the radial Na^{+} flow from the soil into the cortex, therefore reducing the amount of Na^{+} surrounding the endodermal cells. Without this layer, Na^{+} can enter into the cortex through free apoplastic diffusion, and accumulate in the cell walls surrounding endodermal cells. One key difference between *Arabidopis* mutants and wildtype is that the formation of Casparian strips were delayed in *esb1* mutants compared to the wildtype. Plus, as mentioned earlier, the loss of normal *ESB1* function in *esb1* mutants resulted in abnormal localisation of Casparian strips (Hosmani et al., 2013). It was suggested that the defect in the formation of Casparian strip possibly led to ectopic suberisation in *esb1* mutants as there is likely to be a crosstalk between the formation of lignin and suberin deposition in the cell walls (Hosmani et al., 2013). Therefore, it was likely that the defects in both Casparian strips and suberin lamellae in Arabidopsis *esb1* mutants contributed to the higher leaf Na^{+} but lower Ca^{2+} compared to the wildtype. Furthermore, the role of suberin itself is unclear. For example, suberin layers might not completely prevent the apoplastic flow by themselves since they do not prevent the movement of apoplastic tracers (Geldner, 2013; Byrt et al., 2018). Due to the negative association between suberin deposition and water and solute permeability, it is assumed that suberin may contribute to prevent radial Na^{+} flow and water loss, but it may also have a different role (Geldner, 2013).

Barley, relative to other cultivated cereals, can accumulate more salt in leaf tissues whilst maintaining productivity and barley is considered to be more salt tolerant compared to the other cereals (Colmer et al., 2005). However, there is variation in leaf Na^{+} accumulation

within different barley lines, and this could influence yield potential in saline conditions. For example, Flowers and Hajibagheri (2001) found that a salt-tolerant barley, Gerbel, had significantly lower Na^+ in its leaves and apoplast compared to a salt-sensitive line, Triumph, when grown in media containing 200 mM NaCl. It is possible that there might be differences in apoplastic barrier formation that led to the differences in leaf ion accumulation. Further research into the spatial deposition of apoplastic barriers in barley under saline conditions and testing of how this influences ion accumulation is needed to determine what characteristics might be optimal for improving barley salinity tolerance.

1.4.2 Can root barriers limit water permeability?

Salt stress can limit water availability in the roots due to differences in water potential between the root and the soil. Therefore, it is common that salt-affected plants exhibit a similar response to the response exhibited by plants experiencing water-limitation stress. Under increasing salinity and/or water-limited conditions, plants reinforce their root diffusion barriers, presumably to reduce water loss from the roots into the soil. For example, a study demonstrated that maize seedlings grown in aeroponic conditions formed an exodermis in the primary roots, evidenced by an increase in exodermal lignin and suberin deposition; in contrast, no exodermis was observed in the roots of maize grown in a hydroponic system where water would be less limited relative to the aeroponic conditions (Zimmermann et al., 2000).

Impregnation of endodermal and exodermal cell walls with suberin may limit water intake across the plasma membrane. However, endodermal and exodermal barriers may not contribute equally to reducing water permeability in roots and across different plant species. For example, one study by Schreiber et al. (2005b) directly comparing suberin deposition in rice and maize roots found that endo- and exodermal cell walls of rice had 34 and six times higher suberin contents compared to those in maize. It has been suggested that this higher suberin deposition contributes to a relatively reduced hydraulic conductivity in rice compared

to corn. Hence, the authors postulated that endodermal barriers were the main site of hydraulic resistances, at least in rice. Similarly, Arabidopsis *esb-1* mutants had relatively high hydraulic resistances to radial water loss; and this contributed to a reduced transpiration rate and possibly increase in water use efficiency (Baxter et al., 2009). It is clear that suberin deposition in the cell walls and apoplastic barriers can reduce water permeability, but presumably suberin does not completely prevent water and solute flow.

1.4.3 Can root barriers limit K^+ loss?

Maintaining a high cytosolic K^+:Na^+ ratio is crucial for plant survival under salinity (Maathuis and Amtmann, 1999). High cytoplasmic Na^+ can be toxic as Na^+ can displace K^+, and disrupt K^+-dependent metabolic processes. Therefore, restricting Na^+ entry and limiting K^+ loss is important. Previous studies have postulated that apoplastic barriers reduce both, Na^+ entry and K^+ loss (Pfister et al., 2014; Barberon et al., 2016). Arabidopsis mutants with defective Casparian strips had 1.4- to 3.0- fold lower leaf K^+ compared to the wildtype plants indicating that defective Casparian strips might lead to a continuous loss of stelar apoplast K^+ into the outer part of the root (OPR) and eventually into the soil. In K^+ deficient conditions Barberon et al. (2016) found that Arabidopsis plants enhance their root barriers: Casparian strips developed earlier, and root suberisation was increased compared to plants with sufficient K^+. In barley, there is variation in leaf K^+ accumulation under saline conditions (Tilbrook et al., 2017). A study measuring K^+ flux in barley showed that salt-tolerant barley had less root K^+ efflux compared to salt-sensitive barley, and K^+ efflux was greater in the root apex compared to the mature root zone (Chen et al., 2005). Therefore, further investigation is needed into whether there is a correlation between these barriers and K^+ accumulation in barley and whether this influences salt tolerance.

1.4.4 Root barriers limit radial oxygen loss in waterlogged roots

In oxygen-depleted conditions rice and other wetland species respond both morphologically and metabolically to alleviate the effect of the stress. Responses include changes in (i) the formation of root solute barriers in the outer part of the roots to limit radial oxygen loss (ROL), and (ii) the formation of aerenchyma in the cortex to supply internal oxygen from the aerial parts of the plant to the submerged organs (Colmer, 2003; Kotula et al., 2009b).

Root barriers in the OPR limit radial oxygen loss in the basal part of root, and enhance longitudinal oxygen flow towards the root tip. The formation of barriers in rice is inducible: roots grown in stagnant conditions develop barriers in the OPR, whereas roots grown in aerated conditions do not (Kotula et al., 2009b; Kotula et al., 2009c). Histochemical studies by Kotula et al. (2009b) revealed that roots in stagnant conditions had early formation of Casparian strips and suberin lamellae and lignified sclerenchyma cells. This study also reported that the absolute amount of lignin and suberin in the OPR in stagnant conditions was higher compared to roots in aerated conditions. In another study, Abiko et al. (2012) found that a waterlogging tolerant maize, *Z. nicaraguensis* had early deposition of exodermal Casparian strips and suberin lamellae and lignified epidermis compared to inbred maize in waterlogged soil and deoxygenated solutions. These findings affirm that enhanced suberisation, associated with earlier Casparian strip development and suberin deposition in exodermal/hypodermal cell walls has a strong positive correlation to the ROL barriers.

Most of the barriers to ROL are associated with suberisation of the exodermis/hypodermis. To date, there is very little data to show whether the endodermis would influence oxygen permeability. However, histochemical analysis of waterlogged roots has shown an early formation of Casparian strips and suberin lamellae not only in the walls of exodermal cells but also in the endodermal cell walls (Ranathunge and Schreiber, 2011). This indicates that these endodermal barriers may also reduce the permeability of internal oxygen from the shoots into

the cortical cells, causing an energy crisis in the cortical cells due to reducing internal oxygen flow. However, plants respond to cortical oxygen deficit by increasing the formation of aerenchyma. For example, Garthwaite et al. (2008) found that waterlogged sea barleygrass (*Hordeum marinum*) roots developed aerenchyma whereas aerated barley did not. Hence, this reveals that both endodermal and exodermal barriers may limit oxygen flow, and this would influence root respiration and anatomical changes within these two barriers.

Plants enhance diffusion barrier deposition in response to waterlogging and also in response to salinity. For example, Shen et al. (2015) demonstrated that salt stress induces suberisation of an entire cortex in the roots of maize. This strong suberisation in the roots has been shown to reduce solute and water permeability and may also reduce oxygen permeability. However, there is limited information to support whether this salt-induced suberisation influences oxygen permeability as seen in roots in stagnant conditions. A study by Kotula et al. (2015) on sea barleygrass demonstrated that roots in stagnant saline/non-saline conditions had higher porosity compared to roots in aerated non-saline or saline treatment at 100 mM NaCl for 14 days. In modern barley lines, Zeng et al. (2013) showed that combined salinity and waterlogged stress significantly increased leaf Na^+ by two-fold, and reduced K^+ by 40% compared to salinity stress alone. Since modern barley reportedly do not develop exodermal barriers (Kreszies et al., 2019a), there is likely to be increased radial oxygen loss. This might reduce oxygen in the root cells, causing an energy deficit that might contribute to the inability of the root to exclude Na^+ and to retain K^+ at the stele-endodermal region.

1.5 Root respiration under normal and abiotic stress conditions

The ability of a plant to exclude root Na^+ has been correlated with increased root respiration (Drew and Dikumwin, 1985; Malagoli et al., 2008). For example, in aerated hydroponic experiments, salt-tolerant rice had higher root oxygen consumption compared to salt-sensitive rice (Malagoli et al., 2008). Higher oxygen consumption in the roots is presumably due to

higher energy usage to exclude Na^+ through active transporters (Drew and Dikumwin, 1985; Jacoby et al., 2013). Certain halophytes such as mangroves, had a reduction in root respiration under saline conditions (Burchett et al., 1989). The authors suggested that reduction in root respiration may be due to limited supply of substrate (sugar) from the shoots (Burchett et al., 1989) or this could be due to differences in root barriers between the species. Mangroves develop a constitutive exodermal barrier while rice has an inducible root exodermal barrier (Krishnamurthy et al., 2009; Kotula et al., 2009c; Krishnamurthy et al., 2014). In addition, different species might vary in their apoplastic barriers in terms of the composition, structure and spatial deposition in the roots, which could influence the efficiency of the barrier and lead to higher or lower oxygen requirements. Mangroves might build more efficient barriers in saline conditions compared to rice, and this might save the energy cost associated with active Na^+ efflux. Further research is needed to investigate the role of apoplastic barriers, energy requirements and salinity tolerance.

1.6 Wild barley as a source of useful allelic resources for increasing crop salt tolerance

Domestication narrowed down allelic variation in crop species such as barley by creating genetic bottlenecks. Genetic bottlenecks occur due to selective breeding or artificial selection by humans for certain desired traits such as non-shattering seeds or bigger aboveground biomass. This selection process tends to reduce the genetic variation within the subsequent populations (Figure 5) (Tanksley and McCouch, 1997; Abbo et al., 2014). As a result of selective breeding modern barley varieties have less genetic diversity compared to their progenitors. Wild barleys may be useful sources of allelic variation influencing traits such as salt tolerance and root traits that could be re-introduced back into modern barley cultivars. For example, Badr et al. (2020) identified 25 wild barley accessions, which were then subsequently successfully crossed with the modern variety Barke by Maurer et al (2015). These

25 wild barley accessions are also known as the Hordeum Identity Lines (HID). The progenies from the Barke×HID crosses form a Nested Association Mapping (NAM) population and this was the first barley NAM population developed (Maurer et al., 2015). A SNP associated with salt tolerance in this NAM population was identified by (Saade et al., 2016). The 25 wild barley lines may also contain root traits of interest for influencing crop salt tolerance.

The information available in the literature regarding apoplastic barriers in commercial lines and wild barley accessions has grown in the past few years (Kreszies et al., 2019a; Kreszies et al., 2019b; Knipfer et al., 2020). However, in previous studies in barley the plants were grown in hydroponic systems instead of soil-like conditions. Different growth methods can influence deposition of apoplastic barrier differently (Zimmermann and Steudle, 1998; Ranathunge et al., 2017). Towards addressing knowledge gaps regarding the available diversity in root apoplastic barriers in both the parents (HIDs) and the progenies (NAMs) in response to saline treatments, and addressing gaps in our understanding of how soil-like conditions influence apoplastic barrier deposition, we devised a strategy to grow plants from this population in moist paper towels to mimic a soil-like environment, and test root apoplastic barrier formation.

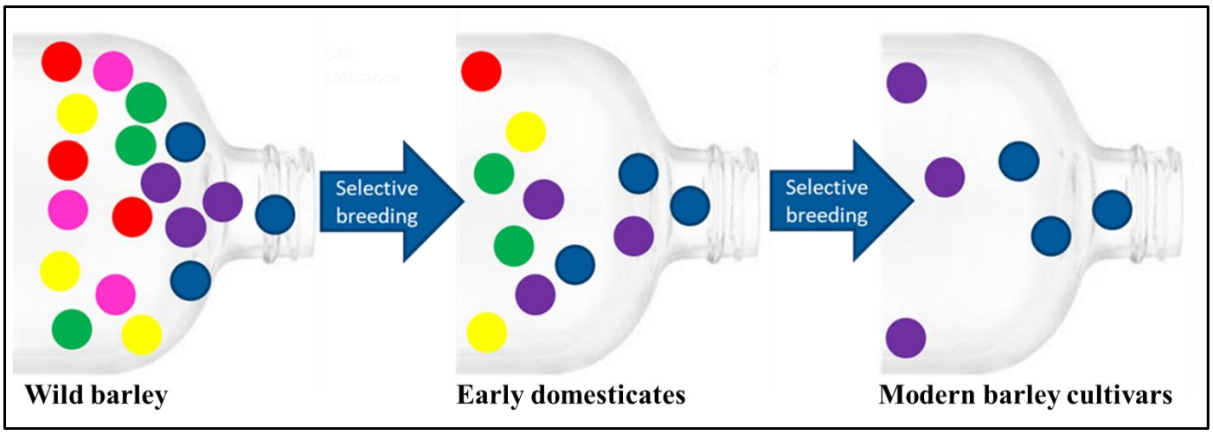

FIGURE 5 Illustration of bottleneck effects on gene pools as a result of steps in crop domestication. The colourful circles represent allelic variants influencing a phenotype of interest. Wild populations exhibit great genetic diversity compared to cultivated counterparts. Selective breeding focussed on just economic and agronomic phenotypes for some traits has narrowed down the allelic variants in modern barley varieties, represented by less colourful circles, relative to wild barleys. This figure was adapted from Tanksley and McCouch (1997).

1.7 Research gaps

Knowledge gaps that inspired the focus of this research project:

- There is limited information about the diversity in apoplastic barriers in barley. Recent literature indicated that there is likely to be variation in apoplastic barriers in wild barley accessions (Kreszies et al., 2019b), providing a precedent that provided justification for looking in additional diverse barley lines.
- It is unclear whether exodermal barrier layers are beneficial for growth in barley under saline conditions.
- It is unclear whether cell wall lignification alters K^+ accumulation in cereals.
- The effects of ABA and ethylene treatments on root suberisation in cereal crops was unknown.
- Little is known about whether development of an additional cell wall barrier might be an energy efficient way to tolerate saline environments.

- Within wild barley accessions it is unclear whether there may be novel variation in a key sodium transport gene, *HvHKT1;5*, or whether there is a correlation between the HvHKT1;5 protein function and apoplastic barrier formation.

1.8 Project aim and objectives

The primary aim of this study was to contribute to our understanding of the importance of apoplastic barriers in influencing salt tolerance in barley, in particular, the potential for some barley accessions to development an exodermis was of interest. The sub-aims were to: (1) explore whether there was variation in spatial deposition of suberin and lignin associated with solute barriers in commercial and wild barley accessions under control and saline conditions; (2) investigate the relationships between the formation of root barriers in selected barley lines with the most diverse root apoplastic barrier traits and ion accumulation characteristics, and also root O_2 oxygen consumption characteristics as a means to measure energy consumption under control and saline conditions; (3) explore the effects of phytohomone treatments, such as ABA and ethylene treatments, on root suberisation in barley. Links between apoplastic barrier deposition and ion accumulation and biomass accumulation in a subset of NAM progenies under saline conditions is also investigated. We checked for any association between the apoplastic barrier trends and variation in a key membrane transporter, HvHKT1;5. *HvHKT1;5* sequences in selected wild barley accessions were compared and gene expression was investigated. We review the potential implications of our findings in relation to diversity in barley root apoplasmic barriers, ion accumulation, root respiration, response to hormone treatments, and membrane transport characteristics and discuss the next steps required to determine how these characteristics relate to each other and barley salt tolerance.

1.9 References

Abbo S, van-Oss RP, Gopher A, Saranga Y, Ofner I, Peleg Z (2014) Plant domestication versus crop evolution: a conceptual framework for cereals and grain legumes. Trends in Plant Science **19:** 351-360

Abiko T, Kotula L, Shiono K, Malik AI, Colmer TD, Nakazono M (2012) Enhanced formation of aerenchyma and induction of a barrier to radial oxygen loss in adventitious roots of *Zea nicaraguensis* contribute to its waterlogging tolerance as compared with maize (*Zea mays* ssp *mays*). Plant Cell and Environment **35:** 1618-1630

Al Nayef M, Solis C, Shabala L, Ogura T, Chen Z, Bose J, Maathuis FJ, Venkataraman G, Tanoi K, Yu M (2020) Changes in expression level of *OsHKT1; 5* alters activity of membrane transporters involved in K^+ and Ca^{2+} acquisition and homeostasis in salinized rice roots. International Journal of Molecular Sciences **21:** 4882

Andersen TG, Barberon M, Geldner N (2015) Suberization - the second life of an endodermal cell. Current Opinion in Plant Biology **28:** 9-15

Andersen TG, Naseer S, Ursache R, Wybouw B, Smet W, De Rybel B, Vermeer JE, Geldner N (2018) Diffusible repression of cytokinin signalling produces endodermal symmetry and passage cells. Nature **555:** 529-533

Anil VS, Krishnamurthy P, Kuruvilla S, Sucharitha K, Thomas G, Mathew MK (2005) Regulation of the uptake and distribution of Na^+ in shoots of rice (*Oryza sativa*) variety Pokkali: role of Ca^{2+} in salt tolerance response. Physiologia Plantarum **124:** 451-464

Barberon M (2017) The endodermis as a checkpoint for nutrients. New Phytologist **213:** 1604-1610

Barberon M, Vermeer JEM, De Bellis D, Wang P, Naseer S, Andersen TG, Humbel BM, Nawrath C, Takano J, Salt DE, Geldner N (2016) Adaptation of root function by nutrient-induced plasticity of endodermal differentiation. Cell **164:** 447-459

Baxter I, Hosmani PS, Rus A, Lahner B, Borevitz JO, Muthukumar B, Mickelbart MV, Schreiber L, Franke RB, Salt DE (2009) Root suberin forms an extracellular barrier that affects water relations and mineral nutrition in Arabidopsis. Plos Genetics **5**

Burchett M, Clarke C, Field C, Pulkownik A (1989) Growth and respiration in two mangrove species at a range of salinities. Physiologia Plantarum **75:** 299-303

Byrt CS, Munns R, Burton RA, Gilliham M, Wege S (2018) Root cell wall solutions for crop plants in saline soils. Plant Science

Byrt CS, Platten JD, Spielmeyer W, James RA, Lagudah ES, Dennis ES, Tester M, Munns R (2007) HKT1; 5-like cation transporters linked to Na^+ exclusion loci in wheat, Nax2 and Kna1. Plant Physiology **143:** 1918-1928

Byrt CS, Xu B, Krishnan M, Lightfoot DJ, Athman A, Jacobs AK, Watson-Haigh NS, Plett D, Munns R, Tester M, Gilliham M (2014) The Na^+ transporter, TaHKT1;5-D, limits shoot Na^+ accumulation in bread wheat. Plant Journal **80:** 516-526

Chen Z, Newman I, Zhou M, Mendham N, Zhang G, Shabala S (2005) Screening plants for salt tolerance by measuring K^+ flux: a case study for barley. Plant Cell and Environment **28:** 1230-1246

Clarkson DT, Robards AW, Stephens JE, Stark M (1987) Suberin lamellae in the hypodermis of maize (*Zea-mays*) roots - development and factors affecting the permeability of hypodermal layers. Plant Cell and Environment **10:** 83-93

Colmer TD (2003) Long-distance transport of gases in plants: a perspective on internal aeration and radial oxygen loss from roots. Plant Cell and Environment **26:** 17-36

Colmer TD, Munns R, Flowers TJ (2005) Improving salt tolerance of wheat and barley: future prospects. Australian Journal of Experimental Agriculture **45:** 1425-1443

Cotsaftis O, Plett D, Shirley N, Tester M, Hrmova M (2012) A two-staged model of Na^+ exclusion in rice explained by 3D modeling of HKT transporters and alternative splicing. PLoS One **7:** e39865

Damus M, Peterson RL, Enstone DE, Peterson CA (1997) Modifications of cortical cell walls in roots of seedless vascular plants. Botanica Acta **110:** 190-195

Drew MC, Dikumwin E (1985) Sodium exclusion from the shoots by roots of *Zea-mays* (cv LG-11) and its breakdown with oxygen deficiency. Journal of Experimental Botany **36:** 55-62

Enstone DE, Peterson CA, Ma FS (2002) Root endodermis and exodermis: Structure, function, and responses to the environment. Journal of Plant Growth Regulation **21:** 335-351

Flowers TJ, Hajibagheri MA (2001) Salinity tolerance in *Hordeum vulgare*: ion concentrations in root cells of cultivars differing in salt tolerance. Plant and Soil **231:** 1-9

Garthwaite AJ, Armstrong W, Colmer TD (2008) Assessment of O_2 diffusivity across the barrier to radial O_2 loss in adventitious roots of *Hordeum marinum*. New Phytologist **179:** 405-416

Garthwaite AJ, von Bothmer R, Colmer TD (2005) Salt tolerance in wild *Hordeum* species is associated with restricted entry of Na^+ and Cl^- into the shoots. Journal of Experimental Botany **56:** 2365-2378

Geldner N (2013) The endodermis. *In* SS Merchant, ed, Annual Review of Plant Biology, Vol 64, Vol 64, pp 531-558

Gong HJ, Randall DP, Flowers TJ (2006) Silicon deposition in the root reduces sodium uptake in rice (*Oryza sativa L.*) seedlings by reducing bypass flow. Plant Cell and Environment **29:** 1970-1979

Harris BN, Sadras VO, Tester M (2010) A water-centred framework to assess the effects of salinity on the growth and yield of wheat and barley. Plant and Soil **336:** 377-389

Hofer R, Briesen I, Beck M, Pinot F, Schreiber L, Franke R (2008) The *Arabidopsis* cytochrome P450 *CYP86A1* encodes a fatty acid omega-hydroxylase involved in suberin monomer biosynthesis. Journal of Experimental Botany **59:** 2347-2360

Hosmani PS, Kamiya T, Danku J, Naseer S, Geldner N, Guerinot ML, Salt DE (2013) Dirigent domain-containing protein is part of the machinery required for formation of the lignin-based Casparian strip in the root. Proceedings of the National Academy of Sciences of the United States of America **110:** 14498-14503

Islam S, Malik AI, Islam A, Colmer TD (2007) Salt tolerance in a *Hordeum marinum-Triticum aestivum* amphiploid, and its parents. Journal of Experimental Botany **58:** 1219-1229

Jacoby RP, Millar AH, Taylor NL (2013) Investigating the role of respiration in plant salinity tolerance by analyzing mitochondrial proteomes from wheat and a salinity-tolerant amphiploid (Wheat x *Lophopyrum elongatum*). Journal of Proteome Research **12:** 4807-4829

James RA, Blake C, Byrt CS, Munns R (2011) Major genes for Na^+ exclusion, *Nax1* and *Nax2* (wheat *HKT1; 4* and *HKT1; 5*), decrease Na^+ accumulation in bread wheat leaves under saline and waterlogged conditions. Journal of experimental botany **62:** 2939-2947

Jbir N, Chaibi W, Ammar S, Jemmali A, Ayadi A (2001) Root growth and lignification of two wheat species differing in their sensitivity to NaCl, in response to salt stress. Comptes Rendus De L Academie Des Sciences Serie Iii-Sciences De La Vie-Life Sciences **324:** 863-868

Kamiya T, Borghi M, Wang P, Danku JMC, Kalmbach L, Hosmani PS, Naseer S, Fujiwara T, Geldner N, Salt DE (2015) The MYB36 transcription factor orchestrates Casparian strip formation. Proceedings of the National Academy of Sciences of the United States of America **112:** 10533-10538

Karahara I, Ikeda A, Kondo T, Uetake Y (2004) Development of the Casparian strip in primary roots of maize under salt stress. Planta **219:** 41-47

Knipfer T, Danjou M, Vionne C, Fricke W (2020) Salt stress reduces root water uptake in barley (*Hordeum vulgare* L.) through modification of the transcellular transport path. Plant, Cell & Environment

Kobayashi NI, Yamaji N, Yamamoto H, Okubo K, Ueno H, Costa A, Tanoi K, Matsumura H, Fujii-Kashino M, Horiuchi T (2017) OsHKT1; 5 mediates Na^+ exclusion in the vasculature to protect leaf blades and reproductive tissues from salt toxicity in rice. The Plant Journal **91:** 657-670

Kotula L, Clode PL, Striker GG, Pedersen O, Lauchli A, Shabala S, Colmer TD (2015) Oxygen deficiency and salinity affect cell-specific ion concentrations in adventitious roots of barley (*Hordeum vulgare*). New Phytologist **208:** 1114-1125

Kotula L, Colmer TD, Nakazono M (2014) Effects of organic acids on the formation of the barrier to radial oxygen loss in roots of *Hordeum marinum*. Functional Plant Biology **41:** 187-202

Kotula L, Ranathunge K, Schreiber L, Steudle E (2009b) Functional and chemical comparison of apoplastic barriers to radial oxygen loss in roots of rice (*Oryza sativa* L.) grown in aerated or deoxygenated solution. Journal of Experimental Botany **60:** 2155-2167

Kotula L, Ranathunge K, Steudle E (2009c) Apoplastic barriers effectively block oxygen permeability across outer cell layers of rice roots under deoxygenated conditions: roles of apoplastic pores and of respiration. New Phytologist **184:** 909-917

Kreszies T, Eggels S, Kreszies V, Osthoff A, Shellakkutti N, Baldauf JA, Zeisler-Diehl VV, Hochholdinger F, Ranathunge K, Schreiber L (2019b) Seminal roots of wild and cultivated barley differentially respond to osmotic stress in gene expression, suberization, and hydraulic conductivity. Plant, Cell & Environment

Kreszies T, Schreiber L, Ranathunge K (2018) Suberized transport barriers in *Arabidopsis*, barley and rice roots: From the model plant to crop species. Journal of Plant Physiology **227:** 75-83

Kreszies T, Shellakkutti N, Osthoff A, Yu P, Baldauf JA, Zeisler-Diehl VV, Ranathunge K, Hochholdinger F, Schreiber L (2019a) Osmotic stress enhances suberization of apoplastic barriers in barley seminal roots: analysis of chemical, transcriptomic and physiological responses. New Phytologist **221:** 180-194

Krishnamurthy P, Jyothi-Prakash PA, Qin L, He J, Lin QS, Loh CS, Kumar PP (2014) Role of root hydrophobic barriers in salt exclusion of a mangrove plant *Avicennia officinalis*. Plant Cell and Environment **37:** 1656-1671

Krishnamurthy P, Ranathunge K, Franke R, Prakash HS, Schreiber L, Mathew MK (2009) The role of root apoplastic transport barriers in salt tolerance of rice (*Oryza sativa* L.). Planta **230:** 119-134

Krishnamurthy P, Ranathunge K, Nayak S, Schreiber L, Mathew MK (2011) Root apoplastic barriers block Na^+ transport to shoots in rice (*Oryza sativa L.*). Journal of Experimental Botany **62:** 4215-4228

Landgraf R, Smolka U, Altmann S, Eschen-Lippold L, Senning M, Sonnewald S, Weigel B, Frolova N, Strehmel N, Hause G, Scheel D, Bottcher C, Rosahl S (2014) The ABC Transporter ABCG1 Is Required for Suberin Formation in Potato Tuber Periderm. Plant Cell **26:** 3403-3415

Li B, Kamiya T, Kalmbach L, Yamagami M, Yamaguchi K, Shigenobu S, Sawa S, Danku JM, Salt DE, Geldner N (2017) Role of *LOTR1* in nutrient transport through organization of spatial distribution of root endodermal barriers. Current Biology **27:** 758-765

Liska D, Martinka M, Kohanova J, Lux A (2016) Asymmetrical development of root endodermis and exodermis in reaction to abiotic stresses. Annals of Botany **118:** 667-674

Liu G, Stirnemann M, Gübeli C, Egloff S, Courty P-E, Aubry S, Vandenbussche M, Morel P, Reinhardt D, Martinoia E (2019) Strigolactones play an important role in shaping exodermal morphology via a KAI2-dependent pathway. iScience **17:** 144-154

Maathuis FJM, Amtmann A (1999) K^+ nutrition and Na^+ toxicity: The basis of cellular K^+/Na^+ ratios. Annals of Botany **84:** 123-133

Malagoli P, Britto DT, Schulze LM, Kronzucker HJ (2008) Futile Na^+ cycling at the root plasma membrane in rice (*Oryza sativa L.*): kinetics, energetics, and relationship to salinity tolerance. Journal of Experimental Botany **59:** 4109-4117

Maurer A, Draba V, Jiang Y, Schnaithmann F, Sharma R, Schumann E, Kilian B, Reif JC, Pillen K (2015) Modelling the genetic architecture of flowering time control in barley through nested association mapping. Bmc Genomics **16**

Munns R (2005) Genes and salt tolerance: bringing them together. New Phytologist **167:** 645-663

Munns R, James RA, Xu B, Athman A, Conn SJ, Jordans C, Byrt CS, Hare RA, Tyerman SD, Tester M, Plett D, Gilliham M (2012) Wheat grain yield on saline soils is improved by an ancestral Na^+ transporter gene. Nature Biotechnology **30:** 360-U173

Munns R, Tester M (2008) Mechanisms of salinity tolerance. Annual Review of Plant Biology **59:** 651-681

Naseer S, Lee Y, Lapierre C, Franke R, Nawrath C, Geldner N (2012) Casparian strip diffusion barrier in *Arabidopsis* is made of a lignin polymer without suberin. Proceedings of the National Academy of Sciences of the United States of America **109:** 10101-10106

Neves GYS, Marchiosi R, Ferrarese MLL, Siqueira-Soares RC, Ferrarese O (2010) Root growth inhibition and lignification induced by salt stress in soybean. Journal of Agronomy and Crop Science **196:** 467-473

Peterson CA, Enstone DE (1996) Functions of passage cells in the endodermis and exodermis of roots. Physiologia Plantarum **97:** 592-598

Peterson CA, Perumalla CJ (1990) A survey of angiosperm species to detect hypodermal Casparian bands. II. Roots with a multiseriate hypodermis or epidermis. Botanical Journal of the Linnean Society **103:** 113-125

Pfister A, Barberon M, Alassimone J, Kalmbach L, Lee Y, Vermeer JEM, Yamazaki M, Li GW, Maurel C, Takano J, Kamiya T, Salt DE, Roppolo D, Geldner N (2014) A receptor-like kinase mutant with absent endodermal diffusion barrier displays selective nutrient homeostasis defects. Elife **3**

Ranathunge K, Kim YX, Wassmann F, Kreszies T, Zeisler V, Schreiber L (2017) The composite water and solute transport of barley (Hordeum vulgare) roots: effect of suberized barriers. Annals of Botany **119:** 629-643

Ranathunge K, Lin JX, Steudle E, Schreiber L (2011a) Stagnant deoxygenated growth enhances root suberization and lignifications, but differentially affects water and NaCl permeabilities in rice (Oryza sativa L.) roots. Plant Cell and Environment **34:** 1223-1240

Ranathunge K, Schreiber L (2011) Water and solute permeabilities of *Arabidopsis* roots in relation to the amount and composition of aliphatic suberin. Journal of Experimental Botany **62:** 1961-1974

Reinhardt DH, Rost TL (1995) Salinity accelerates endodermal development and induces an exodermis in cotton seedling roots. Environmental and Experimental Botany **35:** 563-574

Ren Z-H, Gao J-P, Li L-G, Cai X-L, Huang W, Chao D-Y, Zhu M-Z, Wang Z-Y, Luan S, Lin H-X (2005) A rice quantitative trait locus for salt tolerance encodes a sodium transporter. Nature genetics **37:** 1141

Saade S, Maurer A, Shahid M, Oakey H, Schmockel SM, Negrao S, Pillen K, Tester M (2016) Yield-related salinity tolerance traits identified in a nested association mapping (NAM) population of wild barley. Scientific Reports **6**

Schreiber L, Franke R, Hartmann K (2005a) Effects of NO_3 deficiency and NaCl stress on suberin deposition in rhizo- and hypodermal (RHCW) and endodermal cell walls (ECW) of castor bean (*Ricinus communis L.*) roots. Plant and Soil **269:** 333-339

Schreiber L, Franke R, Hartmann KD, Ranathunge K, Steudle E (2005b) The chemical composition of suberin in apoplastic barriers affects radial hydraulic conductivity differently in the roots of rice (*Oryza sativa L.* cv. IR64) and corn (*Zea mays L.* cv. Helix). Journal of Experimental Botany **56:** 1427-1436

Schreiber L, Hartmann K, Skrabs M, Zeier J (1999) Apoplastic barriers in roots: chemical composition of endodermal and hypodermal cell walls. Journal of Experimental Botany **50:** 1267-1280

Seago J, James L, Peterson CA, Enstone DE, Scholey CA (1999) Development of the endodermis and hypodermis of *Typha glauca* Godr. and *Typha angustifolia* L. roots. Canadian Journal of Botany **77:** 122-134

Shen J, Xu GX, Zheng HQ (2015) Apoplastic barrier development and water transport in Zea mays seedling roots under salt and osmotic stresses. Protoplasma **252:** 173-180

Steudle E (2000) Water uptake by plant roots: an integration of views. Plant and Soil **226:** 45-56

Steudle E, Peterson CA (1998) How does water get through roots? Journal of Experimental Botany **49:** 775-788

Tanksley SD, McCouch SR (1997) Seed banks and molecular maps: unlocking genetic potential from the wild. Science **277:** 1063-1066

Tilbrook J, Schilling RK, Berger B, Garcia AF, Trittermann C, Coventry S, Rabie H, Brien C, Nguyen M, Tester M (2017) Variation in shoot tolerance mechanisms not related to ion toxicity in barley. Functional Plant Biology **44:** 1194-1206

Toda Y, Yoshida M, Hattori T, Takeda S (2013) RICE SALT SENSITIVE3 binding to bHLH and JAZ factors mediates control of cell wall plasticity in the root apex. Plant Signaling & Behavior **8**

Tylova E, Peckova E, Blascheova Z, Soukup A (2017) Casparian bands and suberin lamellae in exodermis of lateral roots: an important trait of roots system response to abiotic stress factors. Annals of Botany **120:** 71-85

Walia H, Wilson C, Zeng L, Ismail AM, Condamine P, Close TJ (2007) Genome-wide transcriptional analysis of salinity stressed japonica and indica rice genotypes during panicle initiation stage. Plant Molecular Biology **63:** 609-623

Wang P, Calvo-Polanco M, Reyt G, Barberon M, Champeyroux C, Santoni V, Maurel C, Franke RB, Ljung K, Novak O (2019) Surveillance of cell wall diffusion barrier integrity modulates water and solute transport in plants. Scientific Reports **9:** 1-11

Wilson A, Robards A (1980) Observations of the pattern of secondary wall development in the hypodermis of onion (*Allium cepa*) roots. Protoplasma **104:** 149-156

Yadav R, Flowers T, Yeo A (1996) The involvement of the transpirational bypass flow in sodium uptake by high-and low-sodium-transporting lines of rice developed through intravarietal selection. Plant, Cell & Environment **19:** 329-336

Yeo AR, Yeo ME, Flowers TJ (1987) The contribution of an apoplastic pathway to sodium uptake by rice roots in saline conditions. Journal of Experimental Botany **38:** 1141-1153

Zeng FR, Shabala L, Zhou MX, Zhang GP, Shabala S (2013) Barley responses to combined waterlogging and salinity stress: separating effects of oxygen deprivation and elemental toxicity. Frontiers in Plant Science **4**

Zhao Q, Dixon RA (2011) Transcriptional networks for lignin biosynthesis: more complex than we thought? Trends in Plant Science **16:** 227-233

Zimmermann HM, Hartmann K, Schreiber L, Steudle E (2000) Chemical composition of apoplastic transport barriers in relation to radial hydraulic conductivity of corn roots (*Zea mays L.*). Planta **210:** 302-311

Zimmermann HM, Steudle E (1998) Apoplastic transport across young maize roots: effect of the exodermis. Planta **206:** 7-19

Chapter 2:

Diversity in root apoplastic barriers deposition in salt treated wild and domesticated barley seedlings

Statement of Authorship

Title of Paper	Diversity in root apoplastic barrier deposition in salt treated wild and domesticated barley seedlings
Publication Status	☐ Published ☐ Accepted for Publication ☐ Submitted for Publication ● Unpublished and Unsubmitted work written in manuscript style
Publication Details	Plant, Cell and Environment (PCE) format

Principal Author

Name of Principal Author (Candidate)	Muhammad Khairul Hisyam Ahmad Sohaimi		
Contribution to the Paper	Contributed to the experimental design, grew the plants, conducted all the microscopy work and root oxygen consumption measurement, quantification of fluoresecence using ImageJ, contributed for growth parameters, growth rate and ion measurement, analysed interpreted the data and contributed for the writing of the manuscript.		
Overall percentage (%)	90%		
Certification:	This paper reports on original research I conducted during the period of my Higher Degree by Research candidature and is not subject to any obligations or contractual agreements with a third party that would constrain its inclusion in this thesis. I am the primary author of this paper.		
Signature		Date	29/12/2020

Co-Author Contributions

By signing the Statement of Authorship, each author certifies that:

i. the candidate's stated contribution to the publication is accurate (as detailed above);

ii. permission is granted for the candidate in include the publication in the thesis; and

iii. the sum of all co-author contributions is equal to 100% less the candidate's stated contribution.

Name of Co-Author	Dr. Stefanie Wege		
Contribution to the Paper	Conceived the work, contributed to the experimental design, contributed in the interpretation of the data, contributed to the supervision, reviewed and commented the manuscript.		
Signature		Date	29/12/2020

Name of Co-Author	Dr. Caitlin Byrt		
Contribution to the Paper	Conceived the work, contributed to the experimental design, contributed in the interpretation of the data, contributed to the supervision, reviewed and commented the manuscript.		
Signature		Date	29/12/2020

Please cut and paste additional co-author panels here as required.

Name of Co-Author	Dr. Rhiannon Schilling		
Contribution to the Paper	Conceived the work, contributed to the experimental design, contributed in the interpretation of the data, contributed to the supervision, reviewed and commented the manuscript.		
Signature		Date	29/12/2020

Please cut and paste additional co-author panels here as required.

Diversity in root apoplastic barrier deposition in salt treated wild and domesticated barley seedlings

Hisyam Sohaimi[1,2], Rhiannon K. Schilling[1,3], Stefanie Wege[1,2#*], Caitlin Byrt[2,4#*]

Author affiliations

[1]School of Agriculture, Food and Wine, The University of Adelaide, Glen Osmond, South Australia, Australia

[2]ARC Centre of Excellence in Plant Energy Biology, The University of Adelaide, Glen Osmond, South Australia, Australia

[3]South Australian Research and Development Institute (SARDI), Department of Primary Industries and Regions, Glen Osmond, South Australia, Australia.

[4]Research School of Biology, The Australian National University, Canberra, Australia

[#]These authors contributed equally

[*]Correspondence to Caitlin.Byrt@anu.edu.au and stefanie.wege@adelaide.edu.au

2.0 Abstract

Salt stress can cause root apoplastic cell wall barriers to change, presumably to support adaptation of transport properties and metabolism. To explore genetic variation in root apoplastic barrier traits a diverse collection of commercial and wild barley accessions were phenotyped to assess the deposition of barriers in root endodermal and exodermal cells. One-week-old seedlings were subjected to non-saline (control) and saline treatments, root suberin and lignin deposition trends were recorded, and root O_2 consumption and tissue Na^+ and K^+ accumulation were measured. Variation in lignin and suberin deposition in endo- and exo-dermal cell walls of roots grown in control and saline conditions was observed. Twenty-two wild barley accessions were identified that formed an exodermis in one-week-old roots in response to salt treatments, whereas a commercial barley cultivar, Barke, did not develop an obvious exodermis. Accessions with pronounced root barrier deposition tended to have lower O_2 consumption relative to the accessions with less obvious barriers. Abscisic acid treatments enhanced suberisation in all accessions and lead to a pronounced formation of an exodermis in wild barley accession, HID138; whereas treatment with an ethylene precursor had no obvious effect on the suberisation, differing from previous observations in Arabidopsis roots. Principal component analysis revealed that there may be associations between the variation in root and shoot Na^+ and K^+ , suberin deposition and root respiration. The variation in root traits within the barley accessions represents a useful resource for determining which root apoplastic barrier traits contribute to crop tolerance to salt stress.

Keywords

endodermis, exodermis, apoplastic barrier, suberin, lignin, saline, wild barley, commercial barley, accession (s)

2.1 Introduction

Enhancing tolerance to salinity and osmotic stresses in commercial cereal crops is an important step towards ensuring the sustainability of food production in the future. Currently, yield losses of 50% are common for many cereals exposed to highly saline conditions relative to non-saline conditions (Islam et al., 2007; James et al., 2012). The domestication of cereals such as barley from their wild grass ancestors led to a decrease in allelic variation, limiting the genetic diversity available for optimising salt tolerance traits in commercial cultivars (Tanksley and McCouch, 1997). However, wild grasses are available as a potential source of salt stress tolerance traits which could be used to increase the productivity of modern cereals in saline soils (Colmer et al., 2006).

There are wild halophytic grasses that display notable capacity for Na^+ and or Cl^- exclusion under high salinity, vacuolization of these ions in mature or senescing leaves, secretion of excess salts by salt glands, accumulation of compatible solutes, reactive oxygen species scavenging and novel cell wall associated properties that may contribute to salt tolerance and yield gains in saline conditions (Colmer et al., 2006; Roy and Chakraborty, 2014; Saade et al., 2016; Isayenkov et al., 2020). These types of halophytic grass features may be useful for limiting yield loss in saline conditions. For example, when exposed to 150 mM NaCl wheat yield loss was in the order of 50% relative to non-saline conditions, whereas there was only a 7% yield loss for halophytic wild barleygrass (*Hordeum marinum*) in saline, 150 mM NaCl, conditions relative to non-saline conditions (Islam et al., 2007). However, it is unclear which of the possible salt tolerance mechanisms in wild barleygrass are key in tolerating saline conditions or whether these would be useful for incorporation into modern cereals.

H. marinum was reported to be able to maintain exclusion of salt from shoots, even in very saline conditions (Garthwaite et al., 2005; Isayenkov et al., 2020). *H. marinum* was also reported to develop a distinct exodermal barrier, in addition to an endodermis, in abiotic stress

conditions (Garthwaite et al., 2008; Kotula et al., 2014). The formation of an exodermis could potentially be a key anatomical feature involved in enabling the roots to restrict excessive ion uptake and prevent nutrient and water loss in saline conditions. However, the extent to which root exodermal barriers influence barley stress tolerance is currently unclear.

Previous studies have suggested that wild and cultivated barley may respond differently to osmotic stress in relation to their deposition of exodermal barriers (Kreszies et al 2019a, Kreszies et al 2019b). These studies reported examples of modern barley lacking an exodermis, and the authors discuss the possibility that exodermal barrier deposition in wild barley could influence osmotic stress tolerance. In comparison to commercial cultivars, wild barley accessions do tend to have greater salt tolerance than commercial cultivars (Tilbrook et al. (2017). Wild barley generally had higher ratios of leaf biomass for the salt stressed plants relative to non-salt-stressed plants, and higher leaf K^+:Na^+ ratios. Interestingly, a commercial line that contained introgressed DNA from wild barley *H. vulgare* L. spp. *spontaneum* maintained a similar ability to tolerate salt as the original salt tolerant wild barley (Tilbrook et al 2017). This indicates the feasibility of transferring useful salt tolerance traits from wild barley to modern cultivars; and similar strategies have been used to increase the salinity tolerance of wheat using traits from wild wheat accessions (James et al., 2011; James et al., 2012; Munns et al., 2012). The challenge remains to identify which traits in wild grasses would be useful for improving modern cereal salinity tolerance.

Salt stress triggers the deposition of apoplastic barriers in roots in many plant species, including some cereals. This trait of forming apoplastic barriers could potentially be used as part of a strategy to increase crop abiotic stress tolerance. Previous studies have reported that rice (*Oryza sativa*) and maize (*Zea mays*) enhanced their apoplastic solute barriers in response to salinity, water- and O_2-deficient environments (Karahara et al., 2004; Krishnamurthy et al., 2009; Kotula et al., 2009c). In a recent study, a comparison of commercial and wild barley

accessions identified differences in the abundance of root suberin in commercial cultivars Barke, Morex and Golden Promise relative to wild accessions (*H. vulgare* spp. *spontaneum* ICB181160, ICB181243 and ICB181466 from Iran, Pakistan and Jordan, respectively) (Kreszies et al., 2019b). This discovery indicates that there is potential to identify root suberin traits of value within wild barley, and scope to test whether these traits enhance the abiotic stress tolerance of modern cultivars. Traits associated with yield gains under saline conditions have been previously identified within a diverse collection of 25 wild barley accessions (*Hordeum vulgare* spp. *spontaneum*), also known as Hordeum Identity (HID) accessions (Saade et al 2016). These 25 accessions were crossed with the elite barley cultivar, Barke, to generate a Nested Association Mapping (NAM) population called "Halle of Exotic Barley (HEB-25)". This collection was used to investigate flowering time traits (Maurer et al 2015), and genetic variation associated with differences in yield in saline conditions were also identified (Saade et al 2016). The HID accessions might therefore be a useful source of diverse barley material for identifying variation in root cell wall traits, such as suberin deposition, that may be associated with environmental stress tolerance.

The enhancement of root diffusion barriers in response to salt stress has been associated with a reduction in leaf Na^+ accumulation in cereals such rice and maize (Karahara et al., 2004; Krishnamurthy et al., 2009; Krishnamurthy et al., 2014). Two rice varieties differing in tolerance to salinity have been shown to differ in root barriers with a tolerant variety having extensive root barrier layers and less root and shoot Na^+ accumulation compared to the less tolerant variety (Krishnamurthy et al., 2011). A two-fold reduction of the NaCl permeability has also been observed with an increase in suberisation of both endodermal and exodermal cell walls in rice under saline conditions (Ranathunge et al., 2011a). In *Arabidopsis thaliana*, root endodermal lignin deposition was reported to influence the ability of plants to prevent K^+ loss under low K^+ conditions; which is important under saline conditions (Pfister et al., 2014;

Barberon et al., 2016). In maize, enhanced root barriers have been linked to preventing water loss under water-limited conditions (Zimmermann et al., 2000). In rice and *H. marinum*, exodermal barriers helped to prevent O_2 loss in O_2-limited environments (Garthwaite et al., 2008; Kotula et al., 2009b; Kotula et al., 2014). These observations indicate that deposition of root apoplastic barriers has the potential to limit NaCl influx and limit the loss of K^+, water and O_2.

Root apoplastic barriers tend to be deposited in endodermal and or exodermal cell layers. All vascular plants except for *Lycopodium* develop an endodermis within the innermost cortical cell layer (Damus et al., 1997; Enstone et al., 2002). The endodermis surrounds the central vasculature, forming a solute barrier or checkpoint for the fluxes of water and solutes in and out of the stele (Barberon, 2017). The formation of the endodermal barrier occurs through a series of stages in cell wall modification associated with the deposition of hydrophobic materials. Initially lignin is deposited in the anticlinal walls of endodermal cells forming a ring-like structure known as a Casparian strip that surrounds the central vasculature (Naseer et al., 2012). After formation of the Casparian strip the free apoplastic pathway is blocked and solute uptake is restricted to selective transport across the plasma membrane of endodermal cells and/or through the symplastic pathway (Sager and Lee, 2014; Byrt et al., 2018). Next a second hydrophobic material suberin is deposited surrounding almost the entire endodermal cell forming a hydrophobic surface, known as suberin lamellae, thus limiting fluxes of water and solutes across the plasma membrane into the cell (Robards et al., 1973; Barberon et al., 2016; Barberon, 2017). At this stage, fluxes can only occur symplastically (Sager and Lee, 2014). Some endodermal cells remain unsuberised even where there is a fully developed lamellae ring, and these cells are known as passage cells (Ranathunge et al., 2017). Unsuberised passage cells are likely to be key sites of exchange of water and solutes across the plasma membrane (Peterson and Enstone, 1996).

Most roots form an endodermis, but not all roots form an exodermis. The location of the exodermis is in the outermost cortical cell layer(s) behind the epidermis, and it can be considered to be present when these cells develop characteristics that are similar to that of the endodermis (Hose et al., 2001). However, unlike in endodermis formation, the development of exodermal Casparian strips and suberin lamellae typically occur simultaneously in this layer and the amount of lignin and suberin is generally lower compared to endodermal cells (Schreiber et al., 1999; Enstone et al., 2002; Schreiber et al., 2005b; Byrt et al., 2018). The exodermis can be single or multilayered depending on the plant species (Peterson and Perumalla, 1990; Seago et al., 1999; Soukup et al., 2002); and can be formed constitutively during root development or formed in response to changes in the external environment (Zimmermann and Steudle, 1998; Ranathunge et al., 2011a). The exodermis is thought to have a similar function to the endodermis; that is to regulate the fluxes of water, solutes and gases in and out of the roots. This is likely to be the case for some cereal crops, where an exodermal barrier could be either constitutive or inducible by abiotic stresses such as salinity, or water- and O_2-limited environments. For example, in rice the formation of an exodermal barrier is induced in response to saline and waterlogged conditions (Krishnamurthy et al., 2009; Kotula et al., 2009c). In maize, the exodermal apoplastic barrier is reinforced in response to drought, most likely to prevent water loss (Karahara et al., 2004). Unlike rice and maize, modern barley and wheat cultivars have not been reported to develop an exodermal barrier, and their growth in stress conditions could hypothetically be improved if this type of trait could be introduced (Ranathunge et al., 2017; Kreszies et al., 2019a; Kreszies et al., 2019b).

Here we screened root diffusion barrier formation in 25 wild barley (HID) accessions, commercial cultivars (Barke and Scarlett) and one *H. marinum* barleygrass, in control (non-saline) and saline conditions. We investigated the relationships between the formation of root apoplastic barriers, root respiration and root and shoot ion accumulation. Our findings reveal

that there are differences in apoplastic barrier deposition, root respiration and ion accumulation within the diverse accessions tested, and that differences in the extent of apoplastic barriers could be contributing to differences in tolerance to salt stress (Saade et al. 2016).

2.2 Material and methods

2.2.1 Plant materials and growth conditions used for screening root barriers

Twenty-eight barley accessions, consisting of 25 wild barley accessions (Maurer et al., 2015), two commercial cultivars (Barke and Scarlett) and one wild barley (*Hordeum marinum*) were used. The 25 wild barley accessions comprised 24 *Hordeum vulgare* ssp. *spontaneum* from the Fertile Crescent, and one accession *Hordeum vulgare* ssp. *agriocrithon* from Tibet (Badr et al., 2000)**.**

Seeds were imbibed in deionised water for 2 h then surface sterilised by rinsing in 1.4 g L^{-1} Thiram solution for 30 s, and placed on filter paper dampened with the same Thiram solution in sterile petri dishes sealed with millipore tape and stratified at 4^{o}C for 4 d. After stratification, the petri dishes were placed in the dark to germinate for 12 h. Uniformly germinated seeds from each accession/line were individually placed onto 18 cm × 22 cm paper towels (Asaleo Care, New Zealand), and fixed into position at 1 cm from the top and in the centre of the paper towel using thin millipore tape. The paper towel was carefully rolled and millipore tape was used to secure the roll to prevent unrolling. The bottom 5 cm of each vertically oriented paper roll was placed into a container (12cm length x 7.7cm wide x 7.7 depth) containing 500 mL of one quarter strength Hoagland's solution, for one week (Table S1). The pH of Hoaglands solution was adjusted to 6.5 using 20µL of 1M KOH. Each container contained 20-24 paper rolls (Figure 1). A 'control' genotype, Barke was included in each experiment and the position of the plants for each accession/line was randomised, blocking for the location within the container. Salt or control treatments were applied at the stage when germinated seeds in paper towels were placed in to Hoagland's solution. Plants were grown in growth room under (12 h

: 12 h, night : dark) with the temperature 22°C : 15°C. Salt treatments of 40 mM NaCl were chosen to impose a moderate salinity stress, sufficient to impose a stress but not so severe as to result in an excessive arrest of plant growth.

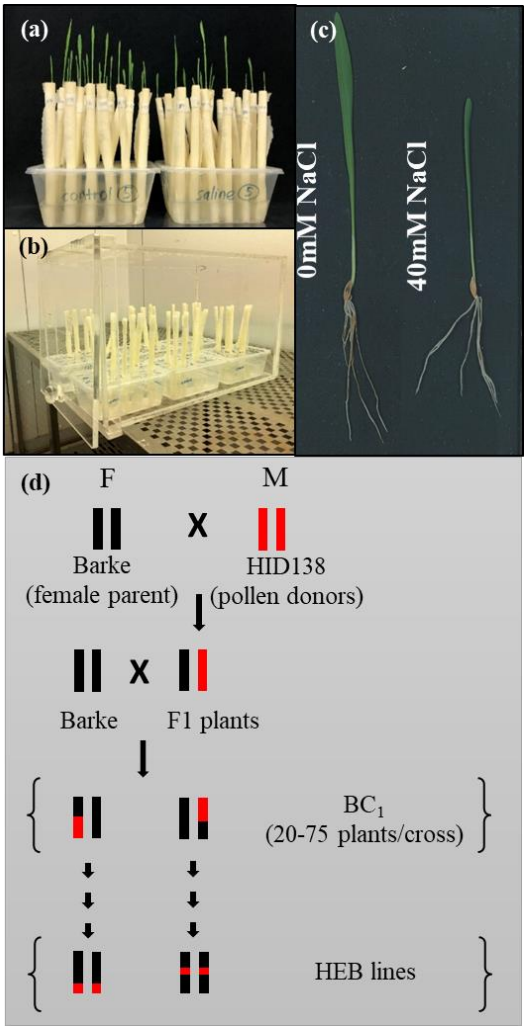

FIGURE 1 Experimental setup and information regarding the plant materials used in the screen for variation in root apoplastic barrier deposition. (a) Pre-stratified seeds were grown in a paper towel roll placed vertically in a small container containing one-quarter strength Hoagland's nutrient solution with or without 40mM NaCl. (b) Plants were grown in a humid, transparent chamber for 7d; the purpose of the container was to prevent excessive evaporation from the paper towel. (c) The cultivar Barke is pictured as an example of the appearance of the plants grown under control and saline conditions in this setup. (d) A pictorial representation of the development of the subsets of NAM HEB25 population, adapted from Maurer et al. (2015). Wild barley accessions, Hordeum Identity 138 (HID 138) is one of

the 25 wild barley accessions that was used as pollen donor which was crossed with a recipient, Barke to develop HEB13 which is a subset of HEB25 NAM population (Maurer et al., 2015).

2.2.2 Root sectioning and screening for the spatial deposition of lignin and suberin

After 7 d of growth in both control and saline conditions the length of the longest seminal root of each plant was measured. A 3-5 mm root segment at the mid-point of the root maturation zone, where the maturation zone was determined by the emergence of root hairs, was cut using a double-sided razor blade and the section was embedded in 5% low melting point agarose gel (Bioline). The embedded root section was then cut transversely in uniform thickness of 100 µm using a vibratome (Vibratome Leica VT1200, Leica Biosystems). To detect lignin sections were stained with a 2:1 ratio of 3% Phloroglucinol:hydrochloric acid stain for a one minute as described in Mitra and Loqué (2014). Stained root sections were viewed under a wide-field microscope (Nikon Ni-E, 20× Magnification) and images were recorded using an attached DS-Ri1-U3 camera. To detect suberin transverse root sections were stained for 1h with 0.01% (w/v) Fluorol Yellow 088 in polyethylene glycol following Brundrett et al. (1991), and the stained sections were viewed using a confocal laser scanning microscope (Confocal Nikon A1R, Nikon A1 Plus; Apo Plan λ 20x objective, excitation wavelength 488 nm, emission collection 500-550 nm. Scale bars were generated using ImageJ.

2.2.3 Hormone treatments

Seeds of Barke, HID003, HID055, HID138 and HID357 were imbibed, sterilised, and stratified as described previously. Seeds were pre-germinated in the dark for 12 h before they were replanted in paper towel under quarter strength Hoagland's solution. Salt (40mM NaCl) and hormones (5µM ABA, 100 µM ACC) were applied at the stage when germinated seeds in paper towels were placed in to Hoagland's solution. After 7 d of growth in each treatment, root length and shoot length and biomass were recorded. A transverse section was made at the maturation zones and stained for lignin and suberin as described previously.

2.2.4 Whole root respiration using a high throughput fluorophore system

Whole roots from individual plants grown in solution containing no additional (control) or an additional 40 mM NaCl were freshly dissected, washed 2 times with MilliQ water, blot dried, weighed and placed in sealed 2 mL tubes fitted with O_2-sensor caps (Astec-Global, Holland). The whole root respiration was then measured using a Q2 meter (Astec-Global, Holland) following a previously reported protocol (Scafaro et al., 2017) with 14 replicates per accession/line per treatment (Figure S1). Tubes were placed in 48 well-plates with the first row including four tubes of which two contained 100% N_2 and two contained ambient air; these were used as standards to calibrate for 0% O_2 and 100 atmospheric O_2 before each set of measurements. The measurements were started immediately and recorded at eight-minute intervals. The rate of O_2 consumption was calculated from 1 h to 3 h after the start of the run for each plate following Scafaro et al. (2017). Molar rate of O_2 consumption was calculated based on the ideal gas law, where the O_2 partial pressure was determined to be 20.95% of atmospheric pressure and the rate of O_2 consumption was then normalised to the fresh and dry weight using an established reported protocol (Scafaro et al., 2017).

2.2.5 Quantification of Na^+ and K^+ accumulation in whole roots of week-old seedlings

Whole root tissues from the respiration experiment were dried in an oven at 65^{o}C for 3 days before the dry weight was recorded. Dried tissue was digested in 10 mL of 1% (v/v) nitric acid at 100°C for 4 h in a 54-well Hotblock (Environmental Express, Mount Pleasant, SC, USA). The Na^+ and K^+ accumulation were measured using a Sherwood 420 flame photometer (Sherwood, Cambridge, UK) following the manufacturers' instructions and Shavrukov et al. (2010).

2.3 Statistical analysis

Data was analysed using GraphPad Prism (version 8) and each genotype was compared with the 'control' genotype, Barke, using one-way ANOVA Dunnet's multiple comparison test. For the comparisons between treatments the data for each individual genotype was compared between the treatments using Sidak's multiple comparison test. For the measurements of respiration for each barley accession/line samples from the control and salt treated plants were placed next to each other in the same plate to limit any potential influence of time between measurements within the plate.

Principle Component Analysis (PCA) analysis was used to transform the data measurements recorded for control and saline treated plants including root ion accumulation, root O_2 consumption and root biomass. The PCA was generated using a "FactoMineR" package, and the biplot graph was drawn using "factoextra" in R programming platform. The 95% confidence eclipse was also added to the graph.

2.4 Results

2.4.1 Variation in apoplastic barrier formation in a diverse barley collection

Variation in the formation of root apoplastic barriers was observed in the roots of the 25 barley accessions tested (Figure S2). Seven of the 25 wild barley accessions, HID003, HID055, HID069, HID101, HID138, HID357 and HID386, displayed the most notable variation in deposition of apoplastic barriers (Figure S2), and these seven accessions along with Barke were selected for further experiments to explore root suberin and lignin deposition, root length, biomass Na^+ and K^+ accumulation, and root O_2 consumption.

2.4.2 Intensity and patterns of root suberin-associated fluorescence signals

Roots were stained with the fluorescent dye Fluorol Yellow 088 to visualise suberin, and care was taken to apply exactly the same staining protocol and duration to all root sections. Variation in the Fluorol Yellow 088 fluorescence signals was observed in microscopy images of the Barke and selected wild accessions; HID003, HID055, HID069, HID101, HID138, HID357 and HID386 under control and saline conditions (Figure 2). The patterns of the fluorescence varied between the cell types, accessions and treatments. The intensity of the fluorescence signal also varied and we observed that there was a clear tendency for the fluorescence signal to increase in saline conditions relative to control conditions for each accession/line tested; however, whilst trends could be observed exact quantification of the signal was not feasible due to the absence of an internal control for normalising the signal between different samples. In most of the accessions tested, the fluorescence signals in the endodermal cell layer appeared brighter compared to the signals in the exodermal cell layer in both control and saline conditions (Figure 2). The quantification of the fluorescence by measuring the gray value shows that, in general, the endodermal cell layer had higher intensity compared to the exodermal under saline conditions (Table S2). HID138 also was found to have the highest intensity in both endodermal and exodermal compared to all of the barley tested under saline conditions (Table S2).

There was no fluorescence signal detected in the epidermal cell wall or in the xylem vessel walls in any of the accessions tested under either control or salt treatments (Figure 2). Some endodermal cells did not display any fluorescence, which is consistent with endodermal passage cells (Figure 2). In response to saline conditions, some of the accessions (Barke, HID003, HID069, HID357 and HID386), had what appeared to be an increase in the fluorescence signal in the cortex cells in saline conditions compared to control conditions (Figure 2). However, the intensity of the fluorescence in the cortex cells appeared considerably

less intense compared to the intensity of the signal observed in both endo- and exodermal cell layers under salt treatment (Figure 2).

We observed that the intensity of endodermal fluorescence signals varied between accessions and treatments. Within the selected accessions, under control conditions, we observed that HID055, HID101, and HID386 had relatively strong intensity of endodermal fluorescence signal, whereas Barke, HID003, HID0069, HID138 and HID357 had relatively weak intensity of endodermal fluorescence (Figure 2). There was variation in the endodermal fluorescence of salt treated root sections relative to the sections from control plants. No obvious differences were observed in the intensity of endodermal fluorescence in Barke, HID055 and HID386 in control relative to salt conditions. HID069 and HID138 had notably stronger endodermal fluorescence in sections from roots that were salt treated relative to the signal in control treatments (Figure 2). HID003 had less intense fluorescent signal in the endodermal cell wall layer of salt treated plants relative to the signal in control plants (Figure 2).

There was variation in the presence of fluorescence signals in the outermost cortex cell layer(s) (Figure 2). This variation depended on the accessions and treatments. No fluorescence was observed under control and salt treatments for Barke, whereas HID069, HID138, and HID357 showed noticeable fluorescence signals in the salt treated plants (Figure 2). For HID003, HID055, HID101 and HID138 clear fluorescent signal was detected for both control and salt treated root sections, indicating the presence of constitutive deposition of suberin, at least under our experimental conditions (Figure 2). In all accessions with an exodermal layer, the layer was composed of one cortical cell layer; no exodermis composed of multiple cell layers was observed in the accessions, developmental stage and conditions tested (Figure 2). In the salt treated conditions HID055, HID101, HID138 and HID386 had a clear fluorescence signal in exodermal cells, which differed from the lack of signal detected for HID069 and HID357 (Figure 2).

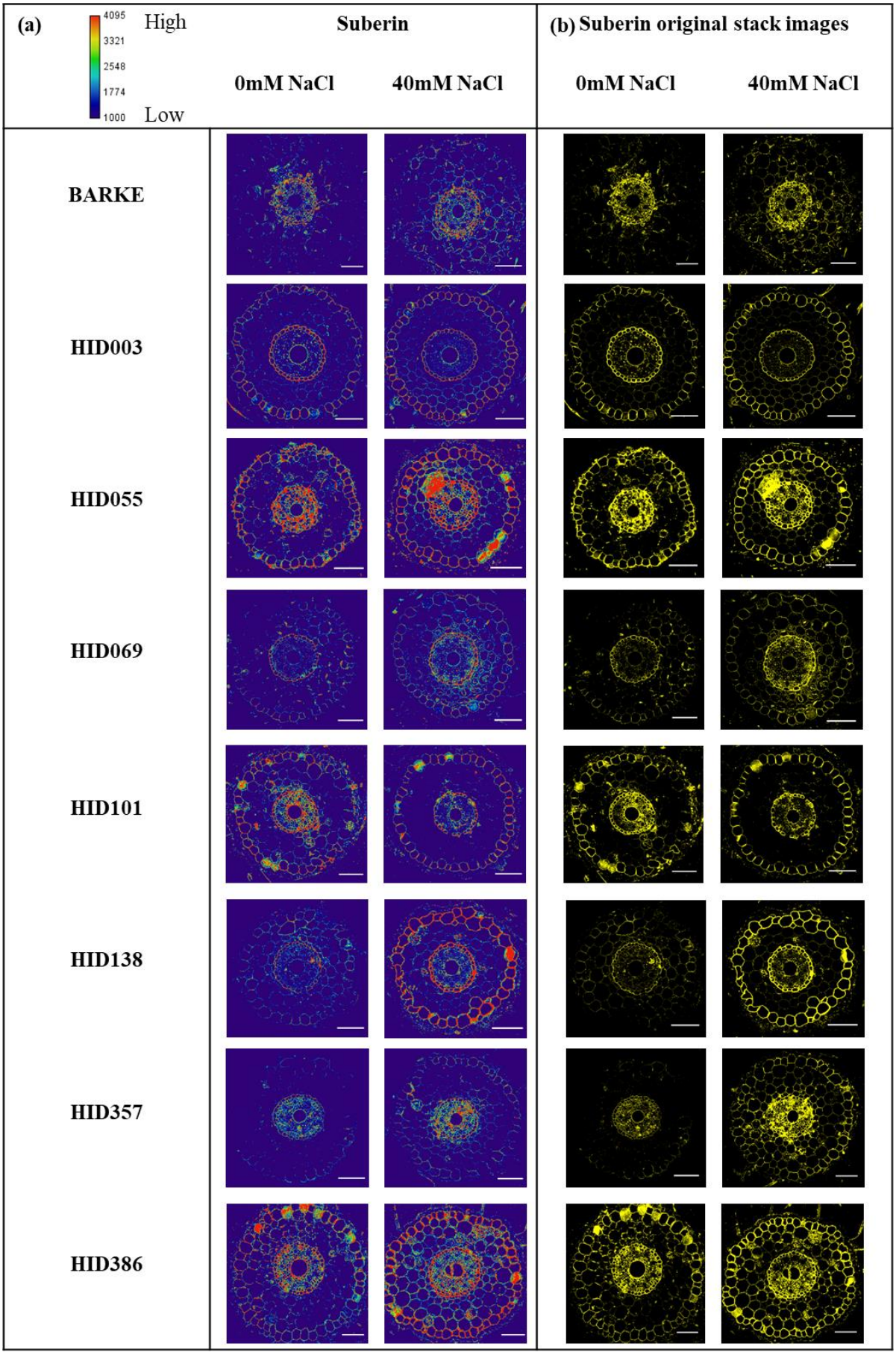
(a)
4095
3321
2548
1774
1000
High
Low
Suberin
0mM NaCl
40mM NaCl
(b) Suberin original stack images
0mM NaCl
40mM NaCl
BARKE
HID003
HID055
HID069
HID101
HID138
HID357
HID386

FIGURE 2 Spatial deposition of suberin in the roots. Spatial deposition of suberin in the longest seminal roots of selected barley accessions grown under control and saline 40mM NaCl treatments for a week; determined using Fluorol Yellow 088 staining. Cross sections of 100µm thickness were made at the maturation zones. Suberin stain signal was obtained by confocal laser scanning microscopy. (a) Stack images of root section with maximum intensity projection visible in a range of colour representing the signal intensity as indicated by the calibration bar on the top left. (b) The original stack images of maximum intensity projection with suberin signal shown in yellow. Scale bars: 100µm.

Variation in the cell-specific patterns of the fluorescence signals were observed in both endodermal and exodermal cell layers in control relative to salt treatments (Figure 2). Accessions such as HID003, HID101, had U-shaped fluorescence signals in the endodermal cell layer, where the open part of the 'U' with narrower fluorescence was facing towards the stele (illustrated in Figure S3 and actual image in Figure S4). In these U-shaped fluorescing endodermal cells, we observed thicker fluorescence signal in the anticlinal walls and in the transverse/tangential section facing the cortex, and narrower fluorescence signal in the transverse section facing the stele (Figure S4). Similarly, we also observed the same U-shaped pattern of fluorescence signals in the exodermal cell layer (Figure S4). The fluorescence signal was thicker in the anticlinal walls of exodermal cells, and in the transverse/tangential section facing outer epidermal cells towards to the other part of the root, but thinner in the transverse/tangential section facing the cortex, towards the inner part of the root (Figure S4). However, there was some variation in these patterns, such as for HID069 and HID357, which both had fluorescence signals in the anticlinal walls but not in the transverse sections (Figure 2). HID138 displayed fluorescence surrounding the entire exodermal cell in roots exposed to the salt treatments (Figure 2).

2.4.3 Intensity and patterns of root lignin-associated staining

Phloroglucinol-HCL staining was used to visualise lignin (Mitra and Loqué, 2014). The cinnamaldehyde end groups of lignin react with phloroglucinol-HCl resulting in a bright red colour that can be observed using the visible light spectrum at a wide-field microscope (Speer, 1987). The intensity of the red stain observed in this study varied between cell types, accessions and treatments. Quantification of the signal is not feasible, due to the lack of an internal control for normalisation. However, staining can be an indicator of the relative deposition of lignin within one section. In all of the accessions, xylem vessels had the greatest intensity of red stain relative to the other cell types in the root sections from both control and salt treatments; and all accessions had lignin deposition in the anticlinal walls of their endodermal cell layers in both control and salt treatments (Figure 3). Lignin staining appeared in the anticlinal walls of additional cortex cell layers consistent with the exodermis, in HID003, HID069, HID101, HID138 and HID386, either in response to salt, or in both conditions (Figure 3).

The elite cultivar Barke lacked any obvious lignin staining in the hypodermal cells in samples from both control and salt treatments, and a similar trend was observed for HID055 and HID357 (Figure 3). Lignin deposition and exodermis formation did appear to be constitutive and was present in both control and saline conditions for HID003, HID069, HID101, HID138 and HID386 (Figure 3). This is consistent with what we observed for suberin deposition except for HID069, which had salt-inducible exodermal suberin. Throughout all experiments, we observed the strongest exodermal lignin staining in HID138 (in salt and control) (Figure 3).

Genotypes	0mM NaCl	40mM NaCl
BARKE	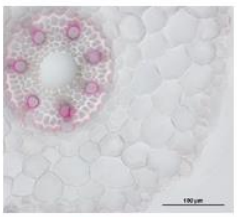	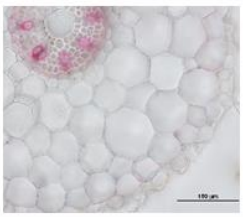
HID003	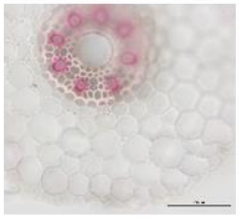	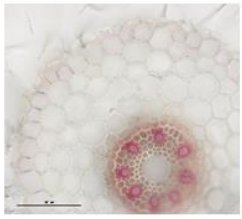
HID055		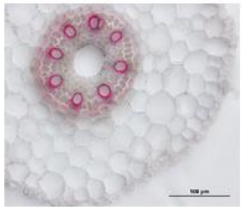
HID069	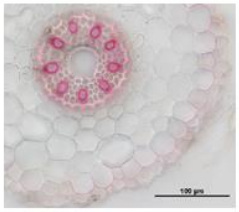	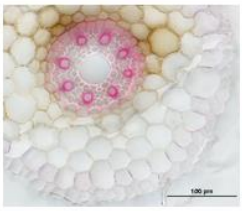
HID101	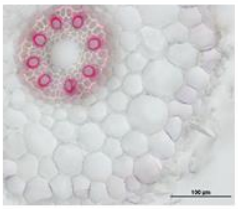	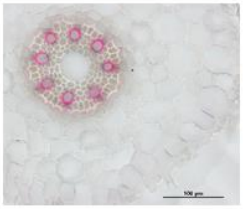
HID138		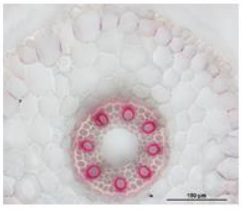
HID357	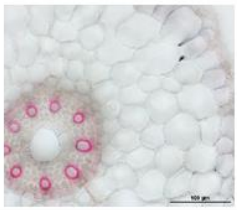	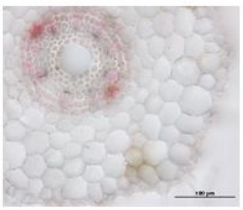
HID386	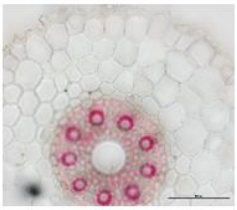	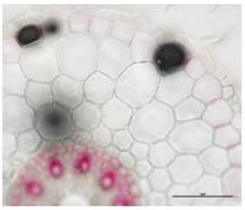

FIGURE 3 Spatial deposition of lignin in the roots. Spatial deposition of lignin in the longest seminal roots of selected barley accessions grown under control and saline 40mM NaCl treatments for a week; determined using Phloroglucinol-Hydrochloric acid. Cross sections were made at the maturation zones. Lignin stain appears in red colour under bright field microscope. Scale bars: 100µm.

2.4.4 Variation in root length and biomass in salt-treated barley seedlings

The phenotypes, in terms of root and shoot biomass accumulation and root length, for these seven wild accessions were compared with Barke, a parent line for the HEB25 NAM population (Maurer et al., 2015) (Figure 4). In the 0 mM additional NaCl conditions the root biomass accumulation of Barke was significantly greater than HID138 and HID357, but Barke's root biomass did not differ to the other five wild accessions (Figure 4a). In the presence of 40 mM NaCl, the root biomass of Barke was less than that of HID003 and significantly greater than HID138 but did not differ to the other wild accessions (Figure 4b). The percentage of root biomass in saline relative to non-saline conditions (40 mM/0 mM NaCl) revealed that the majority of the accessions maintained their growth in the salt treatment conditions relative to control conditions (Figure 4c). In addition, the pattern of the root biomass is quite similar to the total root length (Figure S5).

The longest seminal root of Barke seedlings tended to be shorter relative to the longest seminal root of the wild accessions HID055 and HID101 in both control and saline conditions (Figure 4d, e). The growth rate of seminal root for both HID055 and HID101 was higher compared to Barke (Figure S6a). In saline conditions, HID003, HID069, HID138 and HID357 increased the length of their longest seminal roots relative to the length in control conditions, whereas the other accessions tested did not differ in the length of their longest seminar root in control and salt conditions (Figure 4f).

(a) Root dryweight of one week-old seedlings grown under 0mM NaCl (g)

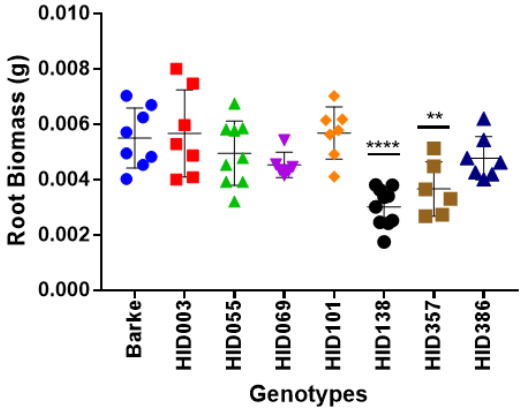

(d) Longest root length of one week-old seedlings grown under 0mM NaCl (cm)

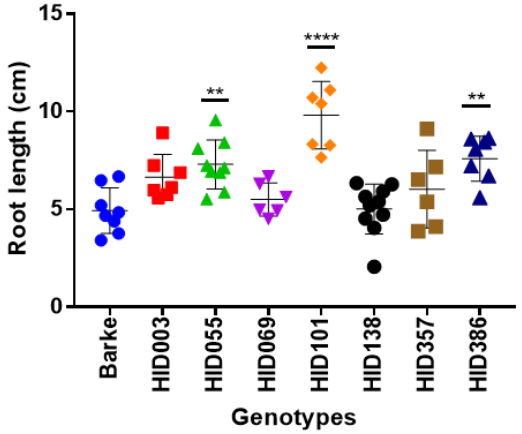

(b) Root dryweight of one week-old seedlings grown under 40mM NaCl (g)

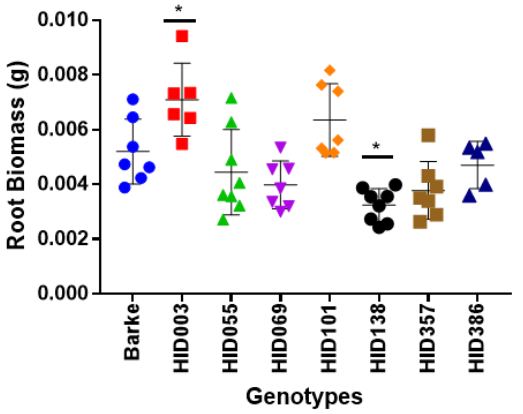

(e) Longest root length of one week-old seedlings grown under 40mM NaCl (cm)

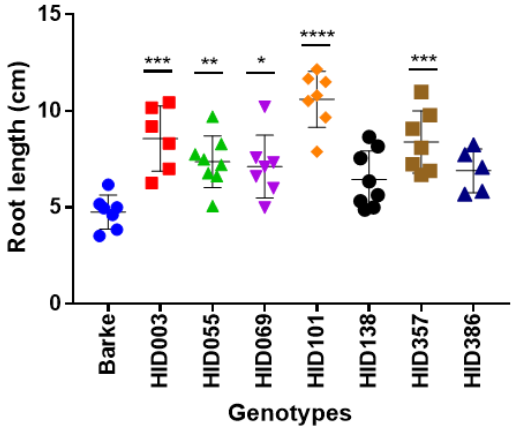

(c) Relative percentage of root biomass under 40mM NaCl (S/C, %)

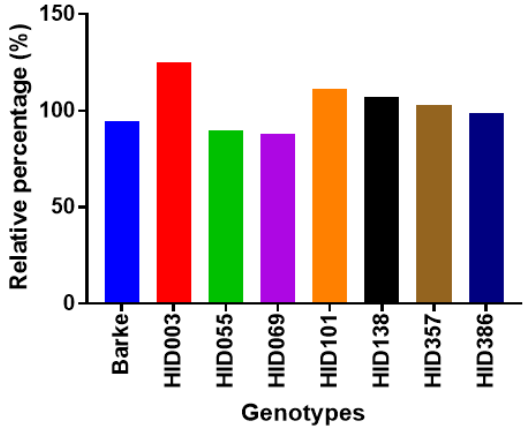

(f) Relative percentage of longest root length under 40mM NaCl (S/C, %)

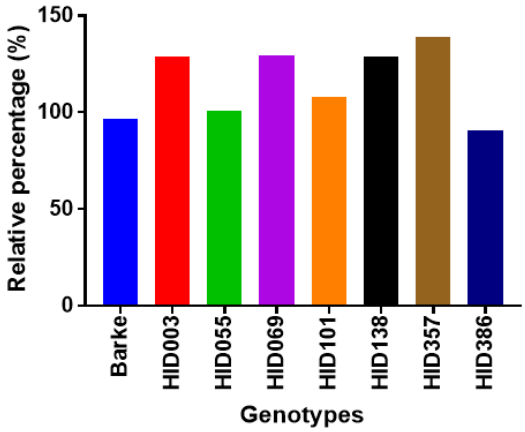

FIGURE 4 Root dry weight and longest seminal root length of one week-old seedlings grown in control (0mM NaCl) and saline (40mM NaCl) conditions. Root dry biomass in (a) control and (b) saline and longest seminal root in (d) control and (e) saline. In figure parts (a), (b), (d) and (e), each HID accession was compared with the elite cultivar (Barke) using one-way ANOVA with Dunnet's multiple comparison test. Data represent individual biological replicates (symbols), means (wide horizontal line) ± SEM (standard error mean) (n = 6-8). ANOVA significant difference $p<0.05$, $p<0.01$, $p<0.001$ and $p<0.0001$ indicated by (*), (**), (***) and (****), respectively. In (c) and (f), the relative percentage of each cultivar in control (C) in relative to saline (S) conditions is shown.

In the control conditions, HID055, HID101 and HID138 accumulated less shoot biomass relative to Barke (Figure S7d). In response to the salt treatment the majority of the accessions, except for HID003, HID101 and HID138, had less shoot biomass compared to the shoot biomass accumulation in control conditions with a 25% reduction in Barke and HID069 and a 10% reduction in HID055, HID357 and HID386 (Figure S7f). The accessions tested did not significantly differ from each other in shoot length either in control or saline conditions, but as expected there were reductions in shoot length in saline relative to control conditions in majority of accession/line (Figure S7a, b, c). The shoot length in salt treated plants, as a proportion of control, revealed that Barke and HID386 had a 15% reduction; and HID003, HID055 and HID069 had less than 10% reduction in shoot length (Figure S7c). Whereas HID101 and HID357 had 10% longer shoot length in salt treated plants relative to the control plants, and HID138 had 20% longer shoots when salt treated relative to the control (Figure S7c).

2.4.5 Analysis of root and shoot ion accumulation in seedlings subjected to control and salt treatments

In general, the accumulation of root Na^+ and K^+ increased in response to saline treatments in the majority of the accessions (Figure 5c, f). In all accessions, there was approximately a two-fold greater accumulation of root Na^+ under saline conditions relative to control conditions (Figure 5c). In comparison to Barke, all of the selected wild barley accessions had relatively low root Na^+ accumulation, under both control and saline conditions (Figure 5a, b). HID138 had significantly higher root K^+ compared to Barke under both treatments, and is the only accession with a significant difference to Barke under salt treatment (Figure 5d, e). Comparison of each accession under control and saline conditions revealed that HID357 was the only accession that did not show greater root K^+ accumulation in saline relative to control conditions (Figure 5f). The accessions that most notably accumulated more K^+ in saline relative to control conditions were Barke, HID003 and HID138; these accessions had about 1.5-fold greater root K^+ accumulation in saline conditions (Figure 5f). Comparison of the root and shoot Na^+:K^+ ratios in each accession/line, and their relative difference in control and saline conditions, revealed that in roots, HID003 was the only accession that had no significant difference in root Na^+:K^+ ratio relative to Barke under control conditions (Figure 5g). In saline conditions HID003 and HID357 had no significant difference in root Na^+:K^+ ratio in roots relative to Barke (Figure 5h).

The Na^+ and K^+ accumulation in the shoots of the wild barley accessions differed. HID069 accumulated significantly less shoot Na^+ compared to Barke under both control and salt conditions, and accumulated less shoot Na^+ in saline conditions (Figure S9a, b, c). HID101 had considerably greater Na^+ accumulation than Barke under control conditions, but interestingly did not show greater accumulation of Na^+ in the salt treatment conditions (Figure S9a, b, c). Relative to shoot Na^+ content values, the shoot K^+ content values were more

homogenous within the accessions tested (Figure S9d, e, f). There was a significant difference in shoot K^+ between the wild barley accessions and Barke under control conditions, with the exception of the accession HID069 which did not differ from Barke (Figure S9d). Under salt conditions, this pattern was not observed, instead HID055 and HID386 were the only two accessions that had less shoot K^+ accumulation compared to Barke (Figure S9d, e). Comparison of the shoot Na^+: K^+ ratio revealed differences between the accessions. HID055 and HID101 both had greater shoot Na^+:K^+ ratios under control conditions compared to Barke, which resulted from HID101 having more Na^+ but not less K^+ than Barke, whereas HID055 had similar Na^+ and less K^+ (Figure S9g). No significant differences in the Na^+:K^+ ratio between Barke and any of other wild barley accessions was observed (Figure S9g, h), and the values for the Na^+:K^+ ratios followed a similar pattern as the Na^+ accumulation values (Figure S9c, i). Interestingly, measured ion accumulation values in all biological replicates of accession HID069 exhibited the least variation relative to values for the other accessions, indicating that ion accumulation may be tightly regulated in this accession (Figure S9).

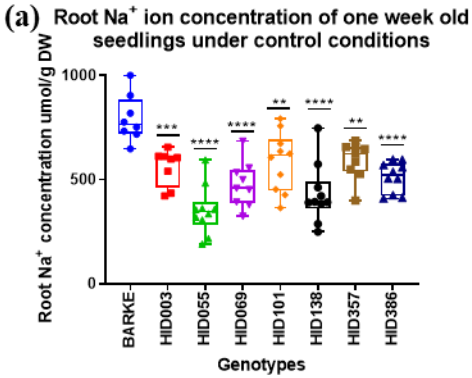
(a) Root Na+ ion concentration of one week old seedlings under control conditions
Root Na+ concentration umol/g DW
1000
500
0
BARKE
HID003
HID055
HID069
HID101
HID138
HID357
HID386
Genotypes

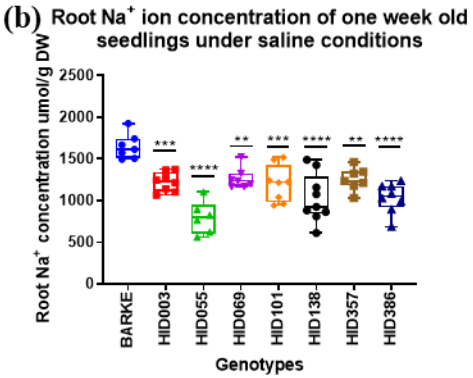
(b) Root Na+ ion concentration of one week old seedlings under saline conditions
Root Na+ concentration umol/g DW
2500
2000
1500
1000
500
0
BARKE
HID003
HID055
HID069
HID101
HID138
HID357
HID386
Genotypes

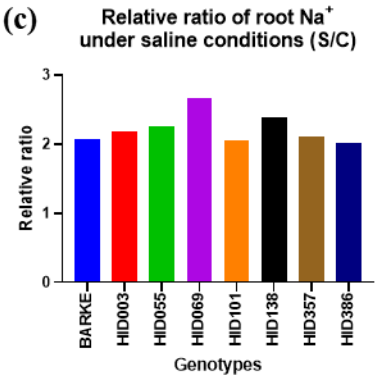
(c) Relative ratio of root Na+ under saline conditions (S/C)
Relative ratio
3
2
1
0
BARKE
HID003
HID055
HID069
HID101
HID138
HID357
HID386
Genotypes

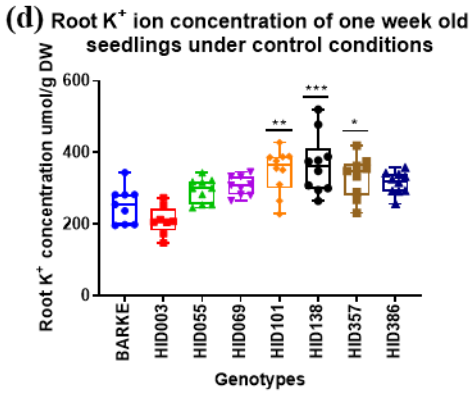
(d) Root K+ ion concentration of one week old seedlings under control conditions
Root K+ concentration umol/g DW
600
400
200
0
BARKE
HID003
HID055
HID069
HID101
HID138
HID357
HID386
Genotypes

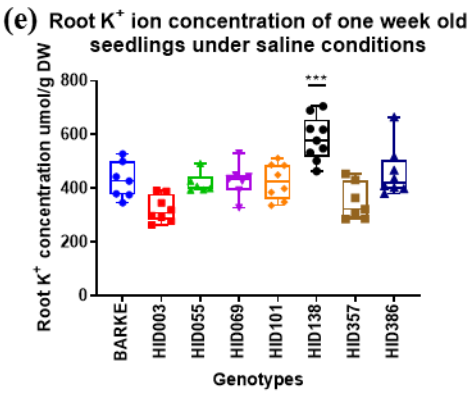
(e) Root K+ ion concentration of one week old seedlings under saline conditions
Root K+ concentration umol/g DW
800
600
400
200
0
BARKE
HID003
HID055
HID069
HID101
HID138
HID357
HID386
Genotypes

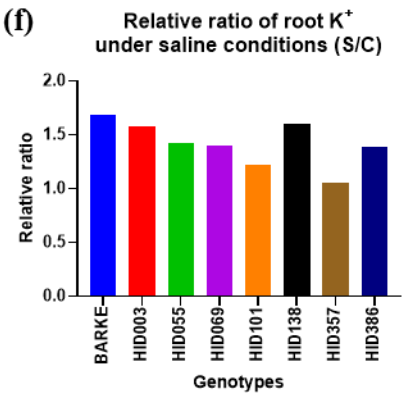
(f) Relative ratio of root K+ under saline conditions (S/C)
Relative ratio
2.0
1.5
1.0
0.5
0.0
BARKE
HID003
HID055
HID069
HID101
HID138
HID357
HID386
Genotypes

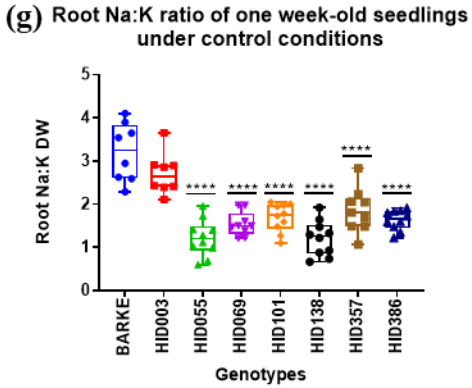
(g) Root Na:K ratio of one week-old seedlings under control conditions
Root Na:K DW
5
4
3
2
1
0
BARKE
HID003
HID055
HID069
HID101
HID138
HID357
HID386
Genotypes

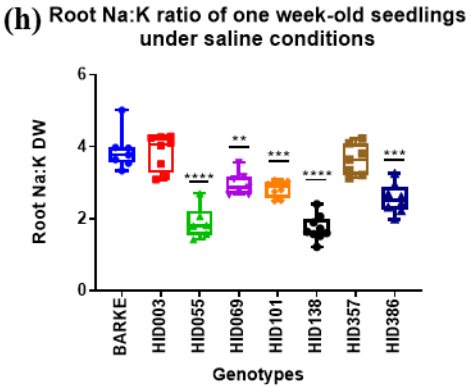
(h) Root Na:K ratio of one week-old seedlings under saline conditions
Root Na:K DW
6
4
2
0
BARKE
HID003
HID055
HID069
HID101
HID138
HID357
HID386
Genotypes

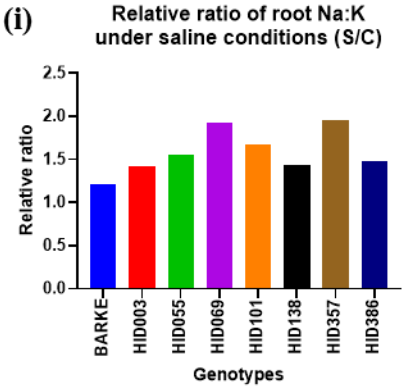
(i) Relative ratio of root Na:K under saline conditions (S/C)
Relative ratio
2.5
2.0
1.5
1.0
0.5
0.0
BARKE
HID003
HID055
HID069
HID101
HID138
HID357
HID386
Genotypes

FIGURE 5 Root ion accumulation in HID accessions of interest which were selected based on the screening of root apoplastic barrier deposition. The accumulation of root Na^+ (a), K^+ (d) and Na^+:K^+ ratio (g) under control (0mM NaCl added) and root Na^+ (b), K^+ (e) and Na^+:K^+ ratio (h) under 40mM NaCl of one-week old seedlings. The ratio of the mean of root Na^+ (c), K^+ (f) and Na^+:K^+ ratio (i) of salt treated plants, S relative to the control plants, C. The amounts of both Na^+ and K^+ were normalised to the tissue dry weight (DW). Data points represent individual biological replicates (symbols) (n=8-10), horizontal line inside the box (median), ends of boxes (lower and upper quartiles), and the whiskers (lowest and highest values). For figures (a), (b), (d), (e), (g) and (h), each wild barley accession was compared to commercial cultivar, Barke using one-way ANOVA with Dunnet's multiple comparison test. ANOVA significant difference $p<0.05$, $p<0.01$, $p<0.001$ and $p<0.0001$ indicated by (*), (**), (***) and (****) respecti

2.4.6 O_2 consumption in control and salt treated barley roots

Whole root O_2 consumption was measured using a Q2 meter, and root samples from plants grown under control and saline conditions. Rate of O_2 consumption in Barke was greater than all the wild barley accessions under control conditions (Figure 6a). In saline conditions, there were no significant differences in the rate of whole root O_2 consumption between Barke and the majority of the accessions (Figure 6b). HID138 was the only accession that had less whole root O_2 consumption compared to Barke in the salt conditions (Figure 6b). The rate of O_2 consumption in saline conditions relative to the control conditions for each accession revealed that HID003 was the only accession that had a similar rate of O_2 consumption under both conditions (Figure 6d). All other accessions had less rate of O_2 consumption in saline conditions relative to control conditions, for example HID138 rate of O_2 consumption in saline conditions was 0.6 the magnitude of consumption in control conditions (Figure 6d). In the other accessions, relative values of rate of O_2 consumption in saline as a proportion of control conditions ranged between approximately 0.1 (HID069) and 0.25 (Barke and HID101) (Figure 6d).

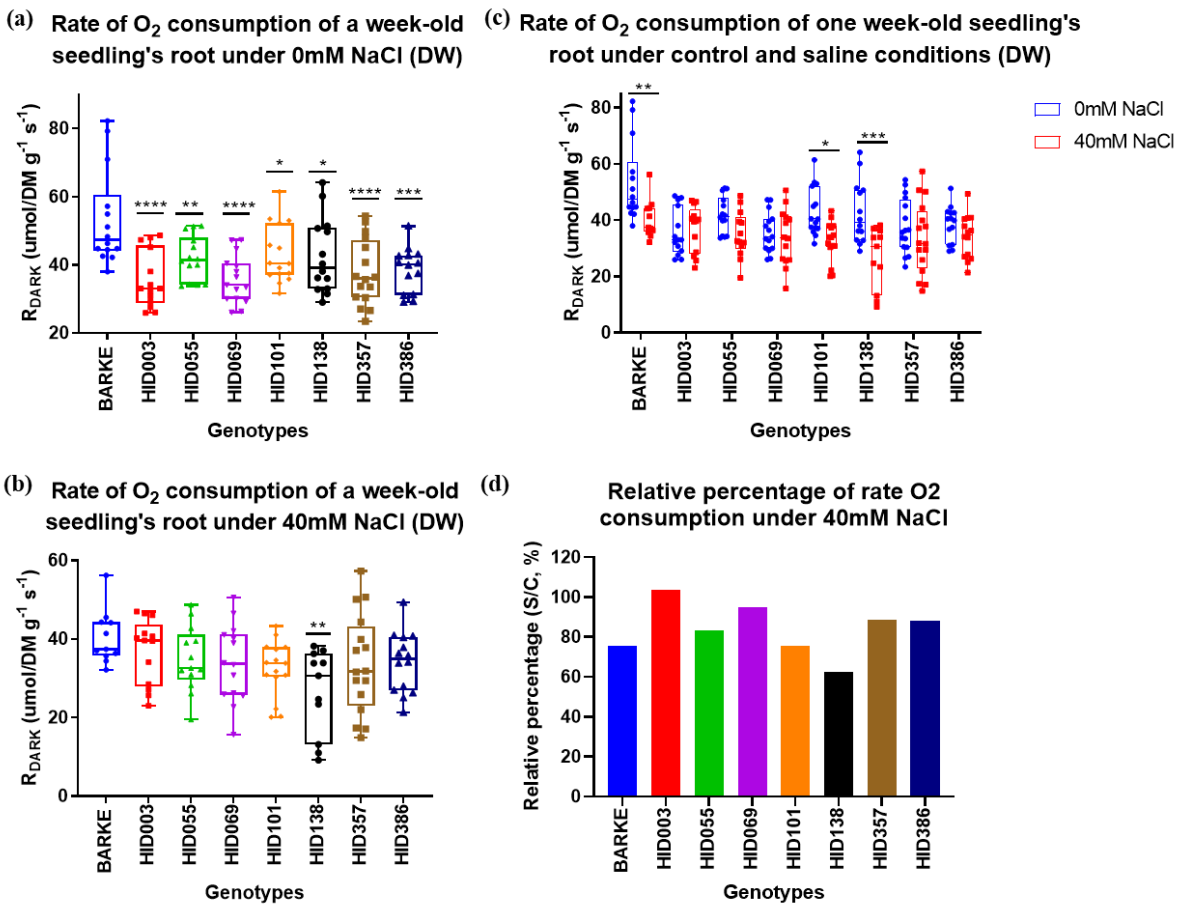

FIGURE 6 Rate of whole root O_2 consumption of one week-old seedlings. Rate of O_2 consumption of seedlings grown under (a) control (0mM NaCl) or (b) saline conditions (40mM NaCl), and (c) in both conditions blue = 0mM and red = 40mM NACl. Rates of respiration were measured in detached root samples over a period of two hours using high throughput Q2 system and normalised to root dry weight. In (a) and (b), rates of O_2 consumption for each wild accession was compared with the commercial barley line, Barke using one-way ANOVA, Dunnet's multiple comparison test. In (c), data for each genotype were compared between the treatments using Sidak's multiple comparison test. For a, b and c, the middle horizontal line is the median. Data points represent individual roots from different biological replicates (n = 6-10). ANOVA significant difference $p<0.05$, $p<0.01$, $p<0.001$ and $p<0.0001$ indicated by (*), (**), (***) and (****) respectively. Dry mass (DM). (d) The percentage mean of rates of O_2 consumption under saline conditions relative to the control is shown.

2.4.7 Principal Component Analysis

PCA was applied to transform the root ion accumulation, O^2 consumption and accumulated root biomass data from plants grown in both control and saline conditions. The analysis revealed a separation between the commercial barley Barke and wild barley accessions (Figure S10). For the wild barley accessions, the majority of the accessions including HID069, HID101, HID357 and HID386 were closely clustered under control and saline conditions. Barke, HID138 and HID003 had a clear separation in the dimensions included in the PCA. HID138 tended to have higher root K^+ accumulation but low Na^+, low O^2 consumption as well as low accumulated biomass compared to Barke in both control and saline conditions. HID003 accumulated more biomass and had higher O^2 consumption compared to HID138 (Figure S10).

2.4.8 Suberin-associated fluorescence detection following root hormone treatments

Hormone treatments can influence suberin deposition, for example in Arabidopsis ABA treatment led to enhanced suberin deposition, and treatment with the ethylene precursor ACC was led to reduced suberin deposition (Barberon et al., 2016). Here, we tested whether similar trends could be observed in barley, and whether different trends in suberin-associated fluorescence would be observed in the Barke relative to the wild barley accessions. Barke and wild barley accessions of interest were treated with applications of 100µM ACC or 5µM ABA and the root suberin-associated fluorescence patterns were compared to the patterns in control conditions. Similar to trends observed in Arabidopsis, the treatments with 5µM ABA enhanced suberin deposition (Figure 7). We observed that ABA-treatment particularly enhanced exodermal suberin deposition, which was not observed in Arabidopsis, as Arabidopsis lacks an exodermis (Figure 7). Moreover, in the ABA treated samples, there appeared to be multiple cortical cell layers where fluorescence was observed for HID003 and HID138 below the epidermis (Figure 7). The intensity of endodermal fluorescence signal was greater in the 5µM ABA treated plants relative to the control plants, but there was not an obvious difference

relative to the salt treated plants (Figure 7). For HID003 there were endodermal cells lacking suberin-associated fluoresence, but in the ABA treated samples all the endodermal cells had suberin-associated fluoresence. All of the accessions except for Barke had fluorescence in their entire endodermal cells when treated with ABA (Figure 7).

In general there were no obvious differences in fluoresence patterns for the 100µM ACC treated root samples relative to controls (Figure 7). It is possible that there may have been a trend where more endodermal cells in control samples had suberin-associated fluoresence than the number of endodermal cells with suberin-associated fluoresence in the ACC treated samples for HID003, but additional sections covering a greater length along the root would be needed to gain sufficient cell numbers to resolve whether there were quantitative differences or not (Figure 7). ACC treatments did not seem to impact the fluorescent signal in HID138. This accession showed a constitutive strong formation of an exodermis in all our tested conditions, which did not disappear under ACC treatment (Figure 7).

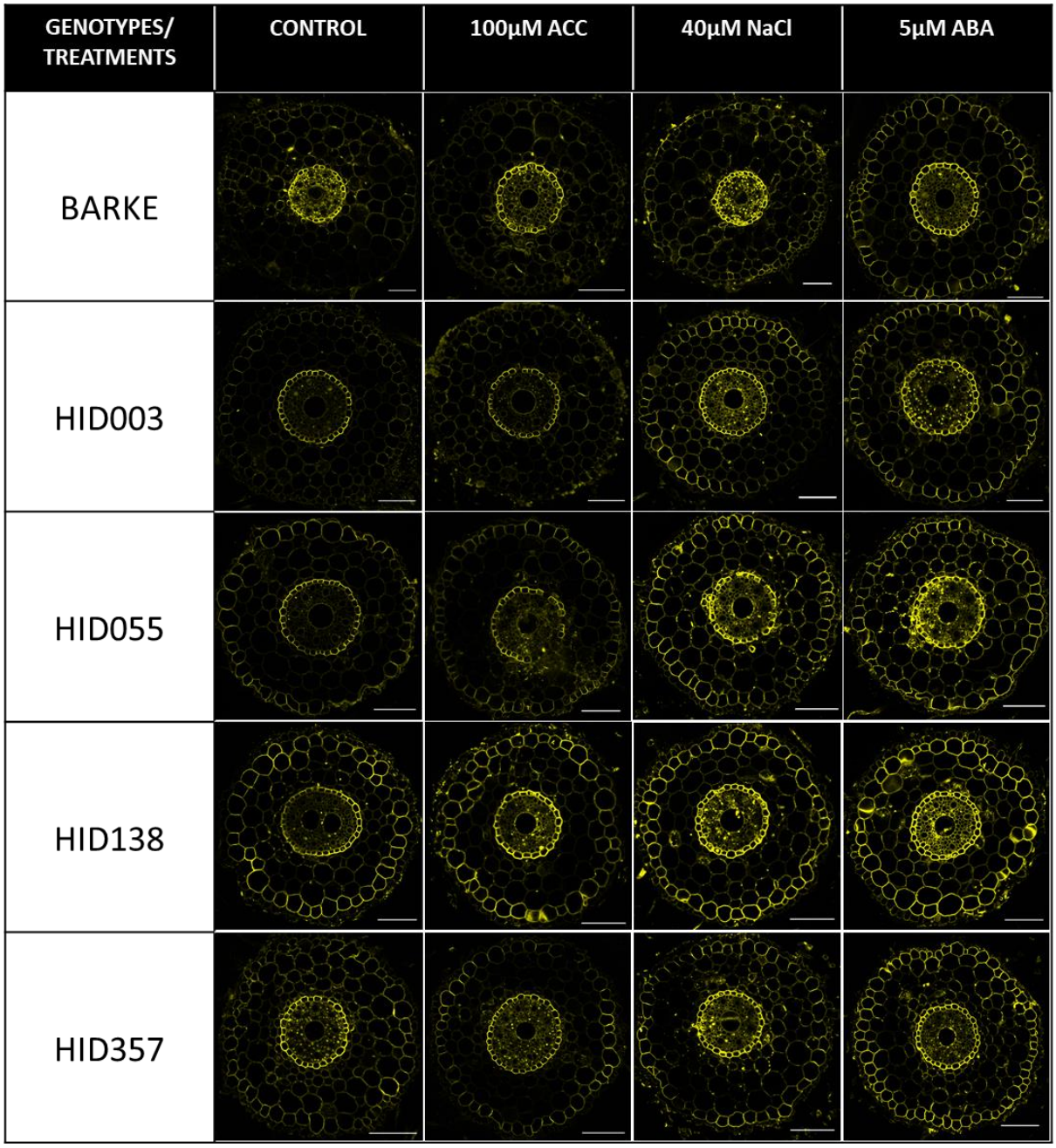

FIGURE 7 Spatial deposition of suberin in the longest seminal roots of Barke and selected wild barley accessions grown under control, 100µM ACC, 40mM NaCl, and 5 µM ABA treatments for one week. Cross sections were made at the maturation zones. Suberin stain signal, observed by Fluorol Yellow 088 staining followed by confocal laser scanning microscopy imaging, is shown in yellow. Scale bars: 100µm.

2.5 Discussion

2.5.1 Phenotypic variation in commercial and wild barley accessions

Seminal roots in particular play an important role in the overall water uptake for seedlings, therefore their development is key in the plant response to abiotic stresses such as salinity (Knipfer and Fricke, 2011). Here, we observed that the roots of the commercial barley line, Barke, were shorter than the wild barley accessions (Figure 4d, e). The observation that commercial barley may tend to have roots that are shorter and less vigorous compared to those of several wild barley accessions has been made previously (Kreszies et al., 2019b). Root length is likely to be a factor that is important in adaptation to different environments; such as the arid environments where the wild barley accessions originated (Badr et al., 2000; Maurer et al., 2015; Kreszies et al., 2019b). In arid and saline conditions, it may have been an advantage to have longer seminal roots, which could be a reason why the accessions HID003, HID069 and HID357 developed longer seminal roots in the salt-treated conditions relative to the seminal root length measured in control conditions. These accessions might have adapted to respond to osmotic stress by prioritising growing longer roots to escape a salty soil layer or explore deeper for useful resources. This strategy could be a beneficial trait that we could introduce into modern cereal cultivars to tailor them for challenging growing environments.

It is easier to select for above ground traits than below ground traits during plant breeding because above ground traits are visible and below ground traits are hidden within the soil. Traits such as grain yield and grain filling have been a priority. Recent strategies to investigate below ground traits involve approaches that enable visualisation of root system architecture, and consideration is being given to the costs and benefits of different root structures in different environmental conditions. Larger root systems use more carbon, potentially leaving less carbon available for partitioning into grain filling, but larger root systems have the potential to access more water and nutrients. Breeding for higher grain yield

in favourable environments could have inadvertently led to selection for smaller root systems where resources were prioritised for above ground tissues and subsequently remobilised for grain filling. Presumably, less carbon was allocated for the development and growth of roots in Barke relative to the carbon allocated to roots in the wild barley accessions with larger root systems than Barke. However, in response to saline conditions, Barke generated 30% less shoot biomass than the shoot biomass produced in control conditions; whereas other wild barley accessions such as HID003, HID101, and HID138 were better able to maintain shoot biomass in the saline conditions (Figure S7f). Selective breeding for yield could have contributed to the loss of salinity and osmotic stress tolerance in modern barley relative to ancestral wild barley accessions (Koevoets et al., 2016). Previous studies have proposed that longer roots systems are beneficial to plants in relation to supporting plant productivity both under favourable conditions and in saline or water-limited environments (Koevoets et al., 2016). Further research is needed to map out the optimal root system size and structure for barley in dry and saline soils.

2.5.2 Exploring associations between apoplastic barriers, ion accumulation and O_2 consumption

Variation in the patterns of suberin-associated fluorescence in both endodermal and exodermal cell walls was observed in the 25 wild barley accessions and Barke. The imaging of Fluorol Yellow 088 fluorescence revealed that suberin deposits were thicker in the anticlinal walls and outer tangential walls compared to the inner tangential walls, see Figure S4 and Figure S3 illustration. Previous characterisation of suberin in the roots of potato *(Solanum tuberosum)* and cotton (*Gossypium hirsutum* L.) revealed similar suberisation patterns in the equivalent cell walls (Reinhardt and Rost, 1995; Landgraf et al., 2014). Thick suberin deposits in the anticlinal walls and outer tangential walls of the endodermal cell layer may have a role as an efficient barrier against the influx of solutes into the stele. This type of barrier may restrict

unregulated apoplastic fluxes of solutes across the cell wall matrix, such that solute flux becomes limited to pathways where membrane transport steps can impose selection on the solutes being transported (Baxter et al., 2009).

In the present study Barke lacked exodermal cell layer suberin deposition in accordance with a previous study in a commercial cultivar, "Golf" (Ranathunge et al., 2017) (Figure 2). Within the wild barley accessions, exodermal suberin deposition was stress-inducible in HID069, HID138 and HID357 or constitutive in HID003, HID055, HID101 and HID386 (Figure 2). Suberin deposition in the exodermal layer forms a hydrophobic surface around the cell that can restrict fluxes of water and solutes (Zimmermann and Steudle, 1998; Zimmermann et al., 2000). Since suberin deposition in the outermost cortical cell layer was absent in Barke in response to saline conditions presumably water and K^+ loss and entry of Na^+ across the plasma membrane could occur to a greater magnitude in Barke relative to accessions that deposit suberin in these cells in response to saline conditions. There were trends observed in the apoplastic barrier deposition and ion accumulation data trends. Each of the wild barley accessions had significantly lower root Na^+ accumulation relative to Barke under saline conditions (Figure 5b). However, it is not clear whether the difference in exodermal suberin influenced the variation in root Na^+ accumulation observed (Figure 5a, b, c). A previous study showed that an Arabidopsis *horst* mutant, which had about 33 % less suberin monomer than wild-type, had greater permeability of NaCl into the roots compared to the wildtype (Ranathunge and Schreiber, 2011). It is also important to note that our investigation of suberin deposition by analysis Fluorol Yellow 088 fluorescence is qualitative rather than quantitative, but despite this limitation it was possible to identify differences in relation to presence or absence of fluorescence in specific cells of the accessions tested. The fluorescence observed in the roots of HID055 and HID138 appeared to be of greater intensity than that of the other accessions (Figure 2), and we also observed that these two accessions had a significantly lower

root Na^+:K^+ ratio compared to Barke (Figure 5g, h). The deposition of suberin in the outermost cortical cell layer of these diverse accessions could have potentially limited Na^+ flux across the plasma membrane into exodermal cells.

The majority of the wild barley accessions tested, with the exception of HID055 and HID357, had some degree of constitutive lignin deposition in the anticlinal walls of their exodermal cell layer, indicating that ancestral barley might have had an exodermis, which was lost during domestication (Krishnamurthy et al., 2011). HID138 tended to deposit more lignin in its exodermal anticlinal walls than the other accessions tested in this study (Figure 3), which indicates that this accession may be better able to restrict apoplastic solute flow relative to the other accessions at the stage of seedling growth. Previous studies revealed that the Casparian strips in maize, where the impermeable component is lignin, increased in thickness with an increase in the accumulation of the salt treatment applied (Karahara et al., 2004). The authors postulated that the radial width of the Casparian strip may be related to the effectiveness of the strip as a barrier. In comparison to salt treated Barke roots, the salt treated HID138 roots had significantly higher root K^+ accumulation whereas HID055 had significantly less root K^+ accumulation compared to Barke (Figure 5d, e). HID055 and HID138 had similar suberisation trends in their exodermal cells but differed in exodermal lignin deposition, with HID138 depositing more lignin in the exodermal cells than HID055 (Figure 3). One possible explanation for this is that HID138 retained more K^+ in the roots than Barke or HID055. Salt treatments generally cause a reduction in root K^+ uptake (Maathuis and Amtmann, 1999; Chen et al., 2007; Cuin et al., 2008). It is possible that the thick lignin deposits in HID138 exodermal cell walls could have reduced K^+ loss to the external environment. Previous analysis of an Arabidopsis Casparian strip mutant, *schengen3* (*sgn3*), revealed that K^+ homeostasis is disrupted in these mutants relative to wildtype controls (Pfister et al., 2014). Despite having similar suberin deposition to the wildtype, these mutants had less root K^+ (Pfister et al., 2014).

The authors suggest that the mutant lacking an intact Casparian strip, which mainly consists of lignin, continuously leaked K^+ out of the root. This indicates that lignin is likely to play a crucial role in limiting K^+ loss in the roots. However, there are likely to be benefits and disadvantages to depositing lignin in root cells. One disadvantage is that significant lignin deposition could limit the uptake of essential nutrients required for growth. Indeed, the root biomass for HID138 revealed that this accession accumulated less biomass than the other accessions tested in both control and saline conditions (Figure 4a, b). Alternatively, the smaller growth of HID138 compared to the other accessions could be due to differences in radial water permeability and associated hydraulic conductivity of the roots. Further research is needed to extrapolate the extent to which variation in exodermal lignin influences nutrient and water transport in barley roots to determine how much exodermal lignin deposition is optimal in different environmental conditions.

Plant roots gain the energy they require for metabolism and active ion transport from the process of respiration (Jacoby et al., 2011; Jacoby et al., 2013). During respiration, roots convert sugar into ATP, a process that consumes O_2. By measuring root O_2, we can assess root respiration. Salinity can cause a greater demand for energy to fuel the processes required for adapting to this osmotic stress, and consequently root respiratory O_2 consumption would be expected to be greater in saline conditions relative to control conditions (Bloom and Epstein, 1984). In response to salt stress, some plants deploy adaptive strategies to maintain growth and metabolic functions; these may include the active efflux of Na^+ out of cells and/or the formation of enhanced diffusion barriers. Different quantities of energy are likely to be required for salt stress adaptation depending on which strategies plants use in their responses to salt stress. These different strategies might also differ in their relative energy efficiency, particularly depending on whether the plant is responding to a short-term or longer-term change in the level of salt stress imposed by the soil environment. The respiration measurements in this study

revealed that the barley accessions lacking in apoplastic barriers had higher root O_2 consumption values relative to the accessions with apoplastic barriers (Figure 6a, b).

Maintaining a low leaf Na^+:K^+ ratio is key in tolerating salinity (Maathuis and Amtmann, 1999). When excess Na^+ accumulates in the shoot, it can be detrimental for photosynthetic processes, osmotic adjustment and other metabolic processes (Maathuis and Amtmann, 1999). One possible strategy to control the Na^+:K^+ ratio is to limit Na^+ accumulation by using membrane transporters to efflux Na^+ from the root via active transport, which requires energy (Munns et al., 2020). In plants with no exodermis, salt can enter the apoplast of the root cortex unrestricted. To maintain a low Na^+:K^+ ratio, plants may need to constantly pump salt out of the cortex cells to the outer part of the root, and back into the external environment; and this would require constant use of energy (Munns et al., 2020). The energy expenditure to actively efflux Na^+ out of the root in saline conditions increases with higher external salinity accumulation, and expending energy on this process results in less energy for plant growth (Munns and Gilliham, 2015).

Another strategy to limit Na^+ accumulation might be to invest energy into the process of building solute barriers in the root. Formation of an exodermal barrier and re-enforcement of endodermal barriers could potentially limit the amount of salt that reaches the cortex cells via the apoplasm, and then presumably less salt could enter the stele and reach the leaves. We are interested in whether or not deposition of apoplastic barriers in roots in saline conditions means that less energy would be needed to pump Na^+ of the roots. Salt stress also has the potential to cause root water loss. There would be an osmotic driving force for water loss from roots due to the differences in osmotic potential between the root and external environment in saline conditions, which would change if there was an increasing concentration of salt in the external environment. Re-enforcement of exodermal apoplastic barriers and suberisation in the cortex cells might prevent water loss from the cortex to the external environment when external

salinity increases. Increasing the accumulation of compatible solutes in roots, such as proline, is another way for plants to manipulate the osmotic potential of the root relative to the soil environment (Ueda et al., 2007; Patterson et al., 2009; Zhu et al., 2020). We are interested in whether it is more economical, in terms of root energy costs, to modify apoplastic barriers relative to increasing root compatible solute content and increasing salt efflux via membrane transport processes.

Barke did not invest in the reinforcement of apopastic barriers in seedling roots to the same extent as the wild barley accessions tested, and Barke had a higher root O_2 consumption under both control and saline conditions than the wild barley accessions (Figure 6a and b). Barke had a relatively low leaf Na^+:K^+ ratio (Figure S9g, h) but a high root Na^+:K^+ ratio (Figure 5g, h) in both control and saline conditions compared to the wild barley. In saline conditions, Barke accumulated a similar amount of leaf Na^+ to the other wild barley accessions (Figure S9), and this raises the possibility that Barke might respond to increasing salinity by more efflux of Na^+ out of the roots than the wild barley accessions. However, further experiments are needed to test this hypothesis, such as measuring root ion efflux. If Barke pumped out more Na^+ then presumably more energy would be required for this work, and therefore more O_2 might be consumed compared to the wild barley accessions. Further research is also needed to test whether the regulation of key membrane transporters known to influence root and root to shoot sodium transport, such as HvHKT1;5 (Amarasinghe et al., 2019; Houston et al., 2020), SOS1 and other ion transporters (El Mahi et al., 2019), differ in the accessions tested (Chen et al., 2007). This would help towards determining whether the wild barley accessions differ in their strategies to manage root Na^+ transport relative to Barke.

Within the selected wild barley accessions, we observed that HID069 had a relatively low shoot Na^+:K^+ ratio compared to the other accessions in both control and saline conditions (Figure S9g, h). However, in contrast to Barke, HID069 also had a low root Na^+:K^+ ratio under

control and salt conditions (Figure 5g, h). HID069 had constitutive exodermal lignin deposition and enhanced exodermal suberin deposition in response to saline treatments relative to many of the other accessions tested. Together, these results indicate that HID069 and Barke use different strategies to manage Na^+ transport and accumulation.

The rate of respiration detected in the roots of the accessions tested did not differ under control and saline conditions with the exception of Barke, HID101 and HID138 (Figure 6c). HID138 had a lower respiration under saline conditions relative to control conditions (Figure 6d). There are few possible explanations for the lower O_2 consumption under saline conditions. HID138 formed notable lignin and suberin deposits in its exodermal cell walls. These barriers might have been effective to prevent the loss of K^+ and limit Na^+ intake into the roots. Therefore, potentially less ATP might have been required to pump Na^+ out of the root and for re-uptake of K^+. It is also possible that the exodermal barrier may have prevented O_2 from entering the roots, which could have confounded the data. Previous studies have reported enhanced exodermal suberisation and lignification in rice and *H. marinum* grown in stagnant, O_2-limited environments helped to limit radial O_2 loss to the environments (Kotula et al., 2009b; Kotula et al., 2014). However, the chemical and physical properties in lignin and suberin in the cell walls could be different depending on which types of stresses roots were exposed to, and this would be likely to contribute to the differences in the permeability of water, solutes and gases. For example, in rice Krishnamurthy et al. (2011) reported that salinity-enhanced suberisation in the roots limited the water permeability while Ranathunge et al. (2011a) showed that hypoxia-enhanced suberisation had the opposite effect. HID138 is generally a slow growing accession (Figure S6a) and has a lower biomass accumulation relative to the other accessions tested (Figure 4, Figure S7). Due to the slow growth of HID138, it is possible that less ATP from respiration is needed for growth. Further research is needed to determine whether it is relevant to compare O_2 consumption in the roots of accessions with

significantly different apoplastic barriers or whether these barriers can confound measurements of O_2 consumption.

We conclude that there is genetic variation within the wild barley accessions that influences the deposition of exodermal diffusion barriers. Differences in these barriers in the wild barley accessions were shown to be inducible by salt or constitutive, to vary relative to suberin and/or lignin abundance, and to differ in spatial and temporal deposition. The root ion accumulation data and O_2 consumption rates indicated that there was also phenotypic variation in the accessions tested for these traits that is likely to contribute to the differences in salinity tolerance previously reported (Saade et al., 2016), and are likely to impact the relative energy efficiency of these accessions. The wild barley accessions identified in this study could be used in future research to determine whether significant lignin deposition in the exodermis limits rapid root growth, and whether increased suberin deposition in exodermal cell walls alters shoot and root Na^+ accumulation. The wild barley accessions we utilised are genetically diverse, and a range of factors are likely to have contributed to the differences in root phenotypes that we observed (Saade et al., 2016). Therefore, the use of sub-sets of material to generate recombinant inbred lines that retain variation in the root barrier traits is needed to create material that can be used to narrow down the loci influencing the root barrier traits of interest.

2.5.3 Treatments with abscisic acid (ABA) and the ethylene precursor, 1-aminocyclopropane-1-carboxylic acid (ACC) triggered different trends in suberin deposition

Barley seedlings treated with ABA had greater suberisation-associated fluorescence in the roots of all of the accessions tested relative to the seedlings grown in control conditions (Figure 7). This is consistent with observations from a previous study testing the influence of ABA treatments on suberin deposition in Arabidopsis roots (Barberon et al., 2016). We

observed that in barley roots, the ABA treatment caused multiple layers of cortex cells to accumulate suberin, whereas in the salt treated plants only a single layer of cells accumulated notable suberin and these particular cells were in the outermost cortical cell layer (Figure 7). In a previous study in maize, it was reported that salt treatment (100mM NaCl) caused a multiseriate suberisation ranging from several layers to an entire cell layer, whereas an osmotic stress (20% PEG) caused only limited deposition in the layer below the epidermis (Shen et al., 2015). This shows that there might have been differences in the levels of stress imposed that caused different response in apoplastic barrier formation. In our case, 40mM NaCl might not cause so much stress compared to those treated with 5µM ABA. A qualitative trend, where fewer passage cells in the ABA treated plants relative to control was observed, but an alternative approach is required to quantify these differences (Figure S12). Nonetheless, a previous study has reported that ABA treatments reduced the number of passage cells in Arabidopsis (Andersen et al., 2018).

Endodermal and exodermal suberin deposits were thicker in ABA treated plants compared to plants in control and salt conditions (Figure 7). Thicker exodermal suberin might limit water and nutrient intake from external environments into the root; and thicker endodermal suberin, with fewer passage cells, might limit water and nutrients reaching the central vasculature, thus limiting transport of essential nutrients and water to the shoot (Kamula et al., 1994; Peterson and Enstone, 1996). Limiting the influx of water and nutrients from external environments would limit plant growth. Plants presumably have to find a compromise between using apoplastic barriers to help in tolerating osmotic stresses such as increasing salinity without excessively hindering water and nutrient uptake.

The influence of ACC treatments on root suberin deposition differed to the influence of the ABA treatments (Barberon et al., 2016). We observed a trend of more passage cells in ACC treated HID003 samples compared to the control (Figure 7). However, the root sections

were cut in a transverse orientation, rather than a longitudinal orientation, thus, the sections do not represent the whole root segment. In a previous study sectioning was made longitudinally in a segment with continuous endodermal suberin lamellae, and the occurrence of passage-cells was calculated by dividing the sum of passage cells to the length of cells in the zone (Andersen et al., 2018). Our sectioning method limited the extent to which we could interpret whether there were differences in passage cells or not, therefore, an alternative approach is required to quantify passage cell number.

We concluded that ABA and ACC had different effects on the suberisation in the root in the barley material tested. Our results support that suberisation in the root can be reversible and change depending on the plant growth conditions. This adaptability in suberisation may allow plants to deposit suberin in response to abiotic stress and subsequently remove this suberin when the external environment becomes more favourable for growth. ABA and ACC had different effects on the suberin deposition, and potentially the number of endodermal passage cells and these differences may have had differing effects on the fluxes of solutes and water in and out of the vasculature.

2.6 Supplementary Figures

TABLE S1 Chemical components of the modified Hoagland's Nutrient Solution. The stock solutions A and B were made in 1L and stock solutions C and D were made in 0.5L. MW = molecular weight. FSH = Full strength of Hoagland.

Stock solution	Compound	MW	Final Concentration	Stock (x125) Amount per 1L (g)	Stock (x1000) Amount per 1L (g)	Amount of stock solution added (ml/L) (FSH)
A	KNO_3	101.11	6.5 mM	82.15	-	8
	$Ca(NO_3)_2.4H_2O$	236.16	4.0 mM	118.08	-	
B	$NH_4H_2PO_4$	115.03	100 µM	1.44	-	8
	$MgSO_4.7H_2O$	246.47	2.0 mM	61.62	-	
C	H_3BO_3	61.83	4.6 µM		0.284	1
	$MnCl_2.4H_2O$	197.9	0.5 µM		0.099	
	$ZnSO_4.7H_2O$	287.54	0.2 µM		0.055	
	$(NH_4)_6Mo_7O_{24}.4H_2O$	1235.95	0.1 µM		0.124	
	$CuSO_4.5H_2O$	249.7	0.2 µM		0.050	
D	NaFe(III)EDTA	367.1	50 µM		18.4	1

TABLE S2 Fluorescence intensity (gray value) of 7d old 40mM NaCl-treated barley plants. The gray value was measured using ImageJ and was set from 0 - 4000. The gray value of the (a) endodermal cell layer and (b) the exodermal cell layer of salt treated roots, n = (3-6) roots; with ~ 30 individual cells. Each genotype was compared with Barke using one-way ANOVA with Dunnet's multiple comparison test. The value shown is the mean ± with standard error of the mean. ANOVA significant difference $p<0.05$, $p<0.01$, $p<0.001$ and $p<0.0001$ indicated by (*), (**), (***) and (****) respectively, no significant different (nsd).

Barley	Endodermal Intensity (Gray Value)	Exodermal Intensity (Gray Value)
BARKE	3298 ± 66.15	1551 ± 169.0
HID003	3136 ± 200.8 (nsd)	2779 ± 211.0 (**)
HID055	3350 ± 29.20 (nsd)	3024 ± 286.6 (**)
HID069	2998 ± 196.7 (nsd)	2089 ± 234.3 (nsd)
HID101	3266 ± 102.3 (nsd)	3024 ± 73.04 (**)
HID138	3864 ± 27.66 (nsd)	3678 ± 60.81 (****)
HID357	3611 ± 106.8 (nsd)	2684 ± 285.7 (**)
HID386	3649 ± 119.1 (nsd)	3305 ± 228.6 (***)

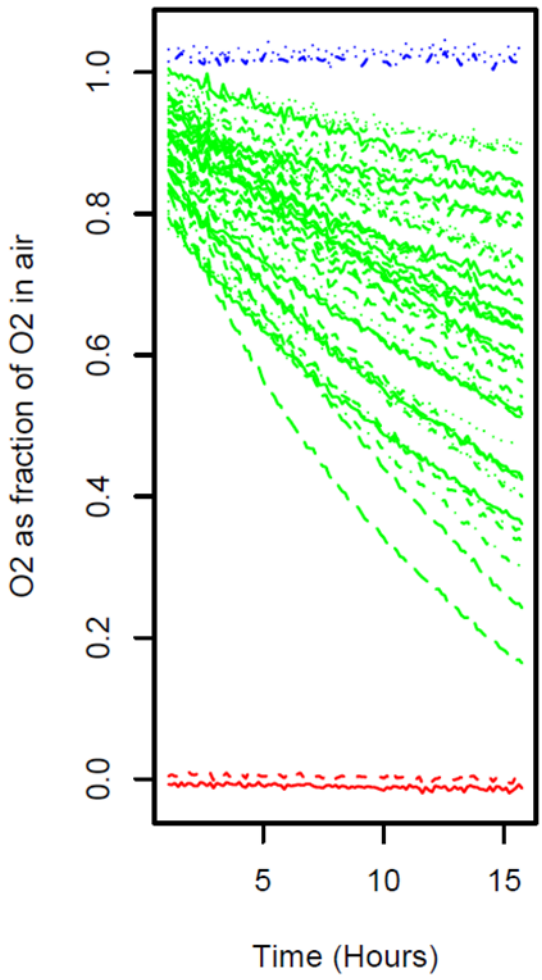

FIGURE S1 Raw/not normalised values of O_2 consumption of one-week old seedling roots over time. Each of the green dot lines represent individual plant placed in the tube with O_2 sensor cap. Two blue dot lines represent the tubes filled with ambient air that was used as standard and this was regard as 100% O_2 and represent as 1.0. Two red dot lines represent the tubes where all the O_2 was purged out and filled with nitrogen and this was regard as 0% O_2 and represent as 0.0. There were two tubes for each standard as only one was used as standard and the other one was used as a backup.

Genotype	0mM NaCl	40mM NaCl
BARKE	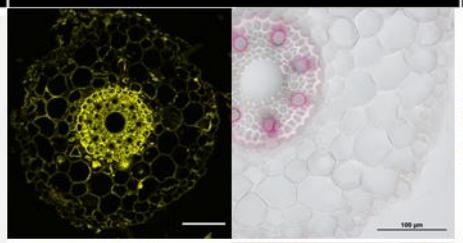	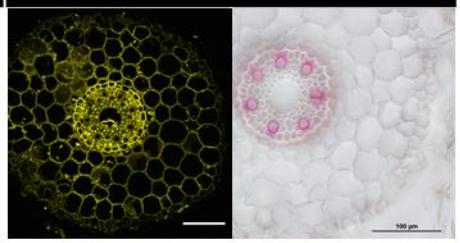
SCARLETT	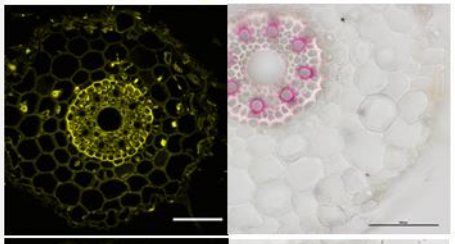	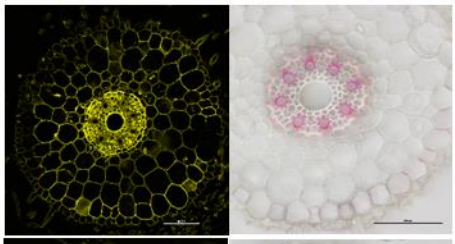
H. marinum	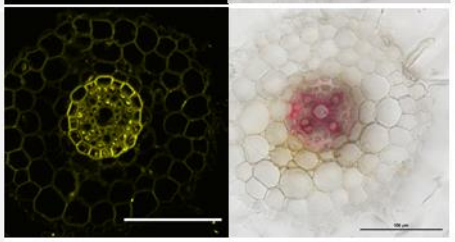	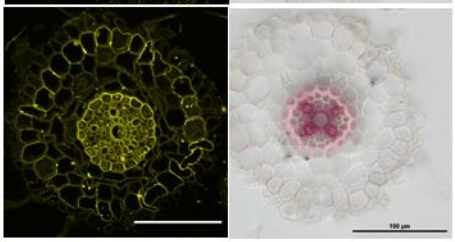
HID003	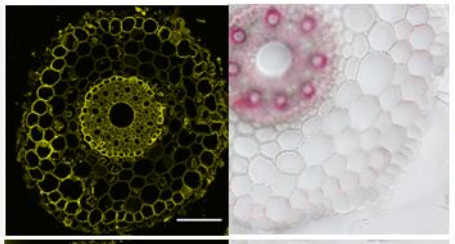	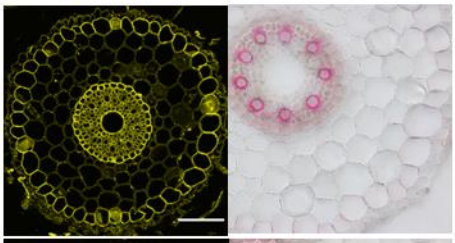
HID004	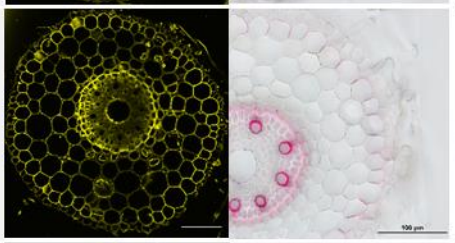	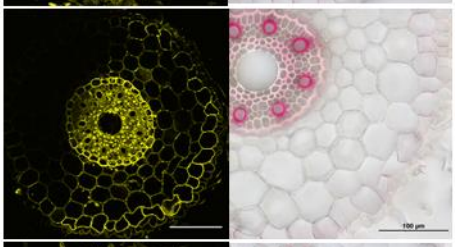
HID055	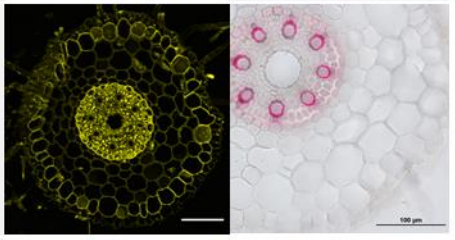	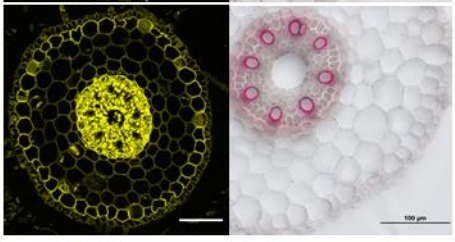
HID062	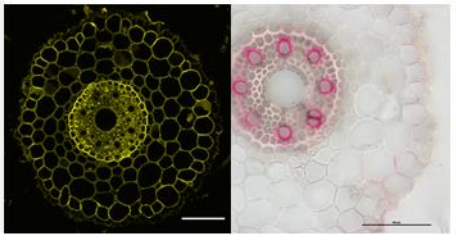	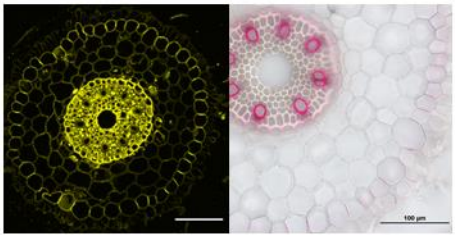

Genotype	0mM NaCl		40mM NaCl	
HID065	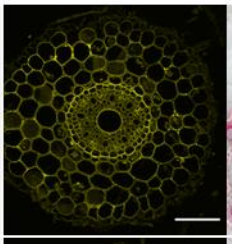	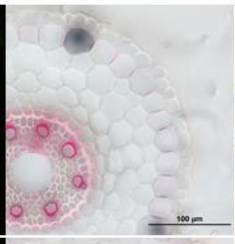	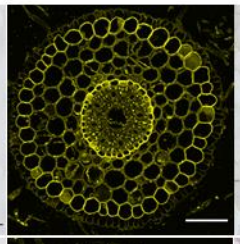	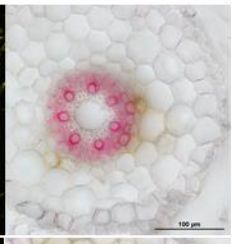
HID069	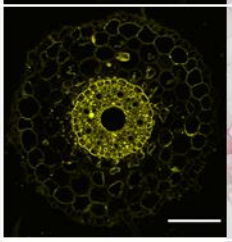	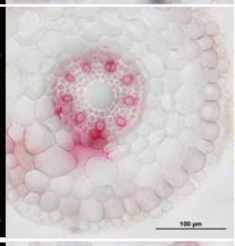	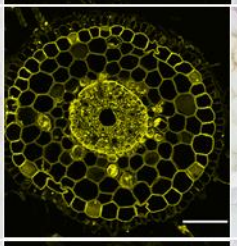	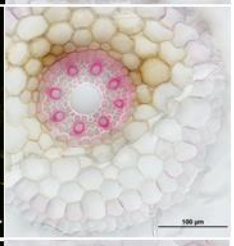
HID080	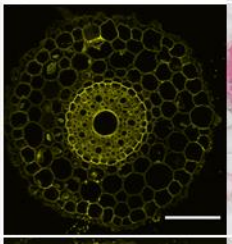	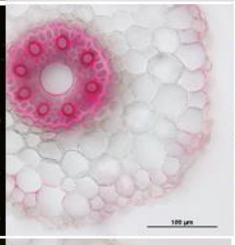	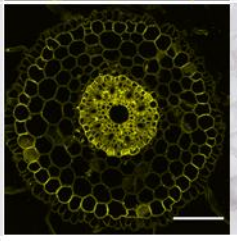	
HID099	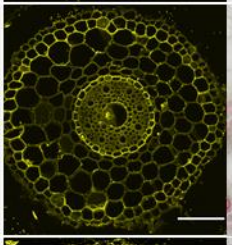	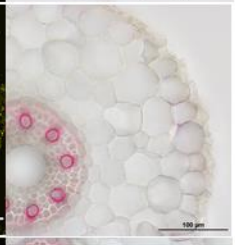	NA	NA
HID101	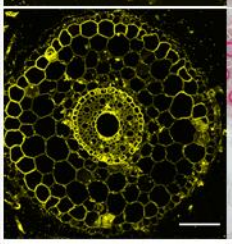	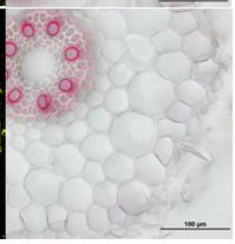	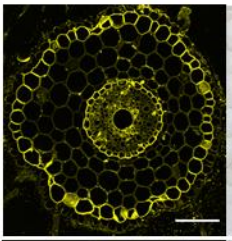	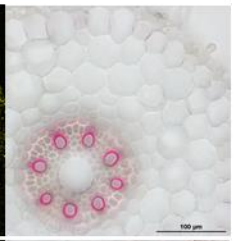
HID102	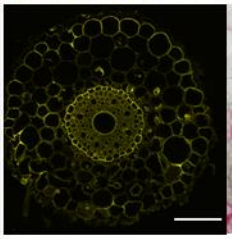	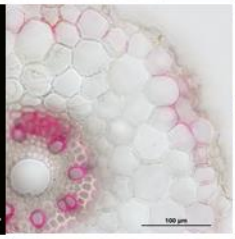	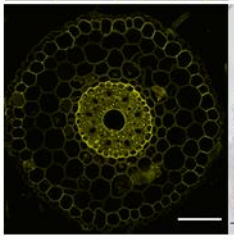	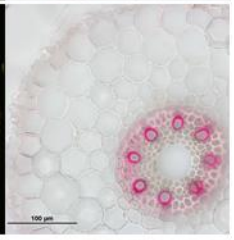
HID109	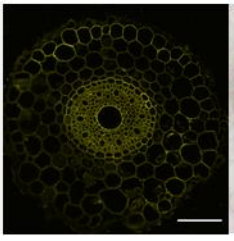	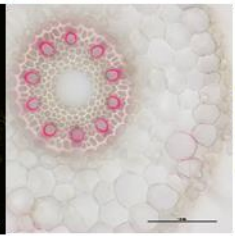	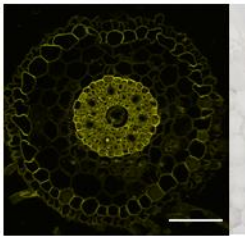	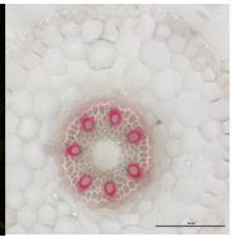

Genotype	0mM NaCl	40mM NaCl
HID114	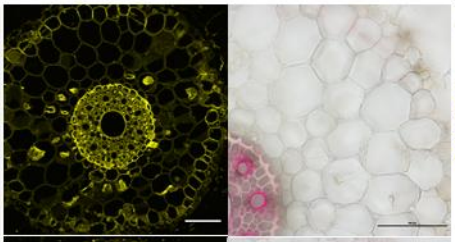	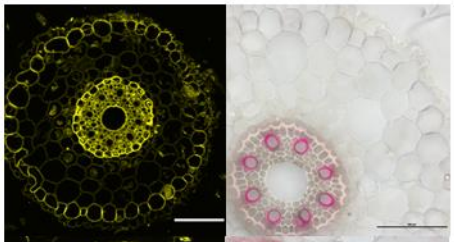
HID138	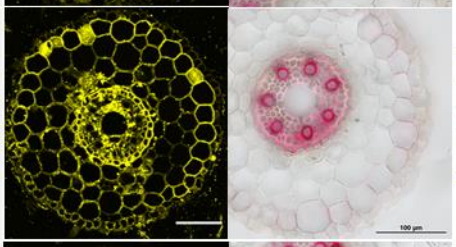	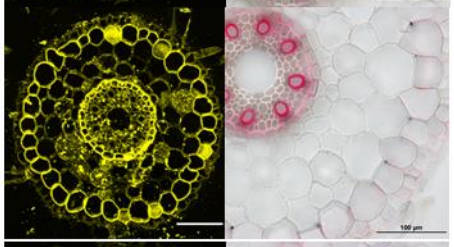
HID140	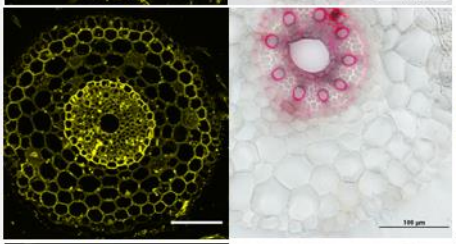	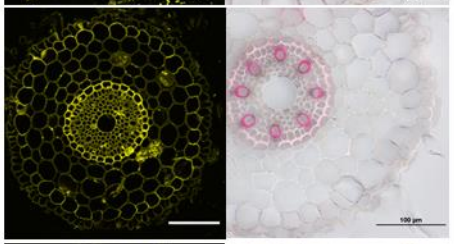
HID144	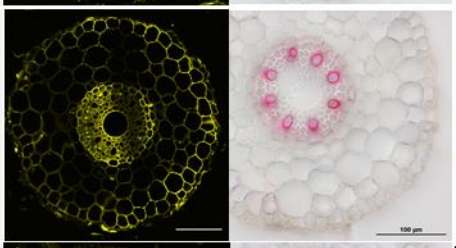	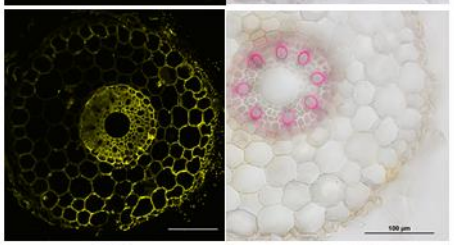
HID219	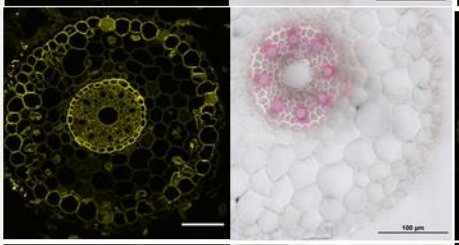	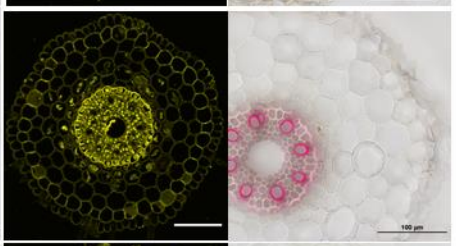
HID249	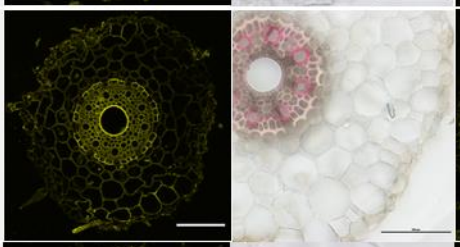	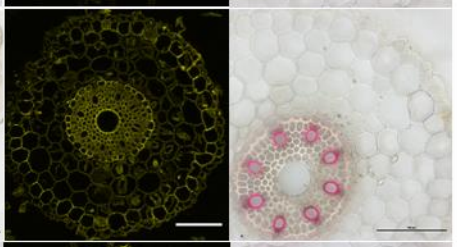
HID270	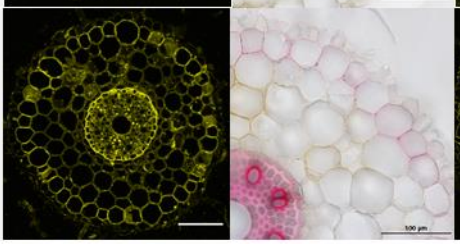	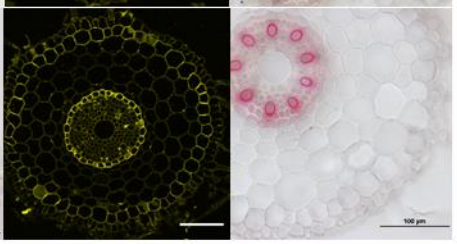

Genotype	0mM NaCl	40mM NaCl
HID294	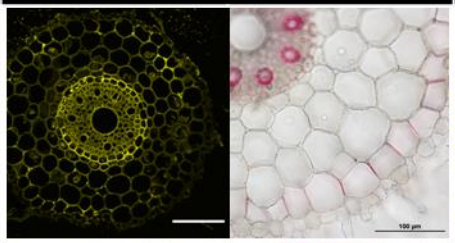	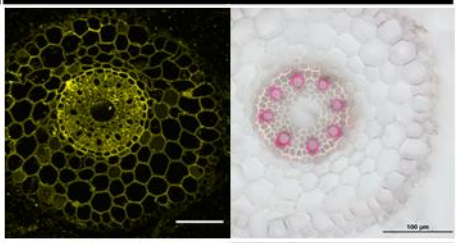
HID295	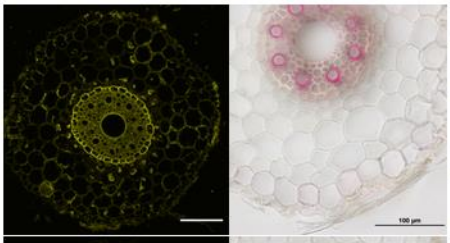	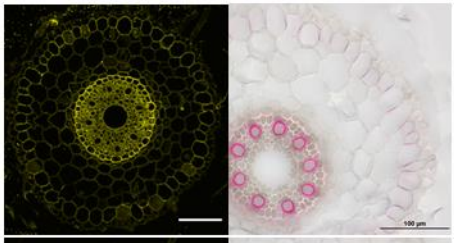
HID357	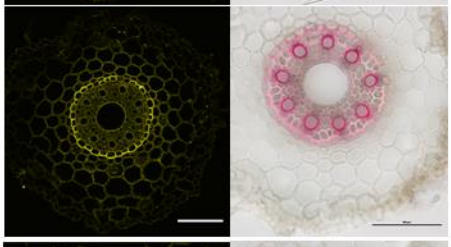	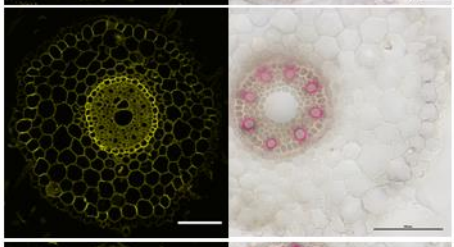
HID358	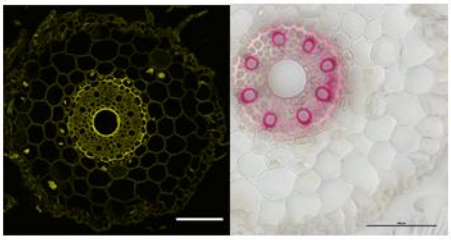	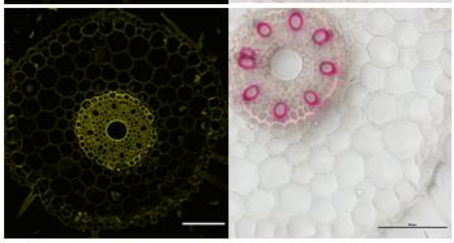
HID359	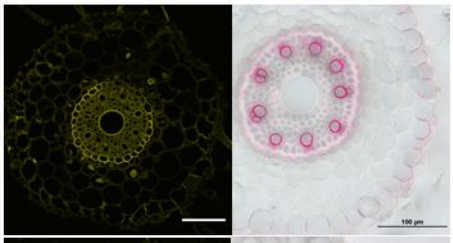	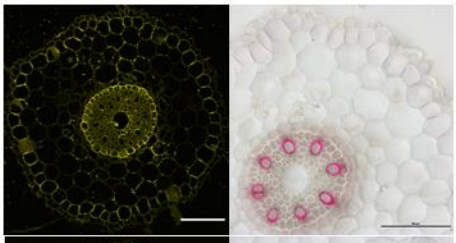
HID380	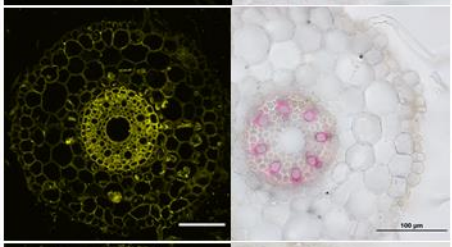	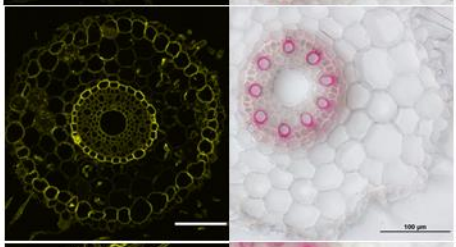
HID386	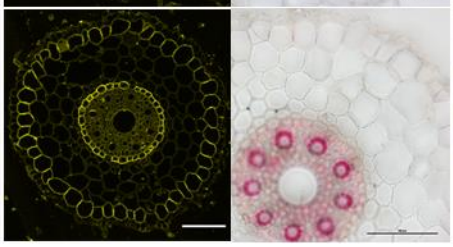	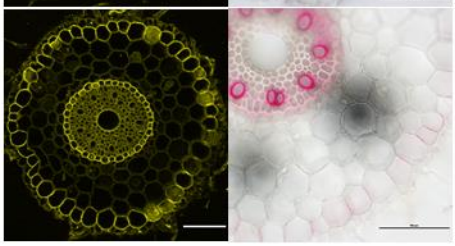

FIGURE S2 Screening for the spatial deposition of suberin and lignin in the longest seminal roots of *H. marinum*, commercial barley cultivars and wild barley accessions grown under 0mM NaCl and 40mM NaCl treatments for one week. Cross sections of 100µm thickness were made at the maturation zones. Suberin and lignin deposition were determined using Fluorol Yellow 088 and Pholroglucinol-HCl, respectively. Suberin stain signal (fluorescence) was obtained by confocal laser scanning microscopy and it is shown in yellow colour. Lignin stain was obtained under bright field microscope and it appears in red colour. Scale bars: 100µm.

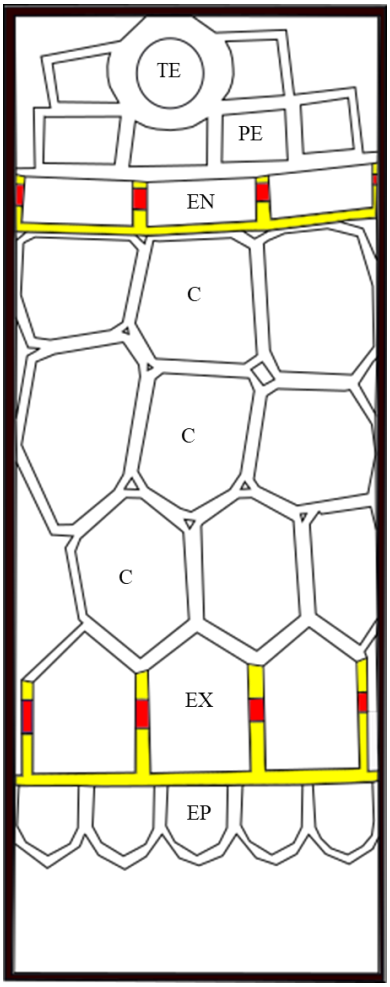

FIGURE S3 Illustration showing deposition of lignin and U-shaped suberin in the root of barley material. Lignin which is shown in red, deposited in the anticlinal wall of the endodermal and exodermal cell. Suberin which is shown in yellow, deposited in the anticlinal walls and transverse section facing to the outer part of the root (outer tangential) in both endodermal and exodermal cell. Abbreviation: TE, tracheary element; EN, endodermal, C; cortex, EX; exodermal, EP; epidermal, SE, soil environments. Image was adapted from Enstone et al. (2002).

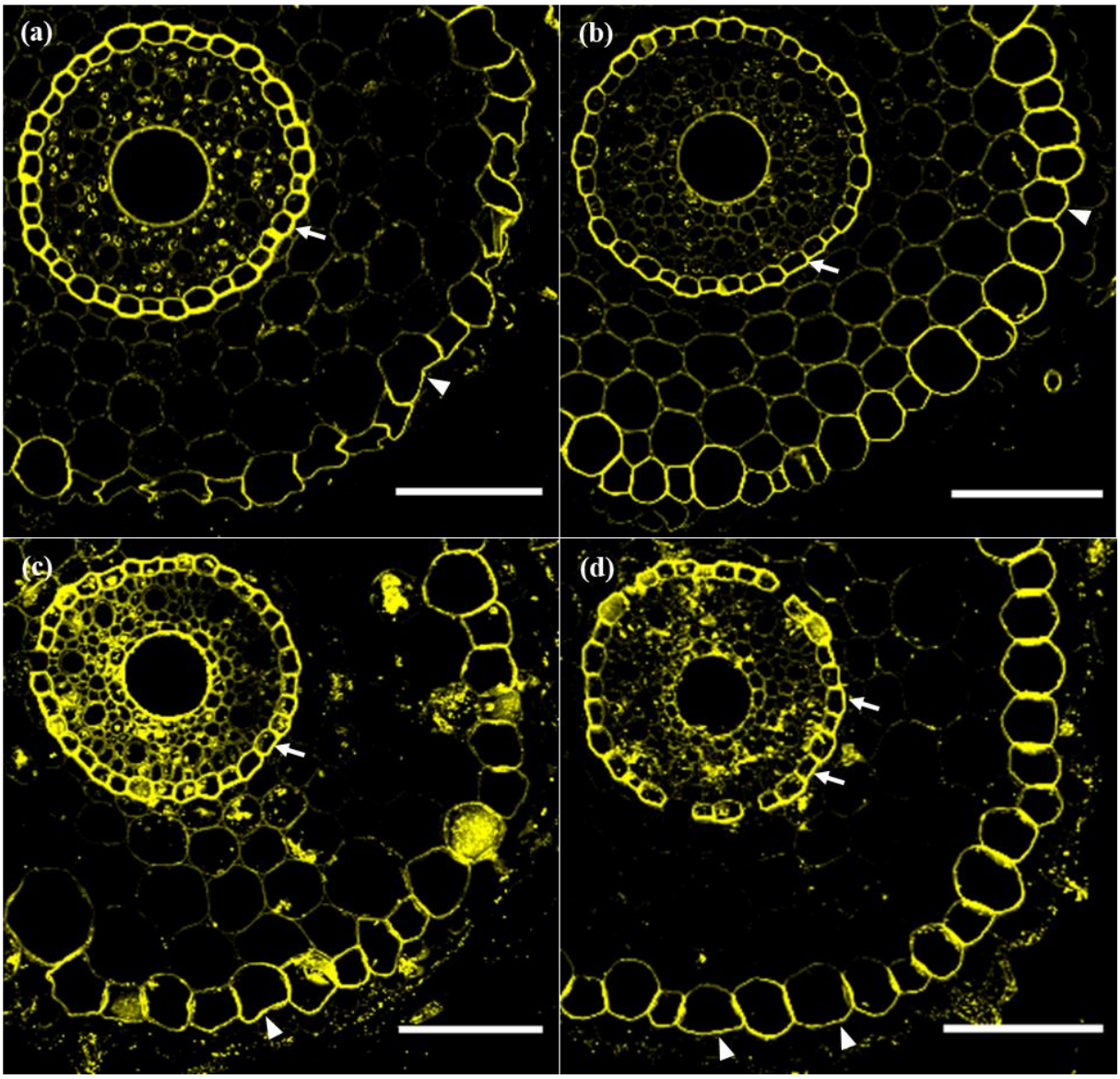

FIGURE S4 The U-shaped suberin deposition in the roots. Stained sections of HID003 and HID101 under control (a, c) and 40mM NaCl (b, d), respectively. All cross sections were stained with Fluorol Yellow 088 with PEG following (Brundrett et al., 1991). The presence of suberin is indicated by a yellowish fluorescence. The U-shaped endodermal and exodermal suberin are shown by the arrows and arrowheads, respectively. Bars = 100µm.

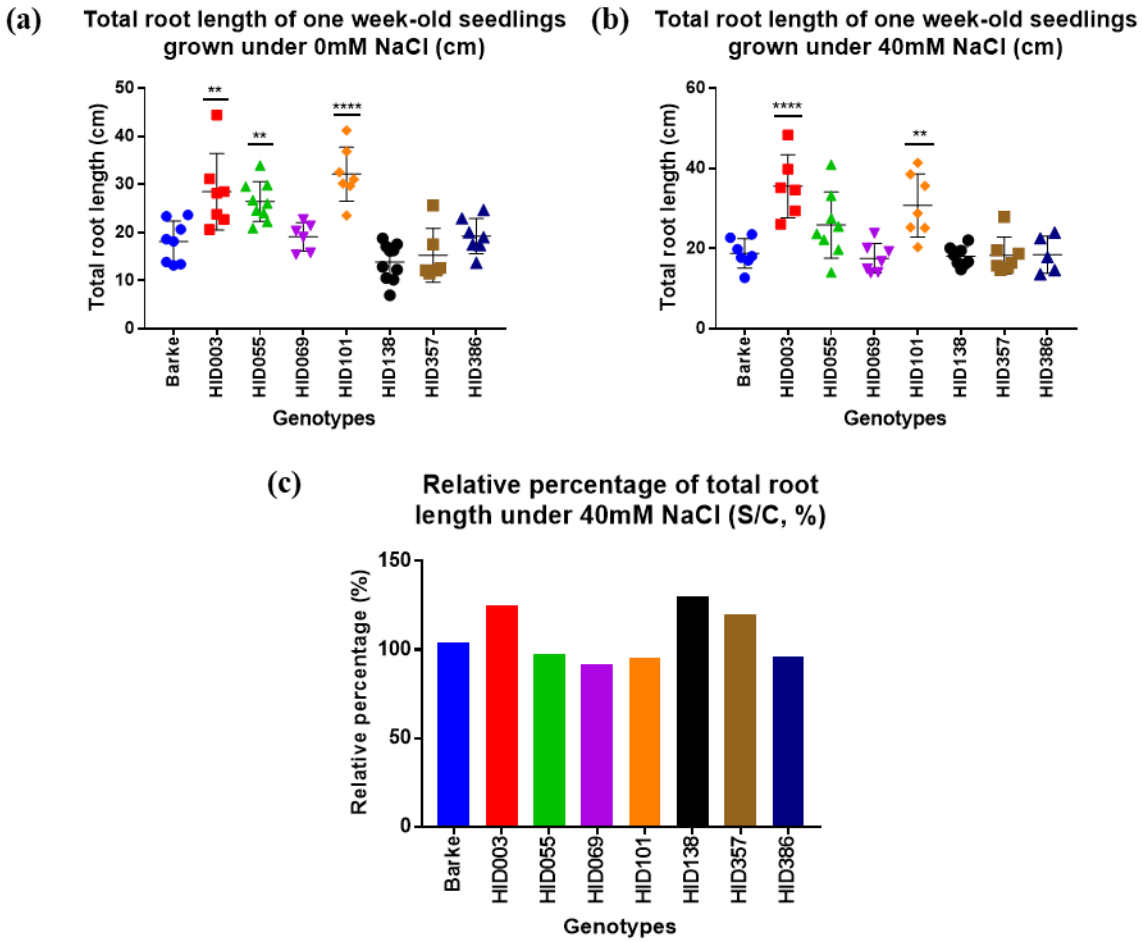

FIGURE S5 Total root length of one-week-old seedlings. Total root length under (a) 0mM NaCl conditions and (b) 40mM NaCl conditions. (c) Relative percentage of root length under saline in relative to those under control conditions. Data of each genotypes in (a) and (b) are compared with an elite cultivar, Barke using one-way ANOVA, Dunnet's multiple comparison test. Data are means (wide horizontal line) ± SEM (standard error mean) (n = 6-8). ANOVA significant difference $p<0.05$, $p<0.01$, $p<0.001$ and $p<0.0001$ indicated by (*), (**), (***) and (****) respectively.

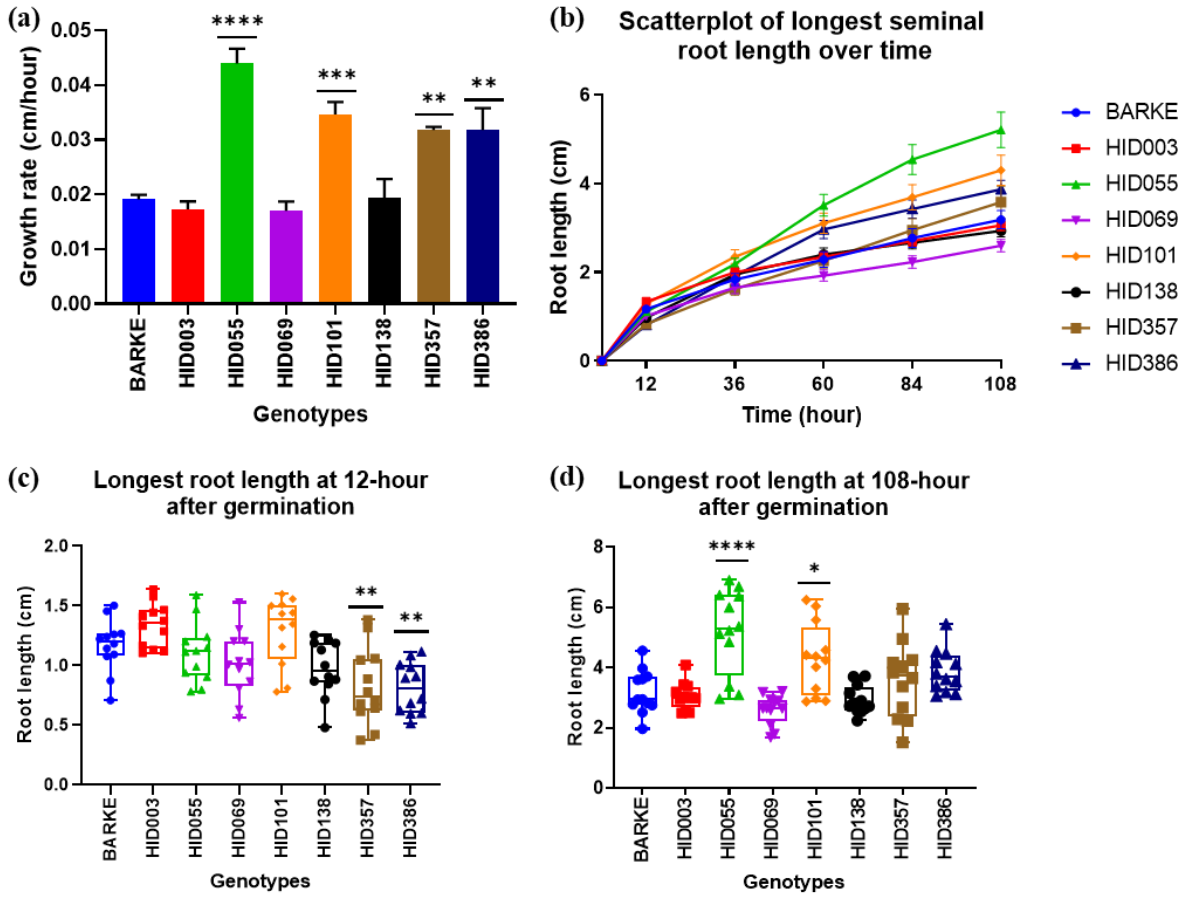

FIGURE S6 Root length and growth rate of longest seminal root of barley seedlings grown in half M/S agar with 40mM NaCl. Seed was first pre-germinated on wet filter paper in a petri dish for 12 h before they were transferred to half-M/S agar with 40mM NaCl. Seedlings were grown on media for 5 days in controlled growth room, and the image of the seedling's growth with a scale was taken every 24 h and the length of the longest seminal root was measured using ImageJ. (a) The growth rate (slope) of the longest seminal root of individual genotypes compared to Barke using one-way ANOVA with SEM shown (b) The longest root length of seedlings over a period of time. (c) The longest root length after 12 hour and (d) 108 hour after germination. Each data is individual biological replicates, and each genotypes were compared with Barke using one-way ANOVA with Dunnet's multiple comparison test. The middle line in box is the median. ANOVA significant difference $p<0.05$, $p<0.01$, $p<0.001$ and $p<0.0001$ indicated by (*), (**), (***) and (****) respectively.

(a)

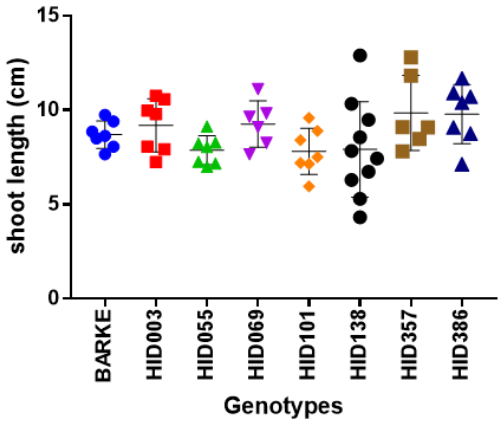
Shoot length of one week-old seedlings grown under 0mM NaCl
shoot length (cm)
15
10
5
0
BARKE
HID003
HID055
HID069
HID101
HID138
HID357
HID386
Genotypes

(d)

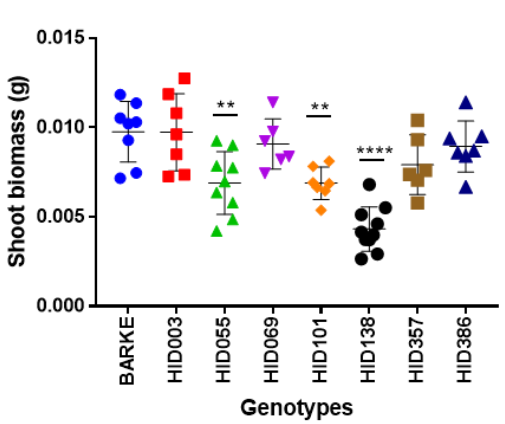
Shoot dryweight of one week-old seedlings grown under 0mM NaCl
Shoot biomass (g)
0.015
0.010
0.005
0.000
**
**
****
BARKE
HID003
HID055
HID069
HID101
HID138
HID357
HID386
Genotypes

(b)

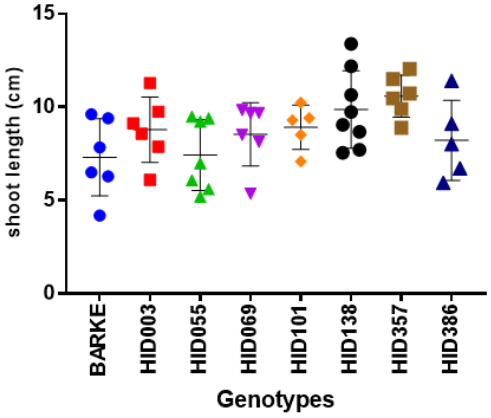
Shoot length of one week-old seedlings grown under 40mM NaCl
shoot length (cm)
15
10
5
0
BARKE
HID003
HID055
HID069
HID101
HID138
HID357
HID386
Genotypes

(e)

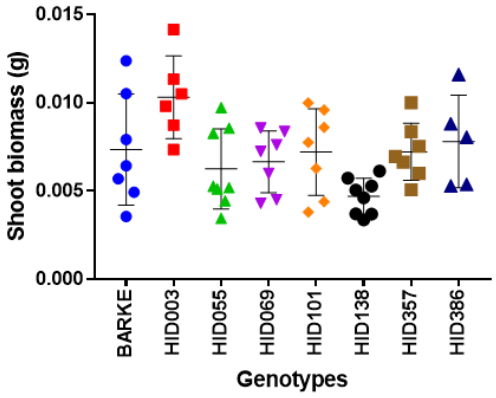
Shoot dryweight of one week-old seedlings grown under 40mM NaCl
Shoot biomass (g)
0.015
0.010
0.005
0.000
BARKE
HID003
HID055
HID069
HID101
HID138
HID357
HID386
Genotypes

(c)

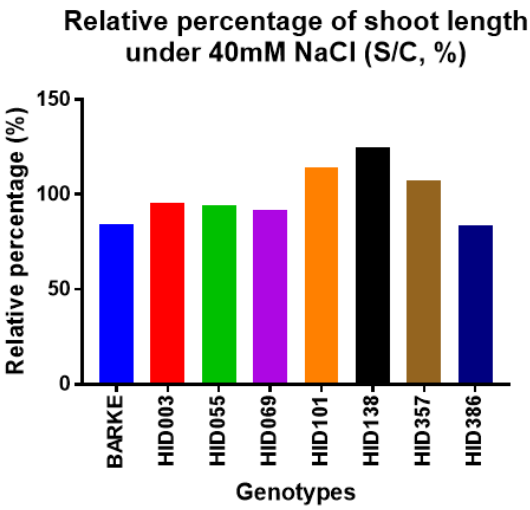
Relative percentage of shoot length under 40mM NaCl (S/C, %)
Relative percentage (%)
150
100
50
0
BARKE
HID003
HID055
HID069
HID101
HID138
HID357
HID386
Genotypes

(f)

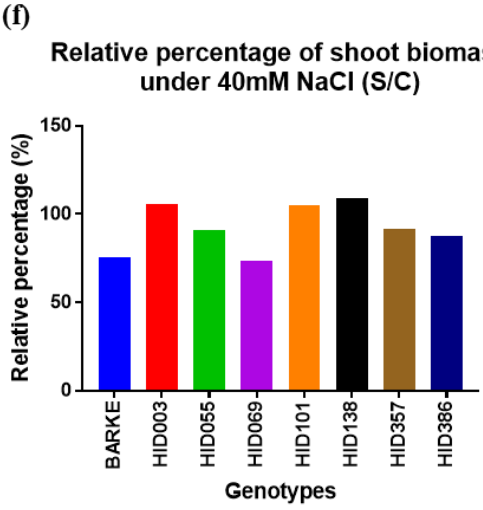
Relative percentage of shoot biomass under 40mM NaCl (S/C)
Relative percentage (%)
150
100
50
0
BARKE
HID003
HID055
HID069
HID101
HID138
HID357
HID386
Genotypes

FIGURE S7 Shoot length and biomass of one-week-old barley seedlings grown under 0mM NaCl and 40mM NaCl. Shoot length in (a) (control) and (b) (saline); shoot biomass in (d) (control) and (e) saline. For (a), (b), (d), (e), each wild accession are compared to Barke using one-way ANOVA, Dunnet's multiple comparison test. Data are individual replicates (symbols), means (wide horizontal line) ± SEM (standard error mean) (n = 6-8). ANOVA significant difference $p<0.05$, $p<0.01$, $p<0.001$ and $p<0.0001$ indicated by (*), (**), (***) and (****) respectively. The percentage relative mean in saline relative to control is shown for (c) shoot length and (f) shoot biomass.

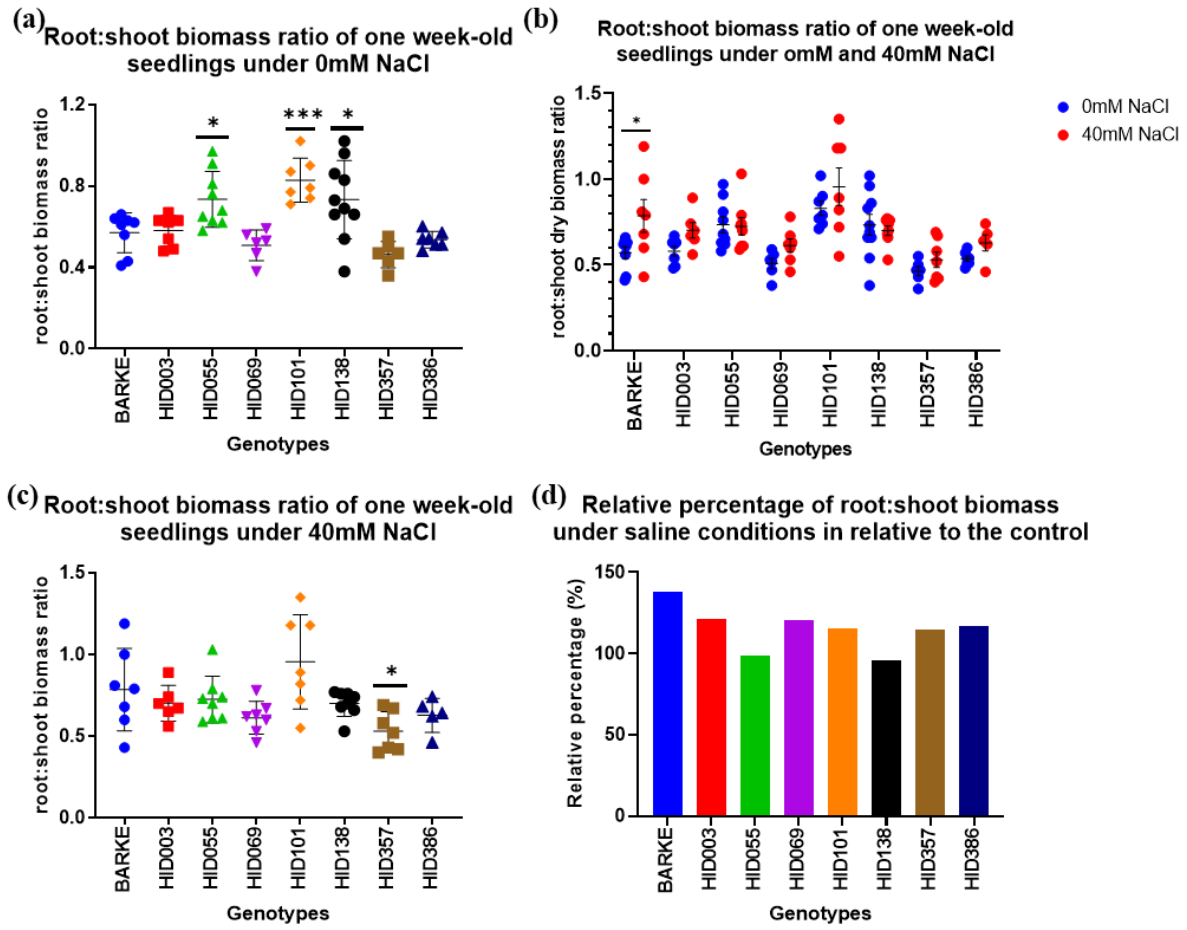

FIGURE S8 Root:Shoot dry biomass ratio of one-week old seedlings under (a) 0mM NaCl, (b) 40mM NaCl and (c) in both conditions. For (a) and (b) the data of each genotypes are compared with elite cultivar, Barke using one-way ANOVA, Dunnet's multiple comparison test. For (c), data for each genotypes were compared between the treatments using Sidak's multiple comparison test. Data are individual replicates (symbols), means (wide horizontal line) ± SEM (standard error of mean) (n = 8-10). ANOVA significant difference $p<0.05$, $p<0.01$, $p<0.001$ and $p<0.0001$ indicated by (*), (**), (***) and (****) respectively. (d) Percentage of mean of root:shoot biomass ratio under saline conditions in relative to the control.

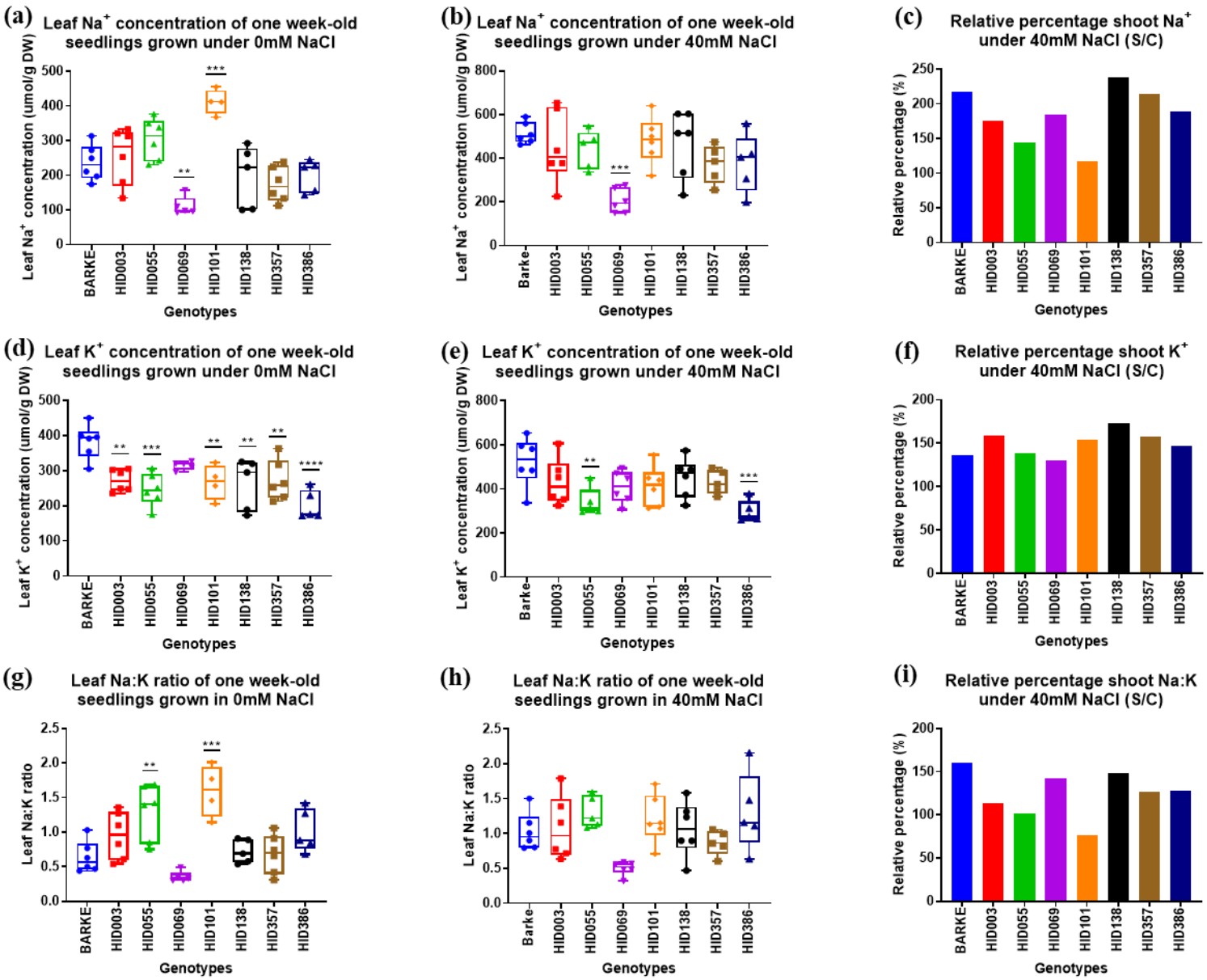
(a)
Leaf Na+ concentration of one week-old seedlings grown under 0mM NaCl
Leaf Na+ concentration (umol/g DW)
Genotypes
BARKE
HID003
HID055
HID069
HID101
HID138
HID357
HID386
(b)
Leaf Na+ concentration of one week-old seedlings grown under 40mM NaCl
Leaf Na+ concentration (umol/g DW)
Genotypes
Barke
HID003
HID055
HID069
HID101
HID138
HID357
HID386
(c)
Relative percentage shoot Na+ under 40mM NaCl (S/C)
Relative percentage (%)
Genotypes
(d)
Leaf K+ concentration of one week-old seedlings grown under 0mM NaCl
Leaf K+ concentration (umol/g DW)
Genotypes
(e)
Leaf K+ concentration of one week-old seedlings grown under 40mM NaCl
Leaf K+ concentration (umol/g DW)
Genotypes
(f)
Relative percentage shoot K+ under 40mM NaCl (S/C)
Relative percentage (%)
Genotypes
(g)
Leaf Na:K ratio of one week-old seedlings grown in 0mM NaCl
Leaf Na:K ratio
Genotypes
(h)
Leaf Na:K ratio of one week-old seedlings grown in 40mM NaCl
Leaf Na:K ratio
Genotypes
(i)
Relative percentage shoot Na:K under 40mM NaCl (S/C)
Relative percentage (%)
Genotypes

FIGURE S9 Profiling of shoot ion accumulation in Barke and HID accessions of interest selected based on the screening of root apoplastic barrier deposition. The accumulation of root Na^+ (a), K^+ (d) and Na:K ratio (g) under control (0mM NaCl added) and root Na^+ (b), K^+ (e) and Na:K ratio (h) under 40mM NaCl of one-week old seedlings. The ratio of the mean of root Na^+ (c), K^+ (f) and Na:K ratio (i) of salt treated plant, S in relative to the control plants, C. The amounts of both Na^+ and K^+ were normalised to the tissue dry weight (DW). Data are individual replicates (symbols), means (wide horizontal line) ± SEM (standard error of mean) (n = 6-10). For figures (a), (b), (d), (e), (g) and (h), each wild barley accession was compared to commercial cultivar, Barke using one-way ANOVA with Dunnet's multiple comparison test. ANOVA significant difference $p<0.05$, $p<0.01$, $p<0.001$ and $p<0.0001$ indicated by (*), (**), (***) and (****) respectively.

(a) PCA – Biplot: 0mM NaCl

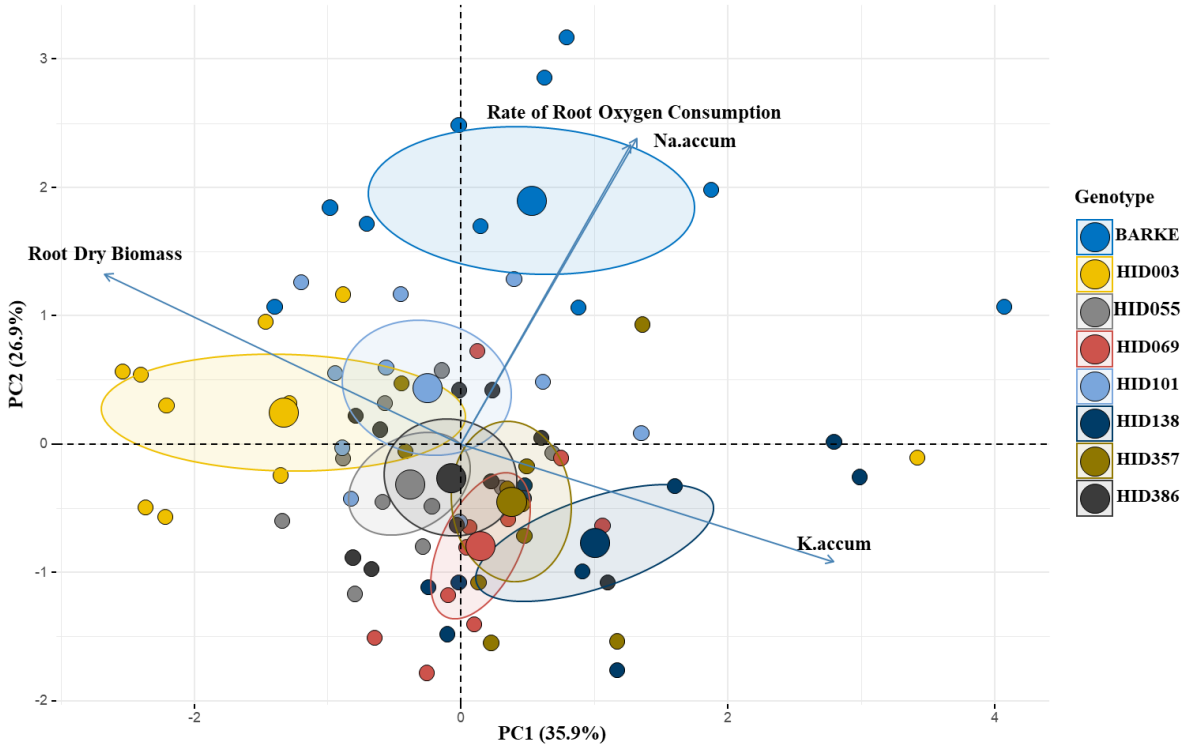

(b) PCA – Biplot:40mM NaCl

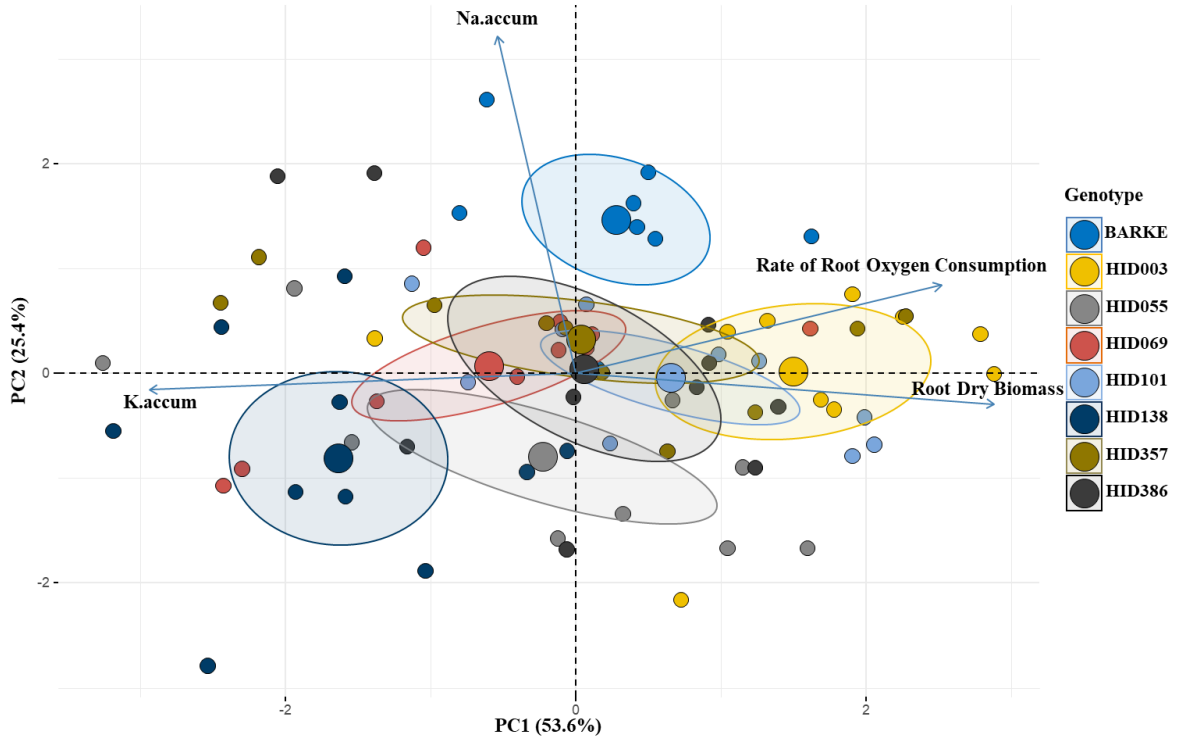

FIGURE S10 Principal Component Analysis for phenotypic characteristics in control and salt treated commercial and wild barley seedlings. PCA biplot showing scores for the two principal components (PC1): x-xis, (PC2): y-axis of the response variables consisting of root dry weight (DW), root O_2 consumption, and root ion accumulation (Na^+, K^+) in Barke and seven wild barley accessions. PCA analysis was conducted using a "FactoMineR" package and the PCA biplot was drawn using "factoextra" package in R software. (a) For the 0mM NaCl data, the principal component 1 (PC1) was accounted for 35.9% data variability, mainly driven by root K^+ accumulation and root dry biomass in the opposing direction. Principal component 2 (PC2) accounted for 26.9% of the data variability and it was mainly driven by root Na^+ accumulation and root O_2 consumption in the same direction. (b) For the 40mM NaCl, PC1 accounted for 53.6% of the data variability and it was mainly driven by root K^+ accumulation in negative direction and root dry biomass and root O_2 consumption in the opposite direction. PC2 accounted for 25.4% of the data variability and it was solely driven by root Na^+ accumulation. The magnitude of the contribution of each variable is shown by the length of the arrows. The large circle represents the mean of each genotype under different treatments. The 95% confidence eclipse is also shown surrounding the mean in each of the genotype.

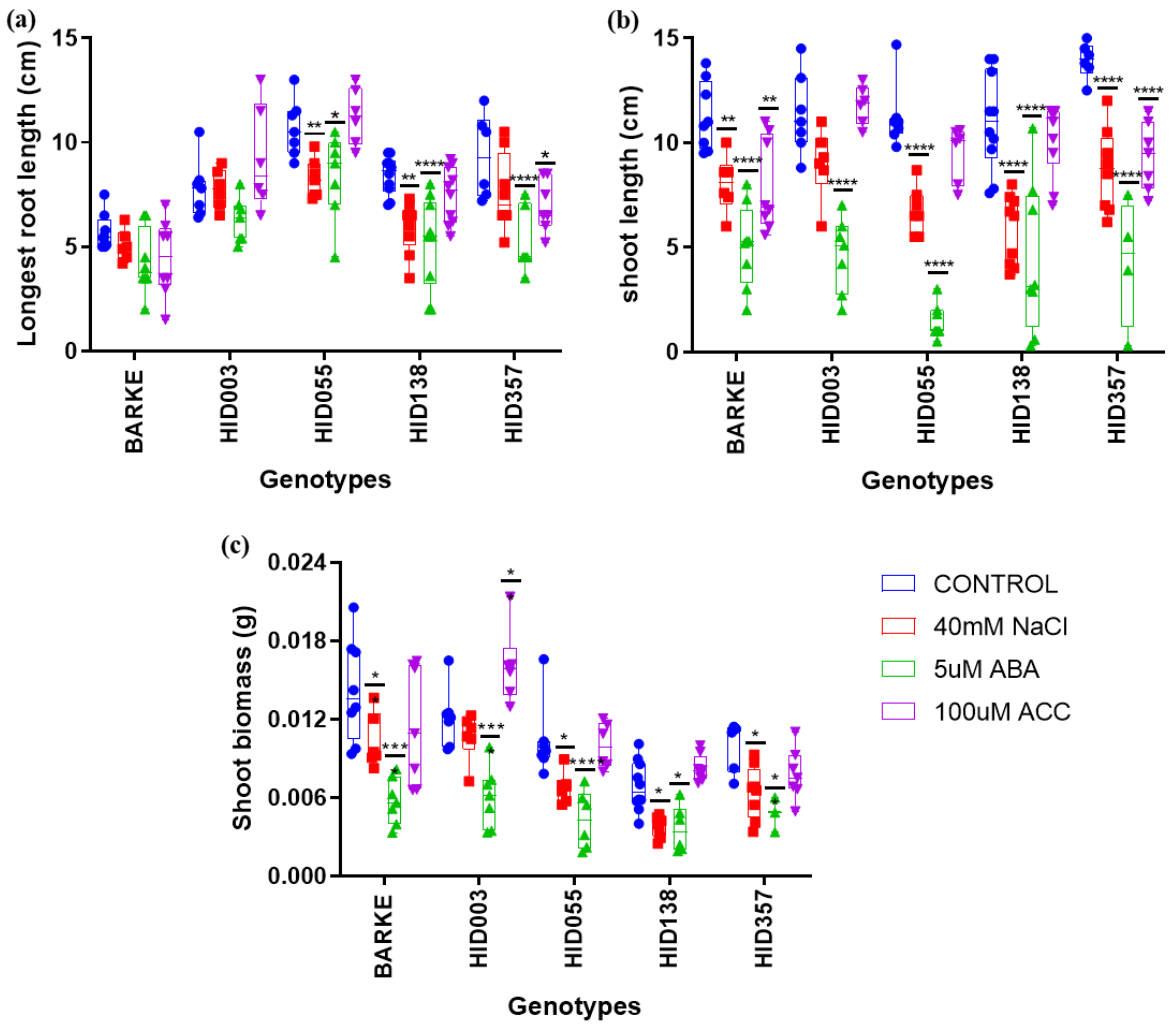

FIGURE S11 Root and shoot length and shoot biomass of one-week old seedlings in control, 40mM NaCl, 5µM ABA, and 100µM ACC and control. (a) Longest root length, (b) shoot length and (c) shoot biomass. For each genotype, data from salt, ABA and ACC treated plants are compared with control plants. The data was compared using a two-way ANOVA with Dunnett's multiple comparison test. Data are individual replicates (symbols), (n = 8-10). The middle horizontal line in the box is median. ANOVA significant difference $p<0.05$, $p<0.01$, $p<0.001$ and $p<0.0001$ indicated by (*), (**), (***) and (****) respectively.

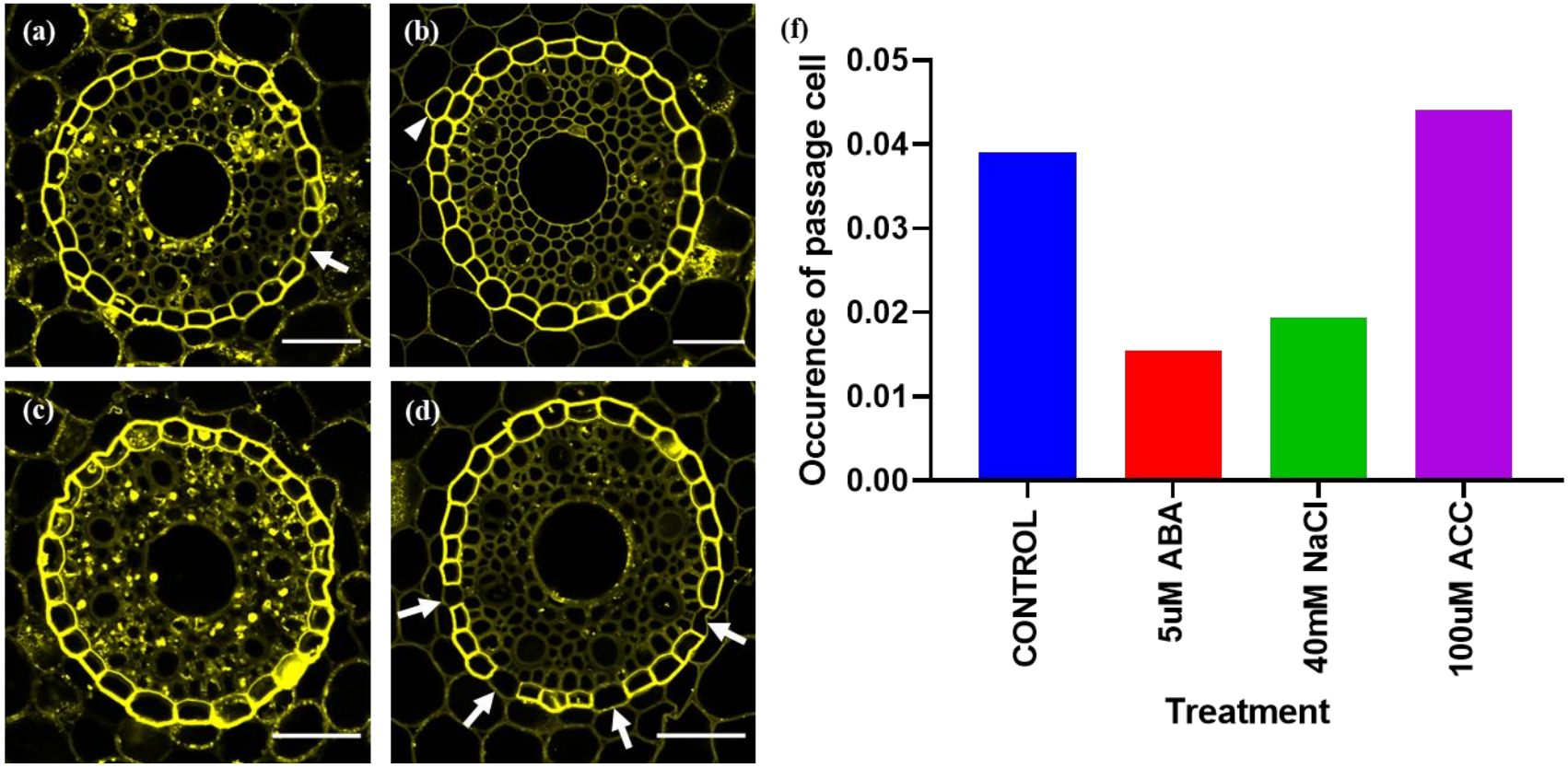

FIGURE S12 The endodermal passage cells under (a) control, (b) 5µM ABA, (c) 40mM NaCl and (d) 100µM ACC in HID138. (f) The occurrence of passage cell was calculated based on the average of percentage of passage cell in endodermal layer of independent biological replicates. The section was stained with Fluorol Yellow 088, and the presence of suberin is shown in yellow. In (a) control and (d) ACC treated plant, the arrow shows the passage cell and in (b) the arrowhead shows the additional suberised cortex cell next to the endodermis.

2.7 Acknowledgements

We gratefully thank the Grains Research and Development Corporation (GRDC) and Australian Centre of Excellence Plant Energy Biology (ARC PEB) for the Rana Munns Scholarship funding for this project. We thank Rana Munns, for critically reading the manuscript; and for her success in advancing our knowledge of crop salinity tolerance, which was the inspiration for this award. We thank Professor Timothy Colmer for providing seed of *Hordeum marinum*, Professor Klaus Pillen for sharing seed for the HID accessions. We also would like to thank Jodie Kretschmer, Dr Daniel Menadue, Andres Garcia and Marie Bee for their support in relation to technical assistance. We also thank the Adelaide Microscopy Facility, especially Dr Gwen Mayo for her support with microscopy. This research was supported by the Australian Research Council in the form of FT180100476 for CB and CE14010008 for SW and HS.

ORCIDs

Hisyam Sohaimi - ORCID ID: 0000-0002-5601-9005

Dr. Stefanie Wege - ORCID ID: 0000-0002-7232-5889

Dr. Caitlin Byrt - ORCID ID: 0000-0001-8549-2873

Dr. Rhiannon Schilling - ORCID ID: 0000-0001-8853-6878

2.8 References

Amarasinghe SL, Watson-Haigh NS, Byrt C, James R, Qiu J, Berkowitz O, Whelan J, Roy SJ, Gilliham M, Baumann U (2019) Transcriptional variation is associated with differences in shoot sodium accumulation in distinct barley varieties. Environmental and Experimental Botany **166:** 103812

Andersen TG, Naseer S, Ursache R, Wybouw B, Smet W, De Rybel B, Vermeer JE, Geldner N (2018) Diffusible repression of cytokinin signalling produces endodermal symmetry and passage cells. Nature **555:** 529-533

Badr A, Muller K, Schafer-Pregl R, El Rabey H, Effgen S, Ibrahim HH, Pozzi C, Rohde W, Salamini F (2000) On the origin and domestication history of barley (*Hordeum vulgare*). Molecular Biology and Evolution **17:** 499-510

Barberon M (2017) The endodermis as a checkpoint for nutrients. New Phytologist **213:** 1604-1610

Barberon M, Vermeer JEM, De Bellis D, Wang P, Naseer S, Andersen TG, Humbel BM, Nawrath C, Takano J, Salt DE, Geldner N (2016) Adaptation of root function by nutrient-induced plasticity of endodermal differentiation. Cell **164:** 447-459

Baxter I, Hosmani PS, Rus A, Lahner B, Borevitz JO, Muthukumar B, Mickelbart MV, Schreiber L, Franke RB, Salt DE (2009) Root suberin forms an extracellular barrier that affects water relations and mineral nutrition in Arabidopsis. Plos Genetics **5**

Bloom A, Epstein E (1984) Varietal differences in salt-induced respiration in barley. Plant Science Letters **35:** 1-3

Brundrett MC, Kendrick B, Peterson CA (1991) Efficient lipid staining in plant-material with Sudan red-7B or Fluoral yellow-088 in polyethylene glycol-glycerol. Biotechnic & Histochemistry **66:** 111-116

Byrt CS, Munns R, Burton RA, Gilliham M, Wege S (2018) Root cell wall solutions for crop plants in saline soils. Plant Science

Chen Z, Pottosin II, Cuin TA, Fuglsang AT, Tester M, Jha D, Zepeda-Jazo I, Zhou M, Palmgren MG, Newman IA (2007) Root plasma membrane transporters controlling K^+/Na^+ homeostasis in salt-stressed barley. Plant Physiology **145:** 1714-1725

Chen ZH, Zhou MX, Newman IA, Mendham NJ, Zhang GP, Shabala S (2007) Potassium and sodium relations in salinised barley tissues as a basis of differential salt tolerance. Functional Plant Biology **34:** 150-162

Colmer TD, Flowers TJ, Munns R (2006) Use of wild relatives to improve salt tolerance in wheat. Journal of Experimental Botany **57:** 1059-1078

Cuin TA, Betts SA, Chalmandrier R, Shabala S (2008) A root's ability to retain K^+ correlates with salt tolerance in wheat. Journal of Experimental Botany **59:** 2697-2706

Damus M, Peterson RL, Enstone DE, Peterson CA (1997) Modifications of cortical cell walls in roots of seedless vascular plants. Botanica Acta **110:** 190-195

El Mahi H, Pérez-Hormaeche J, De Luca A, Villalta I, Espartero J, Gámez-Arjona F, Fernández JL, Bundó M, Mendoza I, Mieulet D (2019) A critical role of sodium flux via the plasma membrane Na^+/H^+ exchanger SOS1 in the salt tolerance of rice. Plant Physiology **180:** 1046-1065

Enstone DE, Peterson CA, Ma FS (2002) Root endodermis and exodermis: Structure, function, and responses to the environment. Journal of Plant Growth Regulation **21:** 335-351

Garthwaite AJ, Armstrong W, Colmer TD (2008) Assessment of O_2 diffusivity across the barrier to radial O_2 loss in adventitious roots of *Hordeum marinum*. New Phytologist **179:** 405-416

Garthwaite AJ, von Bothmer R, Colmer TD (2005) Salt tolerance in wild *Hordeum* species is associated with restricted entry of Na^+ and Cl^- into the shoots. Journal of Experimental Botany **56:** 2365-2378

Hose E, Clarkson D, Steudle E, Schreiber L, Hartung W (2001) The exodermis: a variable apoplastic barrier. Journal of Experimental Botany **52:** 2245-2264

Houston K, Qiu J, Wege S, Hrmova M, Oakey H, Qu Y, Smith P, Situmorang A, Macaulay M, Flis P (2020) Barley sodium content is regulated by natural variants of the Na^+ transporter *HvHKT1; 5*. Communications Biology **3:** 1-9

Isayenkov S, Hilo A, Rizzo P, Tandron Moya YA, Rolletschek H, Borisjuk L, Radchuk V (2020) Adaptation strategies of halophytic barley *Hordeum marinum* ssp. *marinum* to high salinity and osmotic stress. International Journal of Molecular Sciences **21:** 9019

Islam S, Malik AI, Islam A, Colmer TD (2007) Salt tolerance in a *Hordeum marinum-Triticum aestivum* amphiploid, and its parents. Journal of Experimental Botany **58:** 1219-1229

Jacoby RP, Millar AH, Taylor NL (2013) Investigating the role of respiration in plant salinity tolerance by analyzing mitochondrial proteomes from wheat and a salinity-tolerant amphiploid (Wheat x *Lophopyrum elongatum*). Journal of Proteome Research **12:** 4807-4829

Jacoby RP, Taylor NL, Millar AH (2011) The role of mitochondrial respiration in salinity tolerance. Trends in Plant Science **16:** 614-623

James RA, Blake C, Zwart AB, Hare RA, Rathjen AJ, Munns R (2012) Impact of ancestral wheat sodium exclusion genes *Nax1* and *Nax2* on grain yield of durum wheat on saline soils. Functional Plant Biology **39:** 609-618

Kamula S, Peterson C, Mayfield C (1994) The plasmalemma surface area exposed to the soil solution is markedly reduced by maturation of the exodermis and death of the epidermis in onion roots. Plant, Cell & Environment **17:** 1183-1193

Karahara I, Ikeda A, Kondo T, Uetake Y (2004) Development of the Casparian strip in primary roots of maize under salt stress. Planta **219:** 41-47

Knipfer T, Fricke W (2011) Water uptake by seminal and adventitious roots in relation to whole-plant water flow in barley (*Hordeum vulgare* L.). Journal of Experimental Botany **62:** 717-733

Koevoets IT, Venema JH, Elzenga JT, Testerink C (2016) Roots withstanding their environment: exploiting root system architecture responses to abiotic stress to improve crop tolerance. Frontiers in Plant Science **7:** 1335

Kotula L, Colmer TD, Nakazono M (2014) Effects of organic acids on the formation of the barrier to radial oxygen loss in roots of *Hordeum marinum*. Functional Plant Biology **41:** 187-202

Kotula L, Ranathunge K, Schreiber L, Steudle E (2009b) Functional and chemical comparison of apoplastic barriers to radial oxygen loss in roots of rice (*Oryza sativa* L.) grown in aerated or deoxygenated solution. Journal of Experimental Botany **60:** 2155-2167

Kotula L, Ranathunge K, Steudle E (2009c) Apoplastic barriers effectively block oxygen permeability across outer cell layers of rice roots under deoxygenated conditions: roles of apoplastic pores and of respiration. New Phytologist **184:** 909-917

Kreszies T, Eggels S, Kreszies V, Osthoff A, Shellakkutti N, Baldauf JA, Zeisler-Diehl VV, Hochholdinger F, Ranathunge K, Schreiber L (2019b) Seminal roots of wild and cultivated barley differentially respond to osmotic stress in gene expression, suberization, and hydraulic conductivity. Plant, Cell & Environment

Kreszies T, Shellakkutti N, Osthoff A, Yu P, Baldauf JA, Zeisler-Diehl VV, Ranathunge K, Hochholdinger F, Schreiber L (2019a) Osmotic stress enhances suberization of apoplastic barriers in barley seminal roots: analysis of chemical, transcriptomic and physiological responses. New Phytologist **221:** 180-194

Krishnamurthy P, Jyothi-Prakash PA, Qin L, He J, Lin QS, Loh CS, Kumar PP (2014) Role of root hydrophobic barriers in salt exclusion of a mangrove plant *Avicennia officinalis*. Plant Cell and Environment **37:** 1656-1671

Krishnamurthy P, Ranathunge K, Franke R, Prakash HS, Schreiber L, Mathew MK (2009) The role of root apoplastic transport barriers in salt tolerance of rice (*Oryza sativa* L.). Planta **230:** 119-134

Krishnamurthy P, Ranathunge K, Nayak S, Schreiber L, Mathew MK (2011) Root apoplastic barriers block Na^+ transport to shoots in rice (*Oryza sativa L.*). Journal of Experimental Botany **62:** 4215-4228

Landgraf R, Smolka U, Altmann S, Eschen-Lippold L, Senning M, Sonnewald S, Weigel B, Frolova N, Strehmel N, Hause G, Scheel D, Bottcher C, Rosahl S (2014) The ABC Transporter ABCG1 Is Required for Suberin Formation in Potato Tuber Periderm. Plant Cell **26:** 3403-3415

Maathuis FJM, Amtmann A (1999) K^+ nutrition and Na^+ toxicity: The basis of cellular K^+/Na^+ ratios. Annals of Botany **84:** 123-133

Maurer A, Draba V, Jiang Y, Schnaithmann F, Sharma R, Schumann E, Kilian B, Reif JC, Pillen K (2015) Modelling the genetic architecture of flowering time control in barley through nested association mapping. Bmc Genomics **16**

Mitra PP, Loqué D (2014) Histochemical Staining of *Arabidopsis thaliana* Secondary Cell Wall Wlements. JoVE (Journal of Visualized Experiments)**:** e51381

Munns R, Gilliham M (2015) Salinity tolerance of crops–what is the cost? New Phytologist **208:** 668-673

Munns R, Passioura JB, Colmer TD, Byrt CS (2020) Osmotic adjustment and energy limitations to plant growth in saline soil. New Phytologist **225:** 1091-1096

Naseer S, Lee Y, Lapierre C, Franke R, Nawrath C, Geldner N (2012) Casparian strip diffusion barrier in *Arabidopsis* is made of a lignin polymer without suberin. Proceedings of the National Academy of Sciences of the United States of America **109:** 10101-10106

Patterson JH, Newbigin E, Tester M, Bacic A, Roessner U (2009) Metabolic responses to salt stress of barley (*Hordeum vulgare* L.) cultivars, Sahara and Clipper, which differ in salinity tolerance. Journal of Experimental Botany **60:** 4089-4103

Peterson CA, Enstone DE (1996) Functions of passage cells in the endodermis and exodermis of roots. Physiologia Plantarum **97:** 592-598

Peterson CA, Perumalla CJ (1990) A survey of angiosperm species to detect hypodermal Casparian bands. II. Roots with a multiseriate hypodermis or epidermis. Botanical Journal of the Linnean Society **103:** 113-125

Pfister A, Barberon M, Alassimone J, Kalmbach L, Lee Y, Vermeer JEM, Yamazaki M, Li GW, Maurel C, Takano J, Kamiya T, Salt DE, Roppolo D, Geldner N (2014) A receptor-like kinase mutant with absent endodermal diffusion barrier displays selective nutrient homeostasis defects. Elife **3**

Ranathunge K, Kim YX, Wassmann F, Kreszies T, Zeisler V, Schreiber L (2017) The composite water and solute transport of barley (Hordeum vulgare) roots: effect of suberized barriers. Annals of Botany **119:** 629-643

Ranathunge K, Lin JX, Steudle E, Schreiber L (2011a) Stagnant deoxygenated growth enhances root suberization and lignifications, but differentially affects water and NaCl

permeabilities in rice (Oryza sativa L.) roots. Plant Cell and Environment **34:** 1223-1240

Ranathunge K, Schreiber L (2011) Water and solute permeabilities of *Arabidopsis* roots in relation to the amount and composition of aliphatic suberin. Journal of Experimental Botany **62:** 1961-1974

Reinhardt DH, Rost TL (1995) Salinity accelerates endodermal development and induces an exodermis in cotton seedling roots. Environmental and Experimental Botany **35:** 563-574

Robards A, Jackson SM, Clarkson D, Sanderson J (1973) The structure of barley roots in relation to the transport of ions into the stele. Protoplasma **77:** 291-311

Roy S, Chakraborty U (2014) Salt tolerance mechanisms in salt tolerant grasses (STGs) and their prospects in cereal crop improvement. Botanical Studies **55:** 31

Saade S, Maurer A, Shahid M, Oakey H, Schmockel SM, Negrao S, Pillen K, Tester M (2016) Yield-related salinity tolerance traits identified in a nested association mapping (NAM) population of wild barley. Scientific Reports **6**

Sager R, Lee J-Y (2014) Plasmodesmata in integrated cell signalling: insights from development and environmental signals and stresses. Journal of experimental botany **65:** 6337-6358

Scafaro AP, Negrini ACA, O'Leary B, Rashid FAA, Hayes L, Fan Y, Zhang Y, Chochois V, Badger MR, Millar AH (2017) The combination of gas-phase fluorophore technology and automation to enable high-throughput analysis of plant respiration. Plant Methods **13:** 16

Schreiber L, Franke R, Hartmann KD, Ranathunge K, Steudle E (2005b) The chemical composition of suberin in apoplastic barriers affects radial hydraulic conductivity differently in the roots of rice (*Oryza sativa L.* cv. IR64) and corn (*Zea mays L.* cv. Helix). Journal of Experimental Botany **56:** 1427-1436

Schreiber L, Hartmann K, Skrabs M, Zeier J (1999) Apoplastic barriers in roots: chemical composition of endodermal and hypodermal cell walls. Journal of Experimental Botany **50:** 1267-1280

Seago J, James L, Peterson CA, Enstone DE, Scholey CA (1999) Development of the endodermis and hypodermis of *Typha glauca* Godr. and *Typha angustifolia* L. roots. Canadian Journal of Botany **77:** 122-134

Shavrukov Y, Gupta N, Chalmers K, Tester M, Langridge P (2010) Identification of a QTL on chromosome 7H for sodium exclusion from wild barley, *Hordeum spontaneum*. *In* Proceedings of the 10th international barley genetics symposium. ICARDA, Aleppo, pp 241-247

Shen J, Xu GX, Zheng HQ (2015) Apoplastic barrier development and water transport in Zea mays seedling roots under salt and osmotic stresses. Protoplasma **252:** 173-180

Soukup A, Votrubová O, Čížková H (2002) Development of anatomical structure of roots of *Phragmites australis*. New Phytologist **153:** 277-287

Speer EO (1987) A method of retaining phloroglucinol proof of lignin. Stain Technology **62:** 279-280

Tanksley SD, McCouch SR (1997) Seed banks and molecular maps: unlocking genetic potential from the wild. Science **277:** 1063-1066

Tilbrook J, Schilling RK, Berger B, Garcia AF, Trittermann C, Coventry S, Rabie H, Brien C, Nguyen M, Tester M (2017) Variation in shoot tolerance mechanisms not related to ion toxicity in barley. Functional Plant Biology **44:** 1194-1206

Ueda A, Yamamoto-Yamane Y, Takabe T (2007) Salt stress enhances proline utilization in the apical region of barley roots. Biochemical and biophysical research communications **355:** 61-66

Zhu J, Fan Y, Shabala S, Li C, Lv C, Guo B, Xu R, Zhou M (2020) Understanding mechanisms of salinity tolerance in barley by proteomic and biochemical analysis of near-isogenic lines. International Journal of Molecular Sciences **21:** 1516

Zimmermann HM, Hartmann K, Schreiber L, Steudle E (2000) Chemical composition of apoplastic transport barriers in relation to radial hydraulic conductivity of corn roots (*Zea mays L.*). Planta **210:** 302-311

Zimmermann HM, Steudle E (1998) Apoplastic transport across young maize roots: effect of the exodermis. Planta **206:** 7-19

Chapter 3:

Investigating the relationship between root barrier deposition and shoot and root biomass and ion accumulation in selected HEB13 lines

Chapter 3 Investigating the relationship between root barrier deposition and shoot and root biomass and ion accumulation in selected HEB13 lines

3.0 Abstract

Seedlings of the modern barley (*Hordeum vulgare* spp. *vulgare*) cultivar Barke lack an exodermal barrier in control and saline conditions, whereas the wild barley (*Hordeum vulgare* spp. *spontaneum*) accession 'HID138' forms an exodermal barrier under saline conditions. Previously, we observed that the roots of HID138 seedlings accumulated less sodium (Na^+) and more potassium (K^+) than Barke (Figure 5, Chapter 2). In saline conditions the root Na^+:K^+ ratio of HID138 was less than two, whereas for Barke the root Na^+:K^+ ratio was approximately four. Here, we used Recombinant Inbred Lines (RILs) from a Halle Exotic Barley Nested Association Mapping (HEB25 NAM) population of Barke crossed with HID138 to test whether or not there was any association between trends in tissue ion accumulation and the formation of barriers. Our results indicate that in the inbred lines there was greater variation in the K^+ ion accumulation relative to the Na^+ ion accumulation, and that there was no obvious relationship between the differences in K^+ retention and the variation in exodermal barrier deposition. This indicates that other factors are likely to be contributing to the differences in Na^+:K^+ ratios.

3.1 Introduction

Barley (*Hordeum vulgare* L) was domesticated more than 10 000 years ago in an area referred to as the Fertile Crescent in the Middle East (Badr et al., 2000). Barley is one of the earliest crops human civilisation domesticated, and barley is still one of the most important crops, ranked fourth globally based on production (FAOSTAT). Barley is also one of the most salt tolerant crops relative to other cultivated cereals (Munns and Tester, 2008). However, due to climate variability and increasing issues with soil salinity in growing regions, the yield of barley is currently limited (Munns and Gilliham, 2015). In contrast to modern barley, some wild barleys can better tolerate salinity, even at high salt concentrations of 250 mM NaCl

(Tilbrook et al., 2017). For example, *Hordeum marinum* (sea barleygrass), inhabits salt marshes and had only a 7% yield reduction at 150 mM NaCl relative to the control, whereas there was a 50% reduction in yield observed for modern cereals at 150 mM NaCl relative to control (Islam et al., 2007). This indicates that wild barley may contain useful source(s) of genetic variation that enable them to better tolerate high salinity relative to modern lines.

Crop domestication is thought to have led to a genetic bottleneck effect, where some alllelic variation that might be useful for salinity tolerance is likely to have been lost possibly in the process of selecting for yield in favourable conditions (Tanksley and McCouch, 1997). Wild barley progenitors might therefore be useful sources of genetic variation that could be introduced into modern barley lines to improve their tolerance to abiotic stresses. For example, genes from a wild progenitor were successfully introduced into modern barley lines to create amphiploids, which improved salt tolerance by 20% in terms of grains per plant under saline conditions, relative to the controls (Islam et al., 2007).

The Halle Exotic Barley Nested Association Mapping (HEB25 NAM) population is a set of RILS created in Halle, Germany, by crossing 25 highly exotic barley accessions into a common elite cultivar, Barke, and then backcrossing and selfing the progeny (Figure 1) (Maurer et al., 2015). Twenty-four exotic barley accessions categorised as *Hordeum vulgare spp spontaneum* originated in the Fertile Crescent; in the present day, this area constitutes of Afghanistan, Iran, Iraq, Israel, Lebanon, Turkey, and Syria (Appendix 1). One accession, HID380 (*Hordeum vulgare ssp. agriocrithon*) originated from Tibet, and was used to maximise genetic diversity in the HEB25 NAM (Maurer et al., 2015). The set of 25 diverse barley accessions were used as pollen donors and the elite cultivar, Barke was the pollen recipient (Figure 1). The F_1 population from initial crosses was backcrossed to Barke to get a population with mostly Barke background and donor fragments, 'BC_1' (Figure 1). This step was important for maximising the likelihood of retaining sufficient Barke genetics so that comparisons of

traits would be less likely to be confounded by the influence of undesirable wild characteristics, such as seed shattering, that are problematic in breeding programs (Figure 1). About 20-75 BC_1 plants from each cross were then selfed three times through the Single Seed Descent technique, where one seed of each plant was used for creating the next generation (Maurer et al., 2015). The final output was a HEB25 NAM population that is useful for studying the effect of the wild alleles on modern barley traits (Maurer et al., 2015).

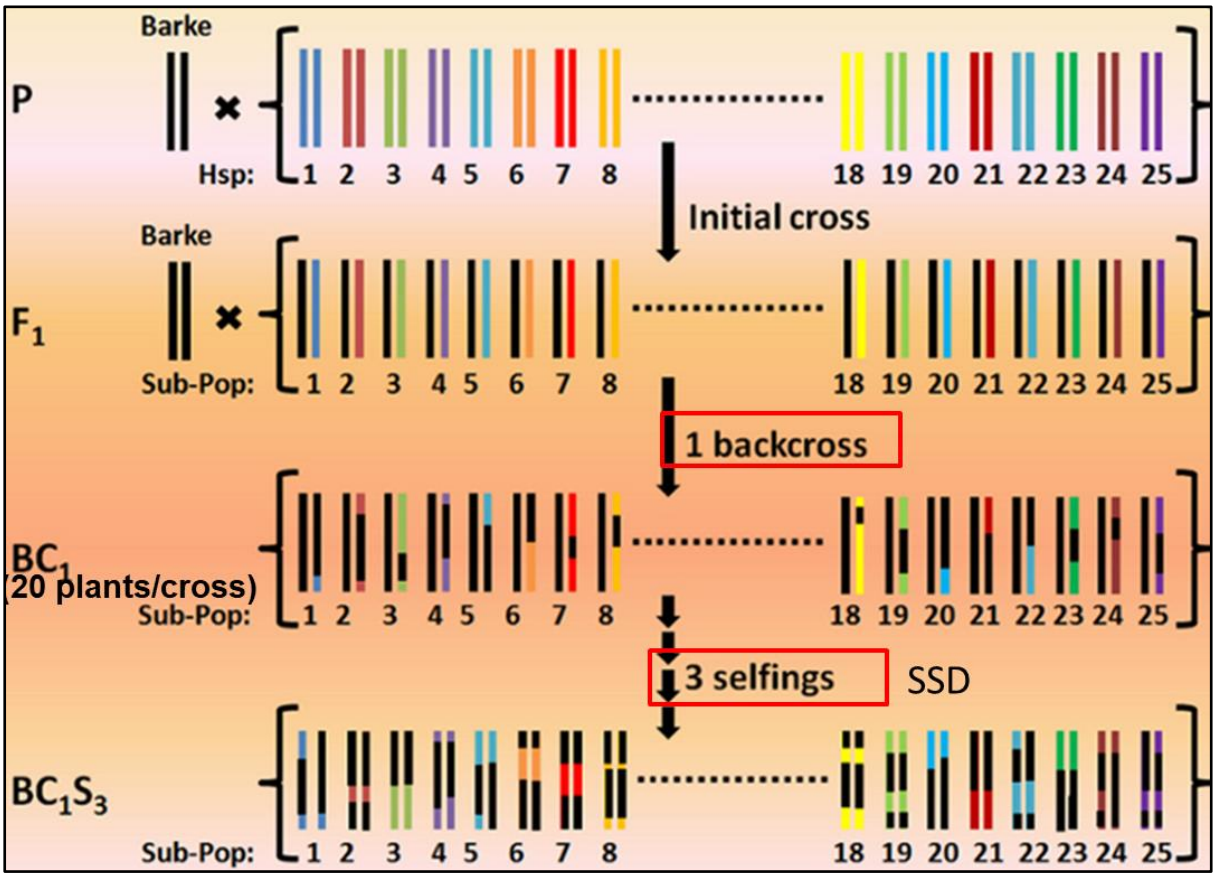

FIGURE 1 Overview of mating strategies used to create the HEB25 Nested Association Mapping (NAM) population (replicated from Figure 1 in Maurer et al 2015). The steps involved crossing of all 25 barleys as donor parents (pollen) to a common parent, Barke as a recipient parent. The F_1 population from the initial cross was backcrossed to Barke. Twenty BC_1s were selfed three times via the Single Seed Descent technique, where one seed of each plant is used to create the next generation. The 1420 BC_1S_3 population includes 25 HEB families with up to 75 lines per family (Source: Maurer et al., 2015).

It has been suggested that one difference that can be observed between commercial barley and some landraces is the ability to form an additional solute barrier, an exodermis, in response to abiotic stress (Kreszies et al., 2019b). Previously, we screened and characterised the apoplastic barrier traits within diverse Hordeum Identity (HID) accessions and selected commercial barley lines; and we screened for lignin and suberin deposition in cell walls (see Chapter 2). Both lignin and suberin are hydrophobic and their deposits in the cell wall are linked to solute barrier formation and are influenced by abiotic stress, such as salinity. One of the HID accessions with notably prominant exodermal lignin and suberin deposition in the exodermal layer based on our analysis was HID138 (see Chapter 2, Figure 2 and Figure 3). We observed that seedlings of the common parent for the HEB25 NAM population, Barke, lacked an obvious exodermal layer (Chapter 2, Figure 2 and Figure 3). Hypothetically, these differences in exodermal solute barriers could influence flux of water, ions and gasses within the roots. Potentially, differences in ion flux could result in differences in tissue ion accumulation in the root and shoot tissues of plants that vary in barrier deposition. However, other factors, such as the potential for differences in membrane transport mechanisms are also likely to vary between the wild HID138 barley, and Barke. In the current study, we investigated the development of the exodermal barriers within HID138 and Barke progeny. The goal was to obtain a better understanding of whether there might be a relationship between variation in barriers and variation in Na^+ and K^+ accumulation. Seed for 57 HEB13s was available for testing. To narrow down which lines would be useful for the planned analysis, we first screened the 57 HEB13s for Na^+ and K^+ content; and subsequently screened for lignin and suberin in a selected sub-set. We used previous leaf ion analysis data as a guide to strategically select lines that had potential to include differences in Na^+ and K^+ accumulation (Figure S1) (Meng et al., 2017). The selected lines were re-tested for leaf and root Na^+ and K^+ accumulation using the protocol we developed for assaying root barrier deposition (see Chapter 2). We then selected a

sub-set of those progeny lines that had the most notable differences in root and shoot Na^+ and K^+ accumulation for use in qualitative imaging for lignin and suberin deposition in roots.

3.2 Materials and methods

3.2.1 Plant materials

The commercial cultivar Barke, HID138 and eleven HEB13 progenies; HEB13-045, HEB13-060, HEB13-104, HEB13-099, HEB13-031, HEB13-066, HEB13-111, HEB13-075, HEB13-081, HEB13-068 and HEB13-097 were selected for this study because variation in leaf Na^+, K^+ and Na^+:K^+ ratios were observed within these lines under saline conditions in previous studies by Saade et al. (2016); Meng et al. (2017) (Figure S1).

3.2.2 Seed imbibition, stratification and paper towel planting

Barley seeds were first imbibed, sterilised and stratified as described in Chapter 2 in material and methods section. After stratification, seeds were first germinated on wet paper towel in dark for 12 h before they were placed in paper towel as described in Chapter 2. For each variety, eight biological replicates per treatment were included. In this experiment, plants were only grown in 40mM NaCl with one quarter strength Hoagland solution as described in Chapter 2.

3.2.3 Root sectioning and screening for the spatial deposition of lignin and suberin

After 7 d of growth in saline conditions, the length of the longest seminal root of each plant was measured. A 3-5 mm root segment at the mid-point of the root maturation zone of the longest seminal root, determined by the emergence of root hairs, was harvested, and embedded in 5 % low melting point agarose gel (Bioline). The embedded root section was then cut transversely in uniform thickness using a vibratome (Vibratome Leica VT1200, Leica Biosystems) prior to staining for suberin and lignin as described in Chapter 2.

3.2.4 Quantification of Na^+ and K^+ accumulation in whole roots of week-old seedlings

Whole roots and shoots of 7d-old HEB13s barley seedlings were harvested, dried and biomass recorded. The ion accumulation in both roots and shoots was measured using the protocol described in Chapter 2.

3.3 Statistical analysis

Data was analysed using GraphPad Prism (version 8). For the phenotypic data, such as biomass accumulation and root length, the data values for each plant were compared using the one-way ANOVA Tukey's multiple comparison test. For the ion analysis data, the values were compared with the 'control' genotype, Barke using the one-way ANOVA Dunnet's multiple comparison test. For each experiment and in each container Barke was included and the replicates of Barke, HID138 and the different HEB13 progeny were randomised in a design that was blocked by the column and row within the container such that replicates were distributed across columns and rows within the containers.

3.4 Results

3.4.1 Root and shoot biomass accumulation, length, root morphology and anatomy

The values for root and shoot biomass accumulation at 40 mM NaCl were similar in their pattern among HEB lines (Figure 2a, b). Root and shoot biomass and root-to-shoot biomass ratio for each of the HEB13 lines were within a range between the values recorded for their parents, Barke and HID138 (Figure 2). With the exception of HEB13-060 and HEB099, the remaining HEBs accumulated less root and shoot dry biomass than Barke (Figure 2a, b). HID138 accumulated the least root and shoot biomass relative to Barke and the majority of the HEB13s tested (Figure 2a, b). HEB13-031, HEB097 and HID138 had greater root-to-shoot biomass ratios than other lines, and no significant differences were observed for other lines in relation to root-to-shoot biomass ratios relative to Barke (Figure 2c). HEB13-097 was the only HEB that did not significantly differ in shoot dry biomass and root-to-shoot biomass ratio

relative to HID138 (Figure 2b, c). HID138 accumulated the least total dry biomass relative to the HEB13s and Barke (Figure 2d). HEB13-060 and HEB13-099 had similar total biomass accumulation to Barke while the remaining HEB13s accumulated less biomass than Barke (Figure 2d).

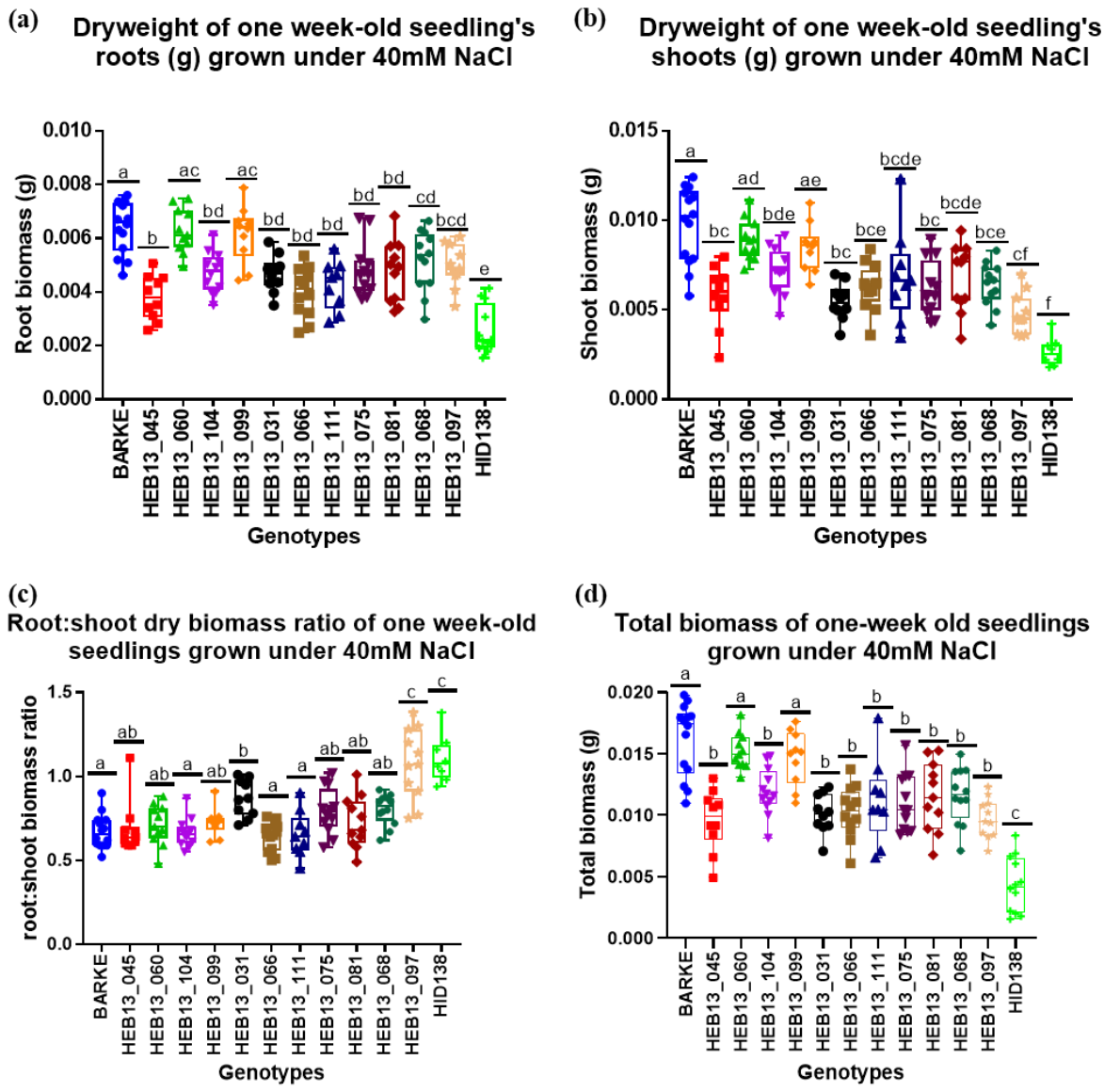

FIGURE 2 Root and shoot biomass of HEB13 plants grown under saline conditions (40 mM NaCl). (a) Root dry biomass of one-week-old seedlings. (b) Shoot dry biomass of one-week-old seedlings. (c) Root to shoot dry biomass ratio of one-week-old seedlings. (d) Total biomass of one-week old seedlings. Data points represent individual biological replicates (n=9-14). The middle horizontal line inside the box is the median value. Each of the genotypes were compared to each other using one-way ANOVA

Tukey's multiple comparison test. Different letters denote a significant difference between means (at least $p < 0.05$).

HID138 had longer root lengths but shorter shoot lengths relative to Barke, whereas the other HEBs did not differ in this parameter (Figure S2a, b). HEB13-097 was the only HEB13 with longer root lengths but similar shoot lengths relative to Barke. In general, the majority of the root and shoot lengths of the HEB13 lines nestled in between both parents (Figure S2).

The mid-point of the root maturation zone of the seminal roots had one large central metaxylem with eight to nine xylem vessels, all plants investigated had this in common (Figure 4 and Figure 5). Differences were found regarding the organisation of the root cortex. Barke, HEB13-060, HEB13-099, HEB13-097 had four cell layers in the cortex, whereas HID138, HEB13-045, HEB13-081, HEB13-068 had three cortex cell layers at the developmental stage investigated (Figure 4 and Figure 5).

3.4.2 Root and shoot ion accumulation in one-week-old seedlings of Barke, HID138 and selected HEB13s following 40 mM NaCl treatments

Barke and HID138 had the largest differences in exodermal barrier under saline conditions compared to the other wild accessions. These differences could hypothetically be one of the key factors contributing to differences in shoot ion accumulation. This raises the possibility that some of the progeny (HEB13) lines from a cross between Barke and HID138 might inherit solute barrier traits from one or other of the parents and this could influence the tissue ion accumulation. One of the advantages of working with these specific wild barley accessions is that they have been included in a NAM population. HEB progeny plants contain predominantly Barke DNA, with sections of DNA from the different HID accessions (Figure 1). This makes it possible to search for putative HID inherited diffusion barrier traits in a Barke background. Using previous data for HEB13 shoot ion accumulation from Meng et al. (2017), we selected a few HEB lines with the biggest differences in ion accumulation to see if there would be any

differences in ion accumulation in both root and shoots in our conditions, and any differences in root barrier layers, using our experimental set-up. Differences were observed for some lines in relation to their tissue Na^+ and K^+ accumulation in a test of HID138 and Barke relative to their HEB13 progeny lines. There were no differences in shoot Na^+ ion accumulation in any of the HEB lines of one-week-old seedlings in saline conditions (Figure 3d). However, both HID138 and HEB13-081 had significantly less root Na^+ accumulation compared to Barke in saline conditions (Figure 3a). There was variation in the K^+ accumulation for both root and shoot within the lines tested (Figure 3b, e). HID138 and all HEB13 progenies except HEB13-045 had significantly had less leaf K^+ accumulation relative to Barke (Figure 3e). HID138 and some of the progeny lines including HEB13-66, HEB13-111, HEB13-075, HEB13-081, HEB13-068 and HEB13-097 had significantly higher root K^+ accumulation relative to Barke, whereas for the rest of the lines there was no difference (Figure 3b). All of the lines, except HEB13-081, did not differ in their shoot Na^+:K^+ ratio relative to Barke (Figure 3f); whereas HID138 and most of the HEB13 progeny lines, except HEB13-45 and HEB13-60, had lower root Na^+:K^+ ratios relative to Barke (Figure 3c).

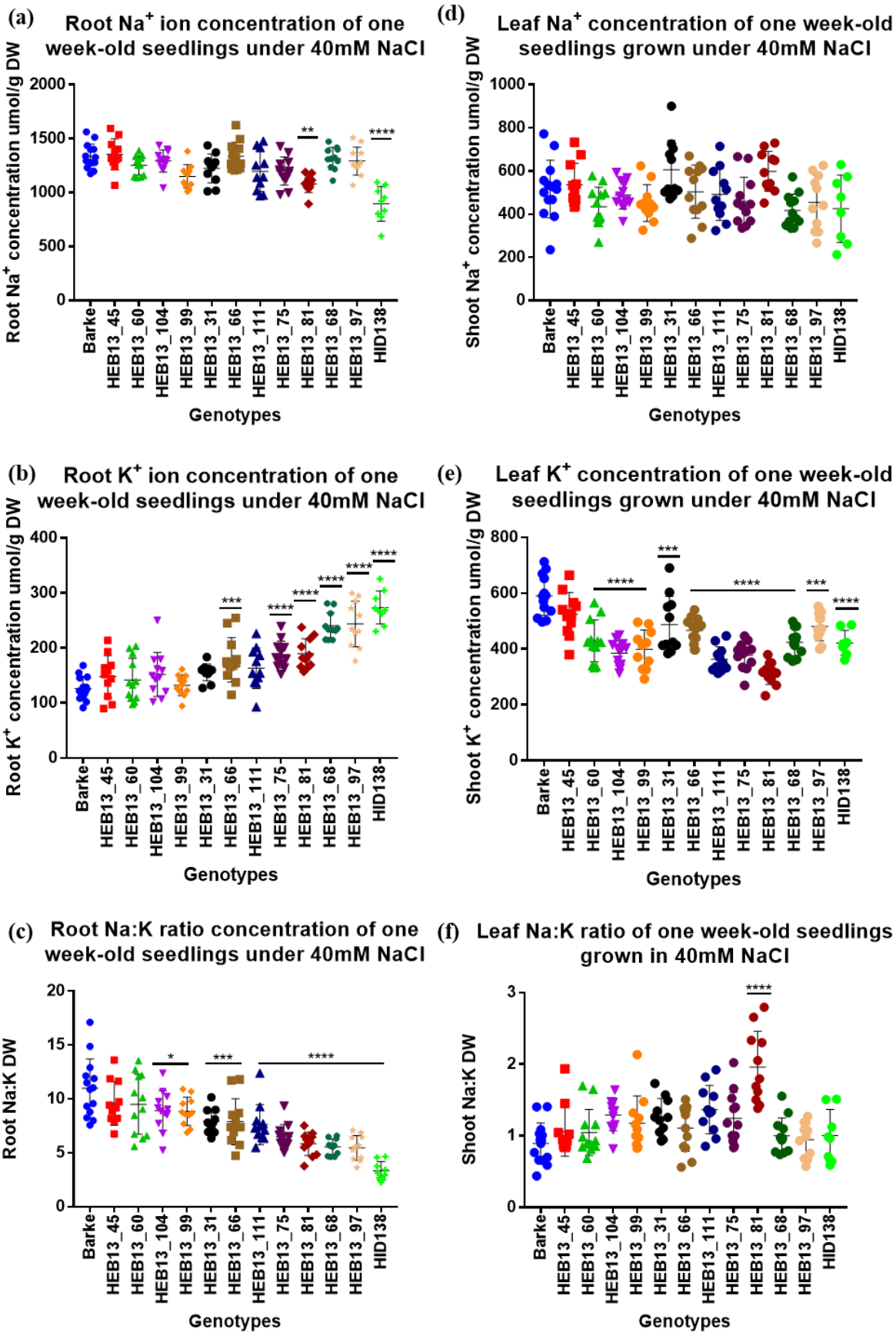
(a)
Root Na+ ion concentration of one week-old seedlings under 40mM NaCl
Root Na+ concentration umol/g DW
2000
1500
1000
500
0
**
****
Barke
HEB13_45
HEB13_60
HEB13_104
HEB13_99
HEB13_31
HEB13_66
HEB13_111
HEB13_75
HEB13_81
HEB13_68
HEB13_97
HID138
Genotypes
(d)
Leaf Na+ concentration of one week-old seedlings grown under 40mM NaCl
Shoot Na+ concentration umol/g DW
1000
800
600
400
200
0
Barke
HEB13_45
HEB13_60
HEB13_104
HEB13_99
HEB13_31
HEB13_66
HEB13_111
HEB13_75
HEB13_81
HEB13_68
HEB13_97
HID138
Genotypes
(b)
Root K+ ion concentration of one week-old seedlings under 40mM NaCl
Root K+ concentration umol/g DW
400
300
200
100
0
***
****
****
****
****
Barke
HEB13_45
HEB13_60
HEB13_104
HEB13_99
HEB13_31
HEB13_66
HEB13_111
HEB13_75
HEB13_81
HEB13_68
HEB13_97
HID138
Genotypes
(e)
Leaf K+ concentration of one week-old seedlings grown under 40mM NaCl
Shoot K+ concentration umol/g DW
800
600
400
200
0
***
****
****
***
****
Barke
HEB13_45
HEB13_60
HEB13_104
HEB13_99
HEB13_31
HEB13_66
HEB13_111
HEB13_75
HEB13_81
HEB13_68
HEB13_97
HID138
Genotypes
(c)
Root Na:K ratio concentration of one week-old seedlings under 40mM NaCl
Root Na:K DW
20
15
10
5
0
*
***
****
Barke
HEB13_45
HEB13_60
HEB13_104
HEB13_99
HEB13_31
HEB13_66
HEB13_111
HEB13_75
HEB13_81
HEB13_68
HEB13_97
HID138
Genotypes
(f)
Leaf Na:K ratio of one week-old seedlings grown in 40mM NaCl
Shoot Na:K DW
3
2
1
0
****
Barke
HEB13_45
HEB13_60
HEB13_104
HEB13_99
HEB13_31
HEB13_66
HEB13_111
HEB13_75
HEB13_81
HEB13_68
HEB13_97
HID138
Genotypes

FIGURE 3 Profiling of the ion accumulation of selected progeny and parents. Root (a) Na^+, (b) K^+, (c) Na^+:K^+ ratio and shoot (d) Na^+, (e) K^+, (f) Na^+:K^+ ratio for Barke and HID138 and selected HEB13 progeny lines grown in media containing 40mM NaCl. The amounts of both Na^+ and K^+ were normalised to the tissue dry weight (DW). The ion contents and ratio for each of the lines were compared with the commercial barley line, Barke using one-way ANOVA, Dunnet's multiple comparison test. Data represent individual biological replicates (symbols), means (wide horizontal line) ± SEM (standard error mean) (n = 7-16). ANOVA significant difference $p<0.05$, $p<0.01$, $p<0.001$ and $p<0.0001$ indicated by (*), (**), (***) and (****) respectively.

3.4.3 Spatial suberin deposition in Barke, HID138 and selected HEB13s in saline conditions

Barke had the lowest fluorescence intensity in its exodermal layer relative to the other plants tested (Figure 4). Only few cells in the Barke cortex layer beneath the epidermis had a weak fluorescence intensity in the anticlinal walls of these cells but not in the tangential walls (Figure 4). All selected HEB13s resembled HID138 and showed suberin deposition in an exodermal cell layer and there was no obvious difference in the intensity of the exodermal fluorescence signal (Figure 4). However, there was variation in the pattern of the distribution of the fluorescence signal. For example, HEB13-045 had strong fluorescence in the anticlinal walls of the exodermal cells, but had a much lower relative signal in the tangential walls of the exodermal cells, compared to HID138 (Figure 4). HEB13-068 and HEB13-081 had strong fluorescent signal and therefore likely high suberin deposition in both anticlinal and tangential walls in the majority of their exodermal cells. HID138, as we had previously found (Chapter 2, Figure 2 and Figure 3), had a high fluorescence intensity in all of its exodermal cell walls, surrounding the entire perimeter connecting with the cortical cells (Figure 4). In addition to variation in exodermis deposition, we also found variations in the endodermis. For HEB13-068, HEB13-081 and HEB13-097, the fluorescence intensity of the outer tangential walls appeared higher relative to that of the inner tangential walls of the endodermal cells (Figure 4).

In general, the intensity of the fluorescence in the endodermal cell layer was stronger relative to the exodermal cell layer in each of the plants tested (Figure 4). This indicates that more suberin was deposited in the endodermal cells compared to exodermal cells, in accordance to the previous studies (Schreiber et al., 1999; Schreiber et al., 2005a). In Barke, HEB13-099 and HEB13-097, endodermal passage cells without extensive suberin deposition were detected (Figure 4). We observed that HEB13-97 plants had the strongest fluorescence signal in the endodermal layer relative to the all the other plants tested (Figure 4). In the majority of the plants tested the fluorescence intensity in the outer tangential walls of the endodermal cells was brighter relative to the intensity from the inner tangential walls. In some lines such as HEB13-97 and HEB13-99, there was noticeable fluorescence in the cortical cells, whereas in other plants such as HEB13-060 and HEB13-068, there was no obvious fluorescence detected in the cortical cells. There was no obvious fluorescence detected in epidermal, xylem or central metaxylem cell walls at the seedling stage tested in majority of the lines (Figure 4). However, it is important to note here that in some lines, for example HEB13-097 and HID138, there was possibly autofluorescence such as in central metaxylem which does not correspond to suberin (Figure 4).

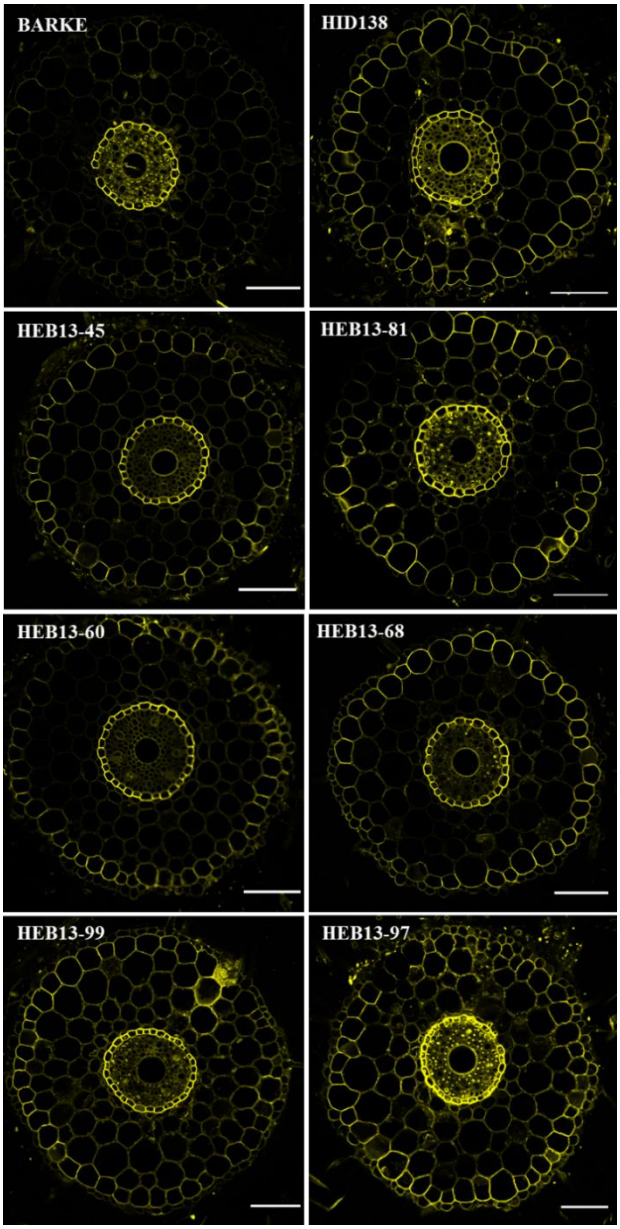

FIGURE 4 Spatial deposition of suberin in the roots of Barke (parent), HID138 (parent), HEB13-45, HEB13-60, HEB13-99, HEB13-81, HEB13-68, HEB13-97. Root sections were from the longest seminal roots of 7 d old 40 mM NaCl treated barley seedlings. Cross sections were made at the maturation zones. Spatial deposition of suberin were determined using Fluorol Yellow 088 (Brundrett et al., 1991). Suberin stain signal was obtained using confocal microscopy and it is shown in yellow. Suberin images and scales were generated using (Fiji is Just) ImageJ. Scale bars: 100µm.

3.4.4 Spatial lignin deposition in Barke, HID138 and selected HEB13s in saline conditions

The intensity of red lignin-associated staining varied between cell types, and between parent and progeny plants tested (Figure 5). In all of the plants tested the xylem vessels had the greatest intensity of red staining relative to other cell types, which was expected. The other two cell layers with the most notable red staining were the anticlinal walls of both endodermal and exodermal cells. The intensity of the lignin staining in the exodermal layer varied between parent and progeny plants. Barke had the least intense red staining in its anticlinal walls of its exodermal cells, relative to HID138 and the HEB13s (Figure 5). HEB13-45 and HEB13-97 had weak red staining, visible as a faint pinkish colour (Figure 5). The other HEB13s such as HEB13-060, HEB13-068 and HEB13-081 had more intense red staining relative to Barke, HEB13-45 and HEB13-97 (Figure 5). However, there was no obvious difference in the intensity of the red staining between HEB13-060, HEB13-081, HEB13-068 and HID138 (Figure 5).

There was variation in the pattern of red staining in the exodermal layer. The red staining could only be observed specifically in the anticlinal walls of both the endodermal and exodermal cell layers, and no red staining was detected in the tangential sections in these cell layers in any plant tested (Figure 5). This is a typical lignin deposition pattern in apoplastic barriers, the Casparian strip (Hose et al., 2001; Geldner, 2013; Kotula et al., 2014). For Barke, HEB13-45 and HEB13-97 we observed that not all of the anticlinal walls of the exodermal cells had red staining (Figure 5). In all of the plants tested the red staining appeared in a pattern equivalent to a straight line covering the length of the anticlinal walls between the cells (Figure 5).

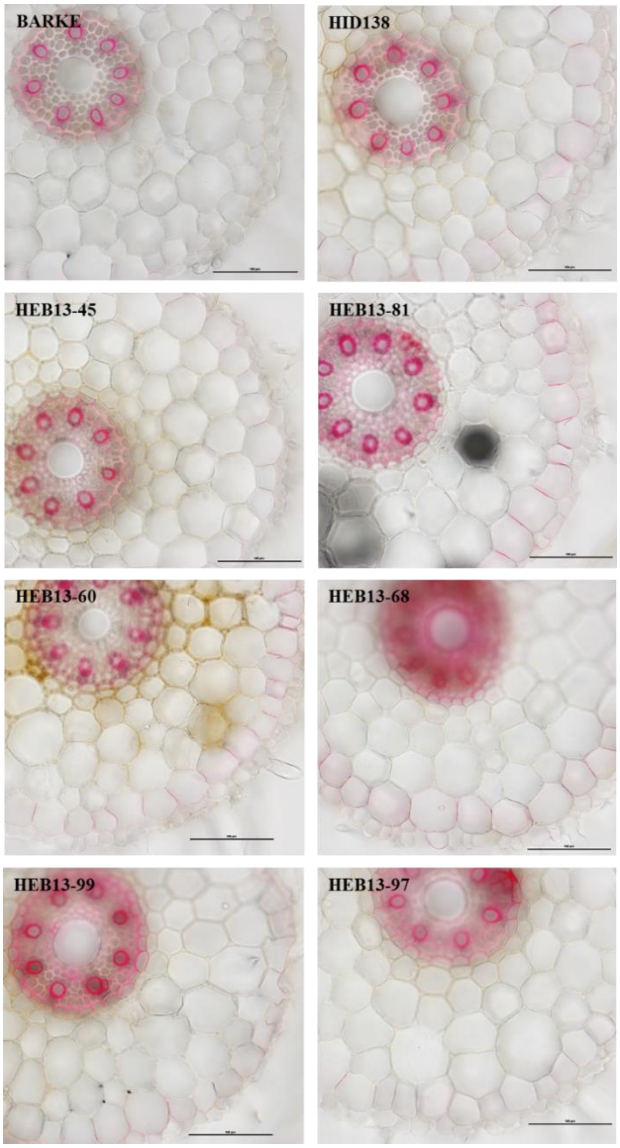

FIGURE 5 Images representing the spatial deposition of lignin in the roots of Barke (parent), HID138 (parent), HEB13-45, HEB13-60, HEB13-99, HEB13-81, HEB13-68, HEB13-97. Root sections were from the longest seminal roots of 7 d old 40 mM NaCl treated barley seedlings. Cross sections were made at the maturation zones. Spatial deposition of lignin was determined using Phloroglucinol-HCl (Mitra and Loqué, 2014) staining. Lignin stain was obtained using bright-field microscope and lignin staining appears as a red colour. Scale bars: 100µm.

3.5 Discussion

One key focus of barley domestication is likely to have been a focus on selecting for maximum seed yield and above ground biomass yield, and selection is likely to have occurred under relatively favourable conditions (Den Herder et al., 2010; Koevoets et al., 2016). This could have inadvertently led to smaller root systems in many modern barley lines relative to wild ancestors (White et al., 2013; Koevoets et al., 2016).

Our investigation of root and shoot biomass accumulation in diverse barley plants revealed that Barke and all of the HEB13 plants tested, except for HEB13-097, accumulated more biomass in the shoot relative to the roots, whereas HID138 and HEB13-097 had similar shoot relative to root biomass accumulation (Figure 2c). This indicates that the majority of the HEB13 plants probably inherited traits from Barke that result in allocation of more carbon and other resources to the shoot rather than to the root at a seedling stage. HEB13-097 was the only HEB13 in our study that maintained approximately equal ratios of root:shoot biomass and longer root length, similar to its wild parent, HID138 (Figure 2c and Figure S2a). HID138 originated in semiarid environments in Iran, where water-stressed conditions are common (Maurer et al., 2015). Water-stressed conditions may cause selection pressure that favours prioritisation of mechanisms that support development of roots over shoots for survival (Zhou et al., 2018). This indicates that the genetic adaptation in HID138 to constitutively exhibit morphological adaptations to low-water environments could have been passed on to HEB-097.

A previous study has suggested that enhanced root lignification could be a contributing factor for the stunted root growth of salt treated soybean seedlings (Neves et al., 2010). Similarly, we found that HID138 with enhanced exodermal lignin deposition had less biomass compared to Barke (Figure 2). However, it is still unclear whether the strong apoplastic barrier caused this. The findings in HEB13s progenies suggest that this may not always be true. For example, we found that HEB-060 with noticeable exodermal lignin (Figure 5) had a total

biomass as large as Barke (Figure 2). Also, HEB13-81 had very strong lignin and suberin deposition similar to those in HID138 (Figure 4 and Figure 5) but had more total biomass compared to HID138 (Figure 2d). This indicates that exodermal lignin alone could not have caused a reduced growth and that other factors could also determine the overall root growth.

It is currently not known whether previously observed variation in root ion accumulation is linked to differences in diffusion barriers between Barke and HID138. Barke lacked exodermal lignin and suberin whereas HID138 deposited exodermal suberin and lignin (Figure 4 and Figure 5). Given that we observed that HEB13-097 was lacking in exodermal lignin but retained K^+ in roots, this indicates that exodermal lignin is unlikely to be the sole factor preventing K^+ loss, at least in the material tested. Rather, we found that HEB13-97 had thick endodermal suberin and obvious deposition of suberin in some exodermal and cortical cells. Hypothetically, it could be that the deposition of suberin in these cells might slow down the root K^+ efflux and root Na^+ influx, leading to lower root Na^+:K^+ ratios. This is suggested to be important for root growth with a previous study, Ranathunge and Schreiber (2011) reporting that Arabidopsis *horst* mutant roots with reduced endodermal suberin had a higher water and NaCl permeability than controls. In contrast, Arabidopsis *esb1* mutants with enhanced suberisation in the endodermis had increased water-use-efficiency and reduced day time transpiration rate, limiting water loss during the vegetative growth stage compared to controls (Baxter et al., 2009). This comes, however, with the cost of a strongly reduced shoot biomass (Neves et al., 2010).

HEB13-081 had low accumulation of leaf K^+ compared to Barke, and a comparable level of Na^+ accumulation (Figure 3). This resulted in a greater leaf Na^+:K^+ ratio in HEB13-81 when compared to Barke (Figure 3f). This was consistent with the trends in the ion data from Meng et al. (2017) showing that HEB13-81 had greater leaf Na^+, but less leaf K^+ and greater leaf Na^+:K^+ ratio (Figure S1). In our study, HEB13-081 had high Na^+:K^+ than Barke and all of

the lines tested, but was still able to maintain shoot growth suggesting another mechanism was used to tolerate high leaf Na^+, such as (but not limited to) compartmentalization of cytosolic leaf Na^+ into the vacuole by tonoplast membrane transporter (Apse et al., 1999). Relative to Barke, HEB13-081 had less root Na^+, and more root K^+ and lower root Na^+:K^+ ratios (Figure 3a, b, c). Both Barke and HEB13-81 also differed in solute barriers (Figure 4 and 5). Barke lacked exodermal lignin and suberin, whereas HEB13-81 had strong lignin deposition based on the intensity of the stain and an obvious exodermal suberin deposition (Figure 4 and Figure 5). These differences in barrier properties suggest that Barke and HEB13-81 may have different strategies in regulating solute uptake. HEB13-81 might have inherited barrier properties from its wild parent, HID138. Hypothetically HID13-081 and HID138 might have invested more resources into root cell wall modification to prevent Na^+ influx and/or K^+ or water efflux. HEB13-81 could be useful for comparison with Barke in future research focussed on studying key factors that influence differences in K^+ retention or other traits that enabled the plant to grow well by tolerating high Na^+:K^+ ratio. Other HEB13s, such as HEB13-45 behaved more similarly to Barke, in that HEB13-45 had significantly greater leaf K^+ but less root K^+ compared to HID138 (Figure 3b, e). HEB13-45 had a weak exodermal barrier which could have potentially influenced fluxes (Figure 4 and Figure 5). Barke and HEB13-45 might regulate fluxes differently to both HEB13-81 and HID138, and further research is needed to test this theory.

In conclusion, this study shows that phenotypic variation in terms of dry biomass and length and root and shoot ion accumulation of the selected progenies lines are nested within their parents, Barke and HID138. We observed heritability of root traits from HID138 at the seedling stage including the development of exodermal layer in most of the progenies tested. There was no obvious relationship between the deposition of exodermal barriers and ion

accumulation and overall biomass in the plants tested suggesting that there were other mechanisms responsible for the variation in leaf ion accumulation in these lines.

3.6 Supplementary Figures

(a)

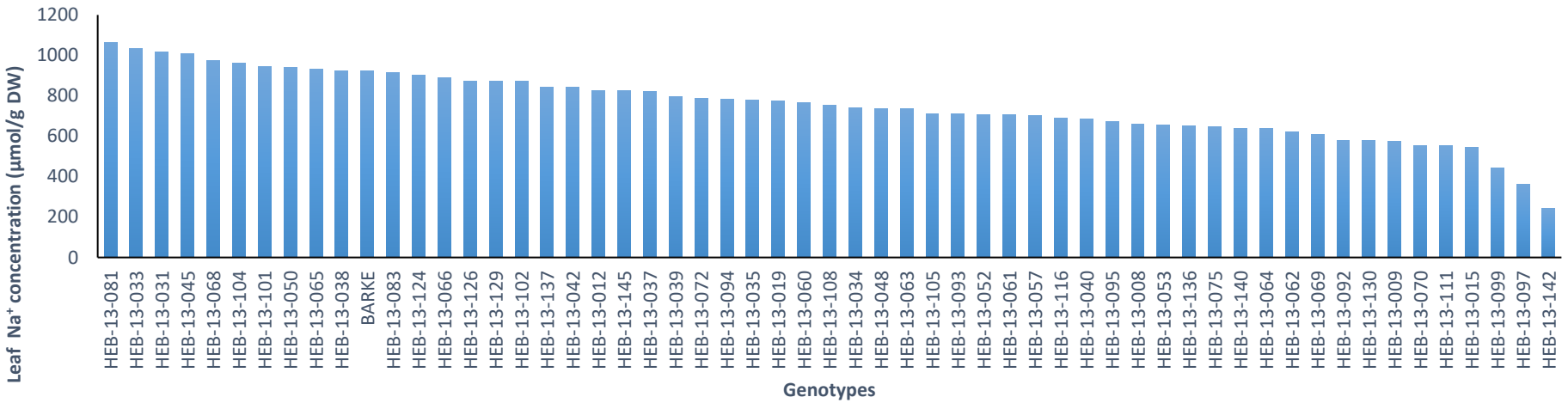
Leaf Na⁺ concentration (µmol/g DW)
1200
1000
800
600
400
200
0
HEB-13-081
HEB-13-033
HEB-13-031
HEB-13-045
HEB-13-068
HEB-13-104
HEB-13-101
HEB-13-050
HEB-13-065
HEB-13-038
BARKE
HEB-13-083
HEB-13-124
HEB-13-066
HEB-13-126
HEB-13-129
HEB-13-102
HEB-13-137
HEB-13-042
HEB-13-012
HEB-13-145
HEB-13-037
HEB-13-039
HEB-13-072
HEB-13-094
HEB-13-035
HEB-13-019
HEB-13-060
HEB-13-108
HEB-13-034
HEB-13-048
HEB-13-063
HEB-13-105
HEB-13-093
HEB-13-052
HEB-13-061
HEB-13-057
HEB-13-116
HEB-13-040
HEB-13-095
HEB-13-008
HEB-13-053
HEB-13-136
HEB-13-075
HEB-13-140
HEB-13-064
HEB-13-062
HEB-13-069
HEB-13-092
HEB-13-130
HEB-13-009
HEB-13-070
HEB-13-111
HEB-13-015
HEB-13-099
HEB-13-097
HEB-13-142
Genotypes

(b)

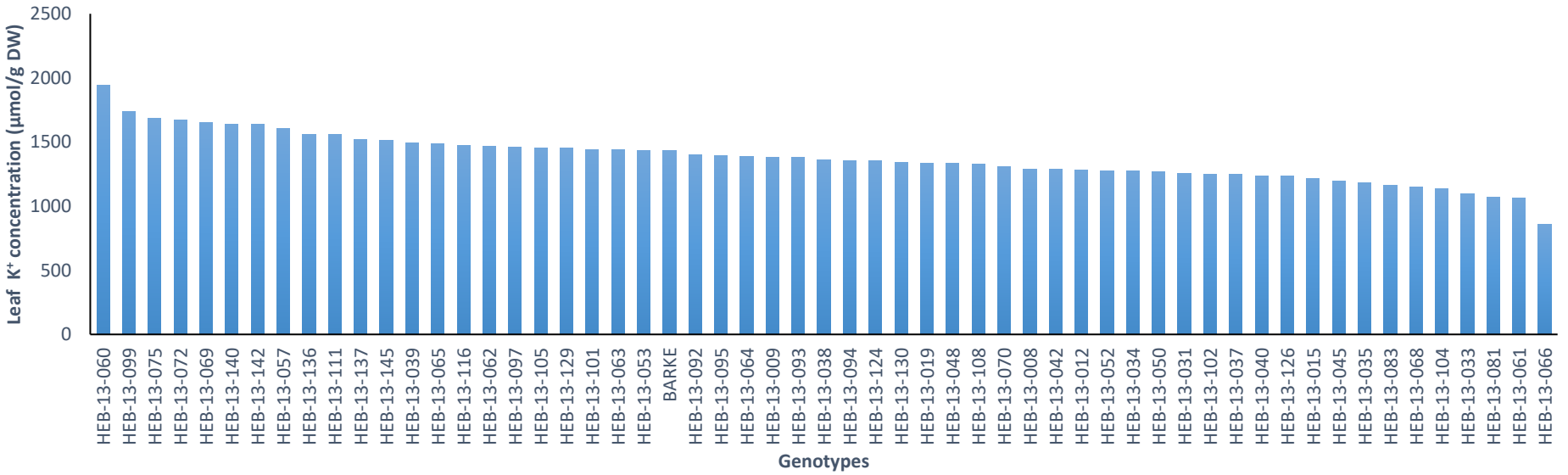
Leaf K⁺ concentration (µmol/g DW)
2500
2000
1500
1000
500
0
HEB-13-060
HEB-13-099
HEB-13-075
HEB-13-072
HEB-13-069
HEB-13-140
HEB-13-142
HEB-13-057
HEB-13-136
HEB-13-111
HEB-13-137
HEB-13-145
HEB-13-039
HEB-13-065
HEB-13-116
HEB-13-062
HEB-13-097
HEB-13-105
HEB-13-129
HEB-13-101
HEB-13-063
HEB-13-053
BARKE
HEB-13-092
HEB-13-095
HEB-13-064
HEB-13-009
HEB-13-093
HEB-13-038
HEB-13-094
HEB-13-124
HEB-13-130
HEB-13-019
HEB-13-048
HEB-13-108
HEB-13-070
HEB-13-008
HEB-13-042
HEB-13-012
HEB-13-052
HEB-13-034
HEB-13-050
HEB-13-031
HEB-13-102
HEB-13-037
HEB-13-040
HEB-13-126
HEB-13-015
HEB-13-045
HEB-13-035
HEB-13-083
HEB-13-068
HEB-13-104
HEB-13-033
HEB-13-081
HEB-13-061
HEB-13-066
Genotypes

c)

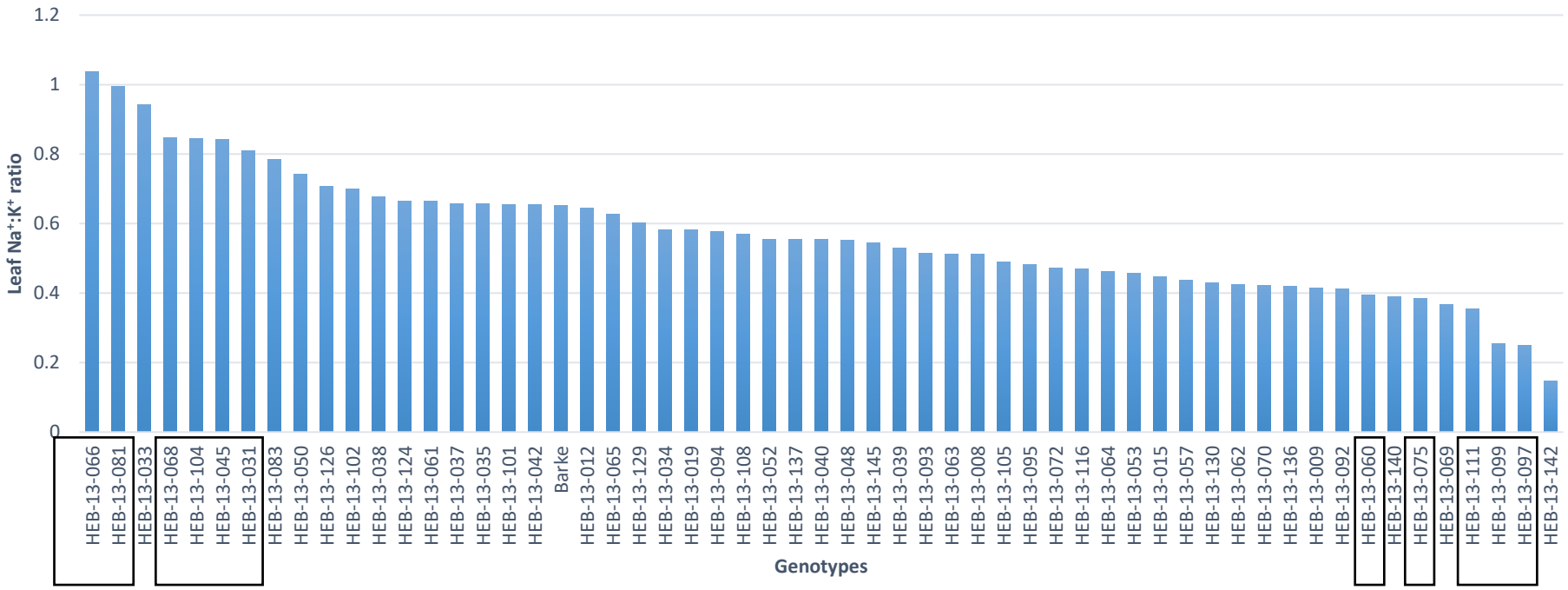

FIGURE S1 The accumulation of Na^+, K^+ and the Na^+:K^+ ratios in fully expanded fourth leaf of 200mM NaCl treated HEB13s and Barke plants (Meng et al., 2017). (a) The accumulation of leaf Na^+. (b) The accumulation of leaf K^+. (c) leaf Na^+:K^+ ion ratio. The data shown here was obtained from a single plant. (c), the highlighted HEB13 lines were selected for this study. Barley material such HEB13-033, HEB13-142 were not available by the time the study was started.

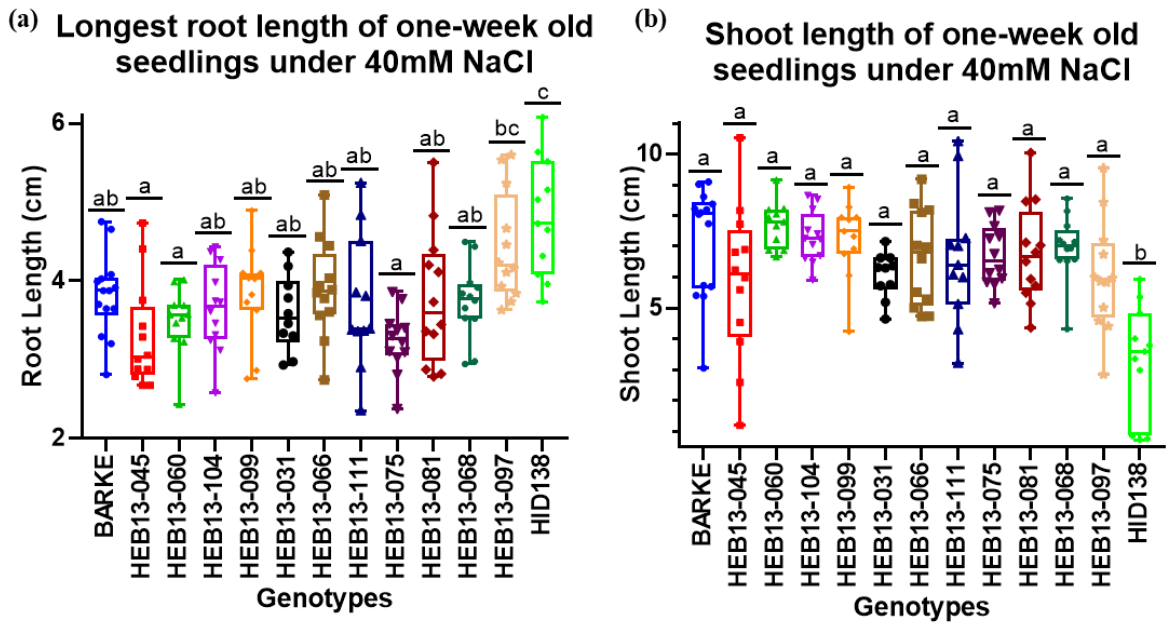

FIGURE S2 Longest root and shoot length of one week-old HEB13 seedlings treated with 40 mM NaCl. (a) Longest seminal root and (b) shoot length. Data points represent individual biological replicates (symbols), median is marked by the horizontal line in the box, the ends of the box are lower and upper quartiles and the whisker are the lowest and highest point. Each genotype was compared to one another using one-way ANOVA Tukey' multiple comparison test. Different letters indicate significant differences between means at a significance level of at least 0.05.

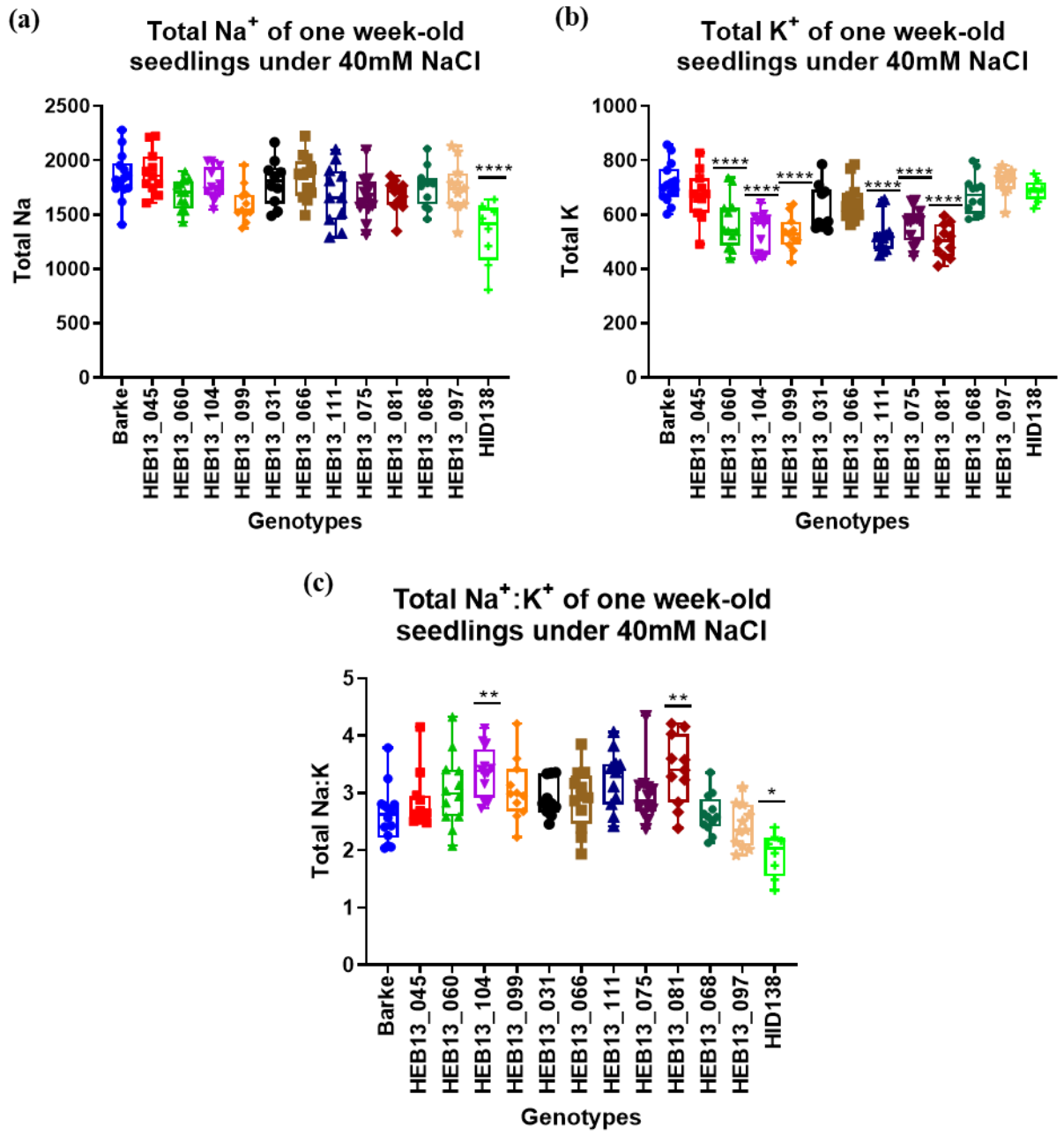

FIGURE S3 Total Na^+ (a), K^+ (b) and Na^+:K^+ ratio (c) of one-week old seedlings treated with 40 mM NaCl. Each genotype (landraces) was compared to Barke using one-way ANOVA Dunnet's multiple comparison test. Data points represent individual biological replicates (symbols), median is marked by the horizontal line in the box, the ends of the box are lower and upper quartiles and the whisker are the lowest and highest point. ANOVA significant difference $p<0.05$, $p<0.01$, $p<0.001$ and $p<0.0001$ indicated by (*), (**), (***) and (****) respectively.

3.7 References

Apse MP, Aharon GS, Snedden WA, Blumwald E (1999) Salt tolerance conferred by overexpression of a vacuolar Na^+/H^+ antiport in Arabidopsis. Science **285:** 1256-1258

Badr A, Muller K, Schafer-Pregl R, El Rabey H, Effgen S, Ibrahim HH, Pozzi C, Rohde W, Salamini F (2000) On the origin and domestication history of barley (*Hordeum vulgare*). Molecular Biology and Evolution **17:** 499-510

Baxter I, Hosmani PS, Rus A, Lahner B, Borevitz JO, Muthukumar B, Mickelbart MV, Schreiber L, Franke RB, Salt DE (2009) Root suberin forms an extracellular barrier that affects water relations and mineral nutrition in Arabidopsis. Plos Genetics **5**

Brundrett MC, Kendrick B, Peterson CA (1991) Efficient lipid staining in plant-material with Sudan red-7B or Fluoral yellow-088 in polyethylene glycol-glycerol. Biotechnic & Histochemistry **66:** 111-116

Den Herder G, Van Isterdael G, Beeckman T, De Smet I (2010) The roots of a new green revolution. Trends in Plant Science **15:** 600-607

Geldner N (2013) The endodermis. *In* SS Merchant, ed, Annual Review of Plant Biology, Vol 64, Vol 64, pp 531-558

Hose E, Clarkson D, Steudle E, Schreiber L, Hartung W (2001) The exodermis: a variable apoplastic barrier. Journal of Experimental Botany **52:** 2245-2264

Islam S, Malik AI, Islam A, Colmer TD (2007) Salt tolerance in a *Hordeum marinum-Triticum aestivum* amphiploid, and its parents. Journal of Experimental Botany **58:** 1219-1229

Koevoets IT, Venema JH, Elzenga JT, Testerink C (2016) Roots withstanding their environment: exploiting root system architecture responses to abiotic stress to improve crop tolerance. Frontiers in Plant Science **7:** 1335

Kotula L, Colmer TD, Nakazono M (2014) Effects of organic acids on the formation of the barrier to radial oxygen loss in roots of *Hordeum marinum*. Functional Plant Biology **41:** 187-202

Kreszies T, Eggels S, Kreszies V, Osthoff A, Shellakkutti N, Baldauf JA, Zeisler-Diehl VV, Hochholdinger F, Ranathunge K, Schreiber L (2019b) Seminal roots of wild and cultivated barley differentially respond to osmotic stress in gene expression, suberization, and hydraulic conductivity. Plant, Cell & Environment

Maurer A, Draba V, Jiang Y, Schnaithmann F, Sharma R, Schumann E, Kilian B, Reif JC, Pillen K (2015) Modelling the genetic architecture of flowering time control in barley through nested association mapping. Bmc Genomics **16**

Meng R, Saade S, Kurtek S, Berger B, Brien C, Pillen K, Tester M, Sun Y (2017) Growth curve registration for evaluating salinity tolerance in barley. Plant Methods **13**

Mitra PP, Loqué D (2014) Histochemical Staining of *Arabidopsis thaliana* Secondary Cell Wall Wlements. JoVE (Journal of Visualized Experiments)**:** e51381

Munns R, Gilliham M (2015) Salinity tolerance of crops–what is the cost? New Phytologist **208:** 668-673

Munns R, Tester M (2008) Mechanisms of salinity tolerance. Annual Review of Plant Biology **59:** 651-681

Neves GYS, Marchiosi R, Ferrarese MLL, Siqueira-Soares RC, Ferrarese O (2010) Root growth inhibition and lignification induced by salt stress in soybean. Journal of Agronomy and Crop Science **196:** 467-473

Ranathunge K, Schreiber L (2011) Water and solute permeabilities of *Arabidopsis* roots in relation to the amount and composition of aliphatic suberin. Journal of Experimental Botany **62:** 1961-1974

Saade S, Maurer A, Shahid M, Oakey H, Schmockel SM, Negrao S, Pillen K, Tester M (2016) Yield-related salinity tolerance traits identified in a nested association mapping (NAM) population of wild barley. Scientific Reports **6**

Schreiber L, Franke R, Hartmann K (2005a) Effects of NO_3 deficiency and NaCl stress on suberin deposition in rhizo- and hypodermal (RHCW) and endodermal cell walls (ECW) of castor bean (*Ricinus communis L.*) roots. Plant and Soil **269:** 333-339

Schreiber L, Hartmann K, Skrabs M, Zeier J (1999) Apoplastic barriers in roots: chemical composition of endodermal and hypodermal cell walls. Journal of Experimental Botany **50:** 1267-1280

Tanksley SD, McCouch SR (1997) Seed banks and molecular maps: unlocking genetic potential from the wild. Science **277:** 1063-1066

Tilbrook J, Schilling RK, Berger B, Garcia AF, Trittermann C, Coventry S, Rabie H, Brien C, Nguyen M, Tester M (2017) Variation in shoot tolerance mechanisms not related to ion toxicity in barley. Functional Plant Biology **44:** 1194-1206

White PJ, George TS, Gregory PJ, Bengough AG, Hallett PD, McKenzie BM (2013) Matching roots to their environment. Annals of Botany **112:** 207-222

Zhou G, Zhou X, Nie Y, Bai SH, Zhou L, Shao J, Cheng W, Wang J, Hu F, Fu Y (2018) Drought-induced changes in root biomass largely result from altered root morphological traits: Evidence from a synthesis of global field trials. Plant, Cell & Environment **41:** 2589-2599

Chapter 4:

HvHKT1;5 SNP detection within diverse barley accessions and expression analysis during early development

Chapter 4: *HvHKT1;5* SNP detection within diverse barley accessions and expression analysis during early development

4.0 Abstract

Regulation of root-to-shoot Na^+ transport is one of the key factors influencing plant survival in saline environments. The Na^+-transporter HKT1;5 plays a major role in limiting root-to-shoot Na^+ transport, and thus maintaining high leaf K^+:Na^+ ratio, which is crucial for most crop plants. Amino acid differences in HvHKT1;5 influence its Na^+ transport function, and plants with a non-functional HKT1;5 variant associated with a proline (P) at position 189 were reported to contain higher leaf Na^+ than plants with a leucine (L) at position 189. In this study, we found that the commercial barley Barke contains the non-functional HvHKT1;5 P189 allele, whereas wild barley accessions HID003, HID055, HID069, HID101, HID138 and HID386 contain alleles with a leucine (L) at the position 189. Within the wild barley accessions, in addition to P189L variants, we found three additional common non-synonymous SNPs, present in all HID accessions; and several more unique SNPs. This indicates that there is large natural variation in HKT1;5 alleles in wild barley. We also probed the expression of *HvHKT1;5* in salt-treated 7d-old barley seedlings, and found that *HKT1;5* was not expressed at this early stage in Barke and wild accessions tested. This indicates that other factors are contributing to the variation in leaf ion accumulation detected in the HID accessions.

4.1 Introduction

Salinity is a major soil constraint reducing crop yields worldwide. Salt stress causes ionic stress (an excess of Na^+ and Cl^+), which can occur days or weeks after the onset of salt stress when ions accumulate, and salt stress causes osmotic stress (an osmolyte imbalance), which occurs rapidly after exposure to salt stress and is not associated with the gradual accumulation of NaCl in leaves (Munns and Tester, 2008; Roy and Chakraborty, 2014). There are three well known salt tolerance mechanisms in plants, including: osmotic tolerance (or the ability to maintain growth under salt stress), tissue tolerance to accumulated Na^+ or Cl^-, and efficient Na^+ and Cl^- exclusion. Osmotic shock at the early stage of salt stress results in stomatal closure and reduction in cell expansion in root tips and young leaves (Munns and Tester, 2008; Abbo et al., 2014). For osmotic tolerance, less is known about the exact mechanism, but this could possibly be achieved by increasing osmotic adjustment and decreasing stomatal closure (Munns and Tester, 2008). Increased tissue tolerance can be achieved by compartmentation of cytosolic Na^+ or Cl^- into the vacuole, the production of compatible solutes such as proline, and efficient reactive oxygen species (ROS) detoxification mechanisms through an increase of antioxidant enzymes, as ROS can cause oxidative stress in plants (Apel and Hirt, 2004; Parida and Das, 2005; Munns and Tester, 2008). In addition, plants also protect sensitive tissues such as leaf blades by translocating NaCl to less salt sensitive tissues such as leaf sheaths and roots via specific membrane transporters; one such ion transporter was named the High affinity potassium K^+ Transporter HKT1;5 (Platten et al., 2006). HKT1;5 is expressed in the root vasculature and despite its name it is selective for Na^+ .(Houston et al., 2020). HKT1;5 is localised on the plasma membrane (PM), it functions as a Na^+ transporter, and in wheat it retrieves Na^+ from the xylem sap, limiting the accumulation in the shoot (Byrt et al., 2014). In roots, Na^+ can be pumped back into the external environment through active PM exporters, for example SOS1 (Shi et al., 2002).

In rice (*Oryza sativa*), bread wheat (*Triticum aestivum*) and barley (*Hordeum vulgare*), HKT1;5s have been identified, and the mechanism of unloading Na^+ from the xylem in the roots to reduce shoot Na^+ accumulation has been characterised. HKT1;5-associated limitation of Na^+ transport to the shoot helps to maintains a high K^+:Na^+ shoot ratio (Maathuis and Amtmann, 1999; Ren et al., 2005; Cotsaftis et al., 2012; Munns et al., 2012; Byrt et al., 2014; Borjigin et al., 2020; Houston et al., 2020).

Previous studies have reported naturally occurring mutations in *HKT1;5* in different plant species that alter its functionality (Cotsaftis et al., 2012). Rice lines with a leucine (L) in position 395 in OsHKT1;5 had higher Na^+ accumulation compared to those with a valine (V) at that same position (Cotsaftis et al., 2012). In other studies, a single nucleotide mutation caused a change of L to P at the position 189 (L189P) in the HvHKT1;5 protein in barley and at 190 (L190P) in TaHKT1;5 protein in bread wheat. This difference disrupts the function of HKT1;5 preventing the retrieving of Na^+ from the shoot in 189P versions, leading to more root-to-shoot transport of Na^+ and higher accumulation of leaf Na^+ (Borjigin et al., 2020; Houston et al., 2020).

Chapter 2 and 3 described variation in the root and shoot ion accumulation from the analysis of 7d-old barley under control and saline conditions (Chapter 2, Figure 5, S9). We found that Barke and HID069 had higher root Na^+:K^+ ratios, 3.9 ± 0.2 and 3.0 ± 0.1, respectively, compared to HID138 which had 1.7 ± 0.1 under saline conditions (Chapter 2, Figure 5h). However, Barke had the same shoot Na^+:K^+ as HID138 (~ 1.0 ± 0.1) whereas HID069 had a shoot Na^+:K^+ ratio of 0.5 under saline conditions (Chapter 2, Figure S9). Barke lacked an exodermal barrier while HID138 had the strongest exodermal barrier compared to HID069 based on their suberin intensity (Chapter 2, Figure 2). In addition to variations in apoplastic barrier formation, other differences between Barke and the wild barley accessions, such as variation in expression of HKT1;5, may be involved in modulating shoot ion

accumulation. Additionally, there might be a relationship between the apoplastic barrier formation and the efficiency of membrane transport mechanisms; higher shoot Na^+ could for example trigger a signalling cascade to induce barrier formation. In this study, we investigated the sequence variation and expression of *HvHKT1;5* in a commercial barley and a collection of wild barley accessions under saline conditions to determine if HKT1;5 function could be influencing the observed variation in root and shoot Na^+ and K^+ accumulation.

4.2 Material and Methods

4.2.1 Plant growth conditions

Seeds of Barke, Morex, HID003, HID055, HID069, HID101, HID138, HID357 and HID386 were imbibed, sterilised and stratified as described in Chapter 2 in the material and methods section. After stratification, seeds were first germinated on wet paper towel in the dark for 12h before they were placed in paper towel as described in the material and methods section in Chapter 2. In this experiment, plants were only grown in 40mM NaCl with one quarter strength Hoagland solution as described in Chapter 2.

4.2.2 DNA extraction

Leaf of one week old seedlings was harvested, freeze dried following Fox et al. (2003) and genomic DNA was extracted following a revised protocol adapted from Rogowsky et al. (1991). In brief, the frozen leaf tissue was homogenized using a 2010 Genogrinder at 1200 rpm for 30 s. Six hundred µL of DNA extraction buffer (pH 8.5) containing 1% sarkosyl, 100mM TRIS-HC1, 100 mM NaC1, 10 mM EDTA, 2% insoluble Polyvinyl-polypyrrolidone (PVPP) and 600 µl phenol/chloroform:iso-amylaleohol (25:24:1) was added to the ground tissue. Samples were mixed for 10 min using the orbital mixer, followed by 10 min centrifuged at 5000 rpm, before supernatant was extracted. DNA in the supernatant was precipitated using 60 µl 3 M Na-acetate (pH 4.8) and 600 µl isopropanol for 2 min at room temperature before centrifuged to pour off the remaining supernatant. The DNA pellet was washed with 1 ml 70%

ethanol, dried, and resuspend overnight in 30 µl R40 at 4ºC. The quantity of DNA was measured in 1 µL of sample using ND-1000 Spectrophotometer (NanoDrop Technologies).

4.2.3 *HvHKT1;5* Genomic Sequence Testing

The genomic sequence of *HvHKT1;5* from Barke and seven wild barley accessions, HID003, HID055, HID069, HID101, HID138, HID357 and HID386 was amplified using Phusion High-Fidelity PCR kit (New England Biolabs, Inc., Beverly, Ma, USA) following the manufacturer's instructions. The primers used for the PCR reaction were as follows: forward primer *HvHKT1;5* (5′ -ATGGGTTCTTTGCATGTCTCC-3′) and reverse primer *HvHKT1;5* (5′ -CTACACTATCCTCCATGCCTGG -3′). PCR conditions were as follows: initial denaturation at 98ºC for 30s, 32 cycles of 98ºC for 10s, 63ºC for 25s, 72ºC for 45s, and final extension at 72ºC for 2 min and held at 10ºC. The PCR product was separated by electrophoresis on a 1% (w/v) agarose gel (Bioline) in 0.5× TAE buffer at 120 V for 45 min with a 1kb Bioline Hyperladder. The PCR products were then visualized under UV light and the 1.7 kb target band was collected for purification prior to sequencing using NucleoSpin Gel and PCR Clean-up kit (Macherey-Nagel) according to the manufacturer's instruction. Sequencing for all samples was conducted by the Sanger sequencing service at the Australian Genome Research Facility (AGRF, South Australia) using the primers listed in the Table S1. The sequencing results were analysed using Geneious (version 8.1.9).

4.2.4 RNA Extraction and cDNA synthesis

RNA was extracted from frozen root tissues using TRIZOL-like reagent. In brief, frozen root tissues were placed in 2.0 ml micro-centrifuge tubes containing 2× 4 mm ball-bearings and were homogenised with a 2010 Genogrinder at 1200 rpm for 30 s. About 1 ml TRIZOL-like reagent was added, followed by 200 µl of chloroform. The solution was mixed for 15 s by vortexing and incubated at room temperature for 3 min prior to centrifuging at 11, 400 rpm for 15 min at 4 ºC. The isolated supernatant was incubated with 500 µl isopropanol for 10 min

before it was centrifuged at 11, 400 rpm for 10 min. The pellet then washed with 11 ml 70 % ethanol air-dried and resuspended in 15 µl sterile water. Any DNA contamination was removed using Turbo DNA-free kit-Invitrogen for Thermo Fisher following manufacturer's instructions. To check the quality of the isolated RNA, 2 µl of RNA was loaded onto a 1% agarose gel in 0.5% TAE buffer for electrophoresis at 120V for 30min. The image of the RNA bands was taken using ChemiScope 2850 gel-doc system (Clinx Science Instruments). The concentration of RNA was measured using a ND-1000 Nanodrop Spectrophotometer. cDNA synthesis was performed on 1 µl purified RNA for 10 µl reaction using Applied Biosystems kit following manufacturer's instructions. cDNA samples were diluted in 1:10 solution and stored at -20^{o}C.

4.2.5 *HvHKT1;5* Gene Expression in Roots

To determine the expression of *HvHKT1;5* in the roots of salt treated commercial Barke and the seven wild barley accessions, a 10 µl PCR reaction was conducted on the synthesised cDNA using One*Taq*® 2X Master Mix with Standard Buffer (New England Biolabs) following manufacturer's instruction. The same primers as described above were used to amplify the coding sequence (CDS): forward primer *HvHKT1;5* (5′-ATGGGTTCTTTGCATGTCTCC-3′) and reverse primer *HvHKT1;5* (5′- CTACACTATCCTCCATGCCTGG-3′). PCR conditions were as following: initial denaturation at 94 ^{o}C for 30 s, 32 cycles of denaturation (94^{o}C) for 10 s, annealing at different temperature (55 ^{o}C, 57 ^{o}C, 59 ^{o}C, 61 ^{o}C and 63 ^{o}C) for 25 s, extension (68 ^{o}C) for 90 s, and final extension at 68 ^{o}C for 5 min and held at 10 ^{o}C. The PCR products were subjected for electrophoresis on a 1% (w/v) agarose gel (Bioline) in 0.5X TAE buffer at 120 V for 30 min, and visualised using Clinx Science Instruments ChemiScope 2850 gel-doc system. The expected length of the *HvHKT1;5* CDS was 1533 bp. *HvGAP* with an expected length of 189 bp gene was amplified as a positive control and milliQ water was used as a negative control. The primer sequences for *HvGAP* amplification used were: forward

primer *HvGAP* (5′-GTGAGGCTGGTGCTGATTACG-3′) and reverse primer *HvGAP* (5′-TGGTGCAGCTAGCATTTGAGAC-3′).

4.3 Results

4.3.1 Synonymous and non-synonymous SNPs identified within the barley material tested

The *HvHKT1;5* sequence of Barke and all wild barley accessions tested consisted of three exons and two introns. The length of all the genomic sequences of *HvHKT1;5* were 1695bp as expected and the CDSs were 1533bp as reported previously (Huang et al., 2020). All of the tested barley plants therefore had HvHKT1;5 variants with 510 amino acid lengths.

The online available genome of the barley cultivar Morex was used as a reference; all of the *HKT1;5* sequences found within our plant material were compared to the Morex *HKT1;5* sequence. We found variation in all *HvHKT1;5* sequences in all wild barley accessions, but not in Barke (Table 1). Barke *HvHKT1;5* was identical in sequence to Morex, no SNPs were detected (Table 1). In the wild barley accessions we detected both synonymous and non-synonymous SNPs. In total, there was one SNPs found in HID003, four in HID055, eight in HID069, HID101, HID138 and HID357, and the highest number of SNPs with a total of 25 was found in HID386 (Table 1).

Some SNPs were common in the wild accessions and there were four particular non-synonymous SNPs shared in the majority of the wild accessions. In all of the wild barley accessions, we found a single SNP at the nucleotide position 566 (C/T), which results in an amino acid change from P to L at the 189th residue in the HvHKT1;5 protein (Table 1). In all the HIDs except for the HID003, there was a single SNP at the 170th base pair (A/G), which results in an amino acid difference, instead of asparagine 57 (N57) these accessions harbour a serine (S) (Table 1). At position 438 within the HvHKT1;5 sequences, we found the inverse

amino acid difference. Half of the accessions including HID069, HID101, HID357 and HID386 had a SNP at 1313bp (G/A) of *HvHKT1;5* CDS sequence, which resulted in an amino acid variation from S438 to N (Table 1). Another common SNP found in some of the wild barley accessions was a difference at 1246bp (G/A); this results in a different amino acid at the 416th position, a change from a valine (V) to isoleucine (I) (Table 1).

Within the wild barley accessions, we identified genotype unique SNPs that cause changes in amino acid residues in the HvHKT1;5 protein that were not found among other genotypes in this study. In HID055, there were two genotype specific non-synonymous SNPs, one SNP at the 321bp (G/A) that results in an amino acid difference at position 107, HID055 harbours a methionine (M) at this position compared to the I found in all other barleys sequenced (Table 1). A second SNP was found in the same accession with the inverse difference in amino acid, specifically HID055 had an I at position 146, while all other barley accessions tested had an M (Table 1). One non-synonymous SNP found in HID138 at 1208bp (A/T) resulted in a 403 residue differences, from K to M. HID386 had in total eleven genotype-specific non-synonymous SNPs (Table 1). Within the wild barleys, HID069, HID01, and HID357 shared the same HvHKT1;5 amino acid sequence (Appendix 10).

There were synonymous SNPs found that did not cause changes in amino acid in HID069, HID101, HID138, HID357 and HID386 (Table 1). There were four common synonymous SNPs at 891bp (A/G), 1008bp (G/A), 1401bp (T/C), and 1494bp (A/G) that corresponded to protein residue 297th Threonine, 336th Glutamine, 467th S and 498th L respectively (Table 1).

TABLE 1 Synonymous and non-synonymous SNPs of Barke and seven indicated wild barley accessions. Non-synonymous resulting differences in the amino acid sequences in the HvHKT1;5 proteins of Barke and seven indicated wild barley accessions; protein sequences are compared to the Morex HvHKT1;5 protein as a reference. The number indicates the position of each amino acid; standard single letters code for amino acids. The highlighted black bold SNPs show the common synonymous SNPs and the highlighted colour (red, green, blue and purple) bold shows the common non-synonymous SNPs found within the wild barley accessions. In HID386, there were two nucleotide substitutions causing the M48L difference, and a total of 25 SNPs detected.

Genotypes	Synonymous SNPs (no change in amino acid)	Non-synonymous SNPs (changes in amino acid)	Total SNPs
BARKE	0	0	0
HID003	0	**P189L**	1
HID055	0	**N57S**, M107I, I146M, **P189L**	4
HID069	**T297**, **Q336**, **S467**, **K498**	**N57S**, **P189L**, **V416I**, **S438N**	8
HID101	**T297**, D327,**Q336**, **S467**	**N57S**, **P189L**, **V416I**, **S438N**	8
HID138	V266, **T297**, **Q336**, L432	**N57S**, **P189L**, K403M, **V416I**,	8
HID357	**T297**, **Q336**, **S467**, **K498**	**N57S**, **P189L**, **V416I**, **S438N**	8
HID386	F43, F44, K119, L251, **T297**, L404, E423, **S467**, **K498**	Q18L, P33L, F46C, M48L (2SNPs), **N57S**, M87S, K131N, M157I, R166H, **P189L**, I224V, T379A, H402A, **V416I**, **S438N**	25

4.3.2 Transcript analysis of *HvHKT1;5*

The full sequence of *HvHKT1;5* was amplified from both genomic DNA from the leaf and cDNA generated from the roots of each genotype. The expected product size of *HvHKT1;5* was sequenced from gDNA and CDS, which was 1695bp and 1533bp, respectively. The expected product for the *HvHKT1;5* sequence from gDNA of all the barley materials were detected (Figure 1a). We did not detect PCR products for the *HvHKT1;5* transcript from the cDNA samples after 35 PCR cycles, in cDNA from any of the wild accessions or Barke indicating no *HvHKT1;5* was expressed in the roots at this growth stage (Figure 1b). All PCR products for the *HvGAP* gene, a house-keeping gene used as positive control was detected in all accessions tested indicating that the CDS from cDNA was viable (Figure 1c).

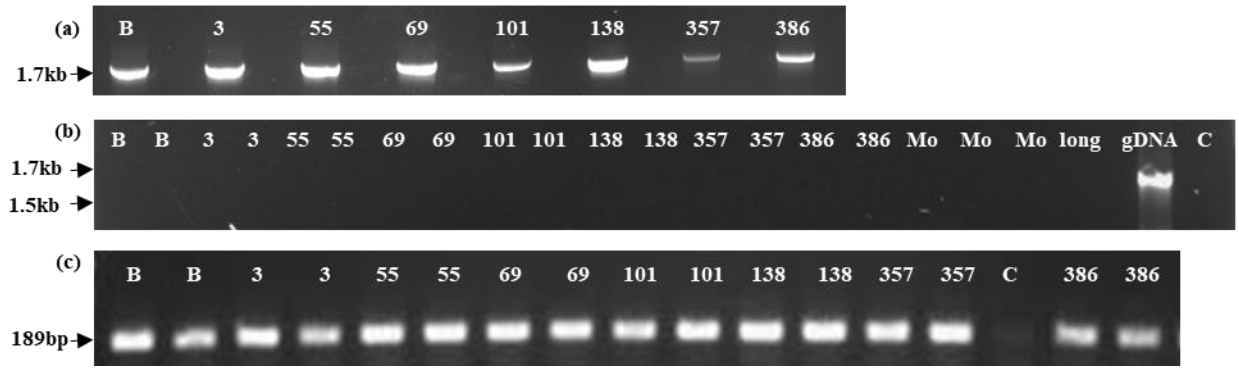

FIGURE 1 *HvHKT1;5* expression in Barke and wild barley accessions. (a) The PCR product of genomic *HvHKT1;5* sequence, using gDNA as template. (b) No PCR products for *HvHKT1;5* CDS were detected, using cDNA generated from roots of one-week old seedlings grown under 40mM NaCl. (c) A PCR product was detected in each sample for the house-keeping gene HvGAP, using the same cDNA as template. Abbreviations; B;Barke, 3; HID003, 5; HID003, 69; HID003, 101; HID101, 138; HID003, 357; HID003, 386; HID003; gDNA; genomic DNA and C; control (milliQ water).

4.4 Discussion

4.4.1 SNP variation within the barley accessions tested

Our results revealed that there is natural variation in the *HKT1;5* sequence in all wild barley accessions tested. Within the sequence variations identified there were some SNPs that have been reported to impact HKT1;5 function, whereas other SNPs could potentially influence the functionality of the HKT1;5, but this remains to be tested.

There were four common non-synonymous SNPs (causing amino acid differences: N57S, P189L, V416I, and S438N) in wild barley accessions in comparison to the reference, Morex. These four common SNPs have have previously been identified in other barley cultivars such as Beecher, Commander, Fleet, Maritime and Sloop when compared to Morex (Amarasinghe et al., 2019). Houston et al. (2020) tested these four common SNPs for their Na^+ transport in *Xenopus laevis* oocytes using two electrode voltage-clamp (TEVC). The authors suggested that three variations (N57S, V416I, and S438N) might not be key in relation to influencing Na^+ conductivity in *X. laevis* oocytes system (Houston et al., 2020). However, Houston et al. (2020) found that HKT1;5 with L189P was common to high Na^+ accumulating genotypes, and that P at 189 severely compromised the HvHKT1;5 functionality. It was proposed that protein misfolding and aberrant subcellular localisation led to the HvHKT1;5189P malfunction as a Na^+ transporter (Houston et al., 2020). Interestingly, another study found a similar SNP in TaHKT1;5 (L190P) in a landrace bread wheat Mocho de Espiga Branca (Borjigin et al., 2020). Similar to the barley HvHKT1;5 (L189P), the TaHKT1;5 (L190P) was also mislocalised in heterologous expression systems (*Nicotiana benthamiana* leaves), and possibly degraded due to misfolding, leading loss of HKT1;5 function (Borjigin et al., 2020). Loss of HKT1;5 function in the plant caused a defect in Na^+ retrieval from the xylem, and led to higher shoot Na^+ accumulation in both, wheat and barley (Borjigin et al., 2020; Houston et al., 2020). In our study, we found that Barke had amino acid P189 whereas all of the wild barley accessions had

L189. This indicates that Barke might have a non-functional HvHKT1;5, therefore unable to retrieve Na^+ from xylem. It is possible that Barke utilised other membrane transporters for Na^+ exclusion from the shoot such as HKT1;4. For example, in other plant species, such as durum wheat, HKT1;4 function has been described to retrieve Na^+ from the xylem and retain in the sheath (James et al., 2006; James et al., 2011). It is also possible that Barke might have adapted other mechanisms, such as tissue tolerance, for example, by compartmentalising leaf cytosolic Na^+ into the vacuoles using Na^+/H^+ antiporter (NHXs) (Blumwald, 2000). In contrast, all of the wild barley accessions had a functional version of HvHKT1;5 (L189). It is possible that at the later stage of development, HvHKT1;5 might play an important role in salt tolerance by retrieving Na^+ from the xylem and retaining it in the root and that this was not observed here due to the early growth stage (seedlings) of the plants tested. It is also important to note that there were other amino acid differences found in HvHKT1;5 among the wild barley accessions, and the impact of these differences in the functionality of HvHKT1;5 is not yet understood.

TABLE 2 The four common non-synonymous SNPs (causing amino acid differences) found within the diverse barley accessions in this study.

Residue number	Amino acid (Genotypes)		Description of the amino acid
189	Proline (BARKE)	Leucine (HID003, HID055, HID069, HID101, HID138, HID357, HID386)	• Both Proline and Leucine are non-polar amino acid. • Proline has R-group joins with its α-amino group forming a secondary amine and a ring. Due to this structure, Proline is the least flexible amino acids. Therefore, this can lead to conformational rigidity in protein, affecting its secondary structure. The presence of Proline in protein disrupt α-helices and β-strands. • Leucine is a branched-chain amino acid that is hydrophobic.
57	Asparagine (BARKE, HID003)	Serine (HID055, HID069, HID101, HID138, HID357, HID386)	• Both Serine and Asparagine are polar amino acids. • Proline has carboxyamide in its R-group while Serine has hydroxyl in its R-group. • Hydroxyl in R-group of Serine can be targeted for phosphorylation by certain protein kinases. • A amino acid substitution from Serine to Asparagine could abolish the phosphorylation site and vice versa.
438	Serine (BARKE, HID003, HID055, HID138)	Asparagine (HID069, HID101, HID357, HID386)	
416	Valine	Isoleucine	• Both Valine and Isoleucine are non-polar amino acid. • The structure of both Valine and Isoleucine quite similar except that Isolecine has a chiral chain.

Within the wild barley accessions, there were also genotype specific (unique) non-synonymous SNPs not found in other genotypes in this study. For example, we found a lysine to methionine amino acid substitution in HID138 and histidine to glutamine in HID386. This amino acid substitution could cause differences in the protein structure as lysine and histidine are positively-charged amino acids while methionine (non-polar amino acid) and Glutamine (polar amino acid) are not. Similar amino acid substitution (K403M) was also detected in certain H.

spontaneum accessions and (H402Q) in certain H. *spontaneum* accessions and in H. *vulgare* cv. Viivi, a low Na^+ accumulating barley (Houston et al., 2020). Another non-synonymous SNP (R166H) in HID386 was also identified previously in certain H. *spontaneum* accessions; this substitution does not alter the residue charge as both Arginine and Histidine are positively charged amino acids. However, the effect of the differences in amino acid on the functionality of HvHKT1;5 protein is unknown.

4.4.2 *HvHKT1;5* was not expressed in roots during early seedling development

HvHKT1;5 transcript was not detected in Barke and any of the accessions at the stage of one week after germination. The most plausible explanation is that at this early growth stage (7d old seedlings), *HvHKT1;5* might not be expressed or maybe the expression was below detection limits in the whole root tissue samples used in our method. In a recent study, Huang et al. (2020) found very low *HvHKT1;5* relative expression in young barley seedlings less than two-week olds under 200mM NaCl indicating that *HvHKT1;5* is likely to be expressed later in development (Houston et al., 2020). Additionally, the amount of salt applied in our experiment might not have been high enough to induce the expression of *HvHKT1;5*. Almost no *HvHKT1;5* relative expression was detected previously when barley lines were treated with 100mM NaCl (Huang et al., 2020). This indicates that the expression of *HvHKT1;5* might be tissue dose dependent (Huang et al., 2020). As we were unable to detect any *HvHKT1;5* transcripts in our study, we propose that differences in HvHKT1;5 are not a contributing factor to the observed ion accumulation differences among the accessions tested (Chapter 2, Figure 5, Figure S9). It is possible that there might be other membrane transporters such as SOS1 or NHXs, involved in regulating ion transport at the early seedlings stage. Future work should investigate the quantitative expression of *HvHKT1;5* in these barley accessions across various growth stages and at higher salt treatment levels to determine if there are any expression differences and, if

so, the extent of expression and how this correlates with ion accumulation or root apoplastic barrier deposition.

In conclusion, our findings reveal that Barke has a non-functional version of HvHKT1;5 similar to the version in Morex, whereas all of the wild barley accessions tested contained other SNPs in HvHKT1;5, which warrant further investigation. Based on the transcript analysis, we conclude that HvHKT1;5 is not the factor causing variation in ion accumulation among the accessions tested at least in this early seedling growth stage.

4.5 Supplementary files

(a)

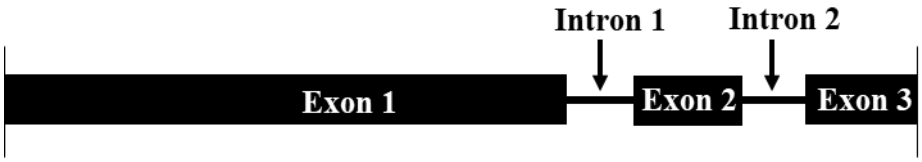

(b)

ATGGGTTCTTTGCATGTCTCCGGCAGTACCACTACTCAACATAGCAGGGTTCAGAGGGCTTA
CCAACTCTTGTTTTTCCATGTGCACCCGTTCTGGCCCCAGCTCCTCTACTTTGTGTCCATCT
CCTTTTTCGGCTTCGTCATGCTGAGAGCCCTCCCCATGAAGACCAACATGCCCACGGACCTA
GACCTGATCTTCACGTCGGTGTCGGCGACGACGGTGTCGAGCATGCAGGCGGTGGAGATGGA
GTCCTTCTCCAACCCCCAGCTCCTCCTCCTAACCCTCCTCATGCTTCTTGGTGGCGAGGTGT
TCACTAGCATGCTTGGCATGTACTTCACCTACGTCAAGTCCAAGAAAAAAGAAGCACAAGCA
CCACATGATGATGGTGCCAAAGTGAAACCAGCACCATCTAGCCTAGAGCTCACGGCCGCTAG
CATCTGCATGGACGACGGCACTGCACAGGACCGTATGGAGCAAGGGTTCAAGGACCAGCCCC
GTTACGGCCGGGCCTTCCTCACCAGGTTGCTCCTGTTCATAGTGGTCGGCTATCACGCGGTG
GTGCACCCGGCCGGTTACTCCCTGATGCTGGTCTACCTGAGCGTCGTGTCCGGCGCGAGGAC
GGTGCTCGCCGGCAAGGGGATCAGCATGCACACCTTCTCCGTCTTCACCATCGTCTCGACGT
TCGCAAACTGCGGCTTCATGCCGAACAACGAAGGGATGGCCTCCTTCCGGTCCTTCCCGGGA
CTCCTCCTACTCGTCATGCCCCACGTCCTCCTCGGAAACACGCTCTTCCCCGTCTTCCTCAG
GCTGGCGATCTGGGCTCTCCAGCGGTTCACCAAGAGGCCTGAACTCGGTGAGCTGCGGAGCA
TCGGCTACGACCACCTCCTGACAAGCCGGCATACAAGGTTCTTGGCTTTCACCGTGGCCGTG
TTCGTGCTGGCGCAGCTGTCGCTCTTCTGCGCCATGGAGTGGGGCTCCGACGGGCTGCGCGG
GCTCACCGCCGCGCAGAAGCTCGTCGCGGCTCTCTTCATGTCGGTCAACTCGAGGCACGCCG
GCGAGATGGTCGTGGACCTCTCCACCGTGTCGTCGGCCGTCGTGGTGGTCTACATGGTCATG
ATGTGTGTTACGTACCTCCACTAAAATCTCTCATGCTTTTTTTGACGGGAATATTCGCTCAT
GCTCGTGTCGTGCCTACACACCACCCTGCAG**GTACCTACCACCTTATACTACATTTCTACCA**
GTGGAAGACAGTAACCAACAAGTGGGAACAGATCAGAAAAGGACAAGCATATGGCACAAGCT
TCTCATGTCGCCCCTCTCGTGCATAGCCATCTTCGTCGTCGTCGTGTGCATCACCGAGAGAC
GGCAGATCTCCGATGACCCACTCAACTTCAACGTCCTCAGCATCGCCGTCGAGGTTATCAGG
TAATCAATCAATTAATTAACAGAACGTAGAAGCGCATGAGACACCAACGTTGTGTGAACTGT
GCATGCAG**TGCGTACGGCAACGTGGGGTTCAGCACGGGGTACAGCTGCGGCCGGCAGGTGAC**
GCCCGACGGCAGTTGCAGGGACGCGTGGGTTGGCTTCTCCGGGAAGTGGAGCAGGGAAGGGA
AGCTCGCCCTCATAGCCGTCATGTTCTACGGCAGGCTCAAGAAATTCAGCATGCATGGCGGC
CAGGCATGGAGGATAGTGTAG

FIGURE S1 Genomic *HvHKT1;5* sequence for Morex and Barke. (a) Illustration of genomic sequence of *HvHKT1;5* consisting of three exons and two introns. (b) The *HvHKT1;5* genomic sequence with the exons in bold in black and introns in bold red.

TABLE S1 List of the primers used for the Sanger sequencing.

	Primers	Length (bp)	5′-3′ primer sequences
Forward primers	*HvHKT1;5*_F	21	ATGGGTTCTTTGCATGTCTCC
	*HvHKT1;5*_F1	20	CGGTTACTCCCTGATGCTGG
	*HvHKT1;5*_F2	21	CCAACAAGTGGGAACAGATCA
Reverse primers	*HvHKT1;5*_R	22	CTACACTATCCTCCATGCCTGG
	*HvHKT1;5*_R1	20	CAGTTTGCGAACGTCGAGAC

TABLE S2 Amino acid, abbreviation and their general characteristic

Name	Abbreviation	Abbreviation	Characteristic
Glycine	Gly	G	Non-polar
Alanine	Ala	A	
Valine	Val	V	
Cysteine	Cys	C	
Proline	Pro	P	
Leucine	Leu	L	
Isoleucine	Lle	I	
Methionine	Met	M	
Tryptophan	Trp	W	
Phenylalanine	Phe	F	
Serine	Ser	S	Polar
Threonine	Thr	T	
Tyrosine	Tyr	Y	
Asparagine	Asn	N	
Glutamine	Gln	Q	
Lysine	Lys	K	Positively-charged
Arginine	Arg	R	
Histidine	His	H	
Aspartic acid	Asp	D	Negatively-charged
Glutamic acid	Glu	E	

4.6 References

Abbo S, van-Oss RP, Gopher A, Saranga Y, Ofner I, Peleg Z (2014) Plant domestication versus crop evolution: a conceptual framework for cereals and grain legumes. Trends in Plant Science **19:** 351-360

Amarasinghe SL, Watson-Haigh NS, Byrt C, James R, Qiu J, Berkowitz O, Whelan J, Roy SJ, Gilliham M, Baumann U (2019) Transcriptional variation is associated with differences in shoot sodium accumulation in distinct barley varieties. Environmental and Experimental Botany **166:** 103812

Apel K, Hirt H (2004) Reactive oxygen species: metabolism, oxidative stress, and signal transduction. Annu. Rev. Plant Biol. **55:** 373-399

Blumwald E (2000) Sodium transport and salt tolerance in plants. Current Opinion in Cell Biology **12:** 431-434

Borjigin C, Schilling RK, Bose J, Hrmova M, Qiu J, Wege S, Situmorang A, Brien C, Berger B, Gilliham M (2020) A single nucleotide substitution in *TaHKT1; 5-D* controls shoot Na+ accumulation in bread wheat. bioRxiv

Byrt CS, Xu B, Krishnan M, Lightfoot DJ, Athman A, Jacobs AK, Watson-Haigh NS, Plett D, Munns R, Tester M, Gilliham M (2014) The Na^+ transporter, TaHKT1;5-D, limits shoot Na^+ accumulation in bread wheat. Plant Journal **80:** 516-526

Cotsaftis O, Plett D, Shirley N, Tester M, Hrmova M (2012) A two-staged model of Na^+ exclusion in rice explained by 3D modeling of HKT transporters and alternative splicing. PLoS One **7:** e39865

Fox R, Warner P, Eglinton J (2003) The application of rapid DNA extraction methods for MAS in barley and wheat improvement programs. *In* Proceedings of the 53rd Australian Cereal Chemistry Conference,

Houston K, Qiu J, Wege S, Hrmova M, Oakey H, Qu Y, Smith P, Situmorang A, Macaulay M, Flis P (2020) Barley sodium content is regulated by natural variants of the Na^+ transporter *HvHKT1; 5*. Communications Biology **3:** 1-9

Huang L, Kuang L, Wu L, Shen Q, Han Y, Jiang L, Wu D, Zhang G (2020) The HKT transporter HvHKT1; 5 negatively regulates salt tolerance. Plant Physiology **182:** 584-596

James RA, Blake C, Byrt CS, Munns R (2011) Major genes for Na^+ exclusion, *Nax1* and *Nax2* (wheat *HKT1; 4* and *HKT1; 5*), decrease Na^+ accumulation in bread wheat leaves under saline and waterlogged conditions. Journal of experimental botany **62:** 2939-2947

James RA, Davenport RJ, Munns R (2006) Physiological characterization of two genes for Na+ exclusion in durum wheat, Nax1 and Nax2. Plant Physiology **142:** 1537-1547

Maathuis FJM, Amtmann A (1999) K^+ nutrition and Na^+ toxicity: The basis of cellular K^+/Na^+ ratios. Annals of Botany **84:** 123-133

Munns R, James RA, Xu B, Athman A, Conn SJ, Jordans C, Byrt CS, Hare RA, Tyerman SD, Tester M, Plett D, Gilliham M (2012) Wheat grain yield on saline soils is improved by an ancestral Na^+ transporter gene. Nature Biotechnology **30:** 360-U173

Munns R, Tester M (2008) Mechanisms of salinity tolerance. Annual Review of Plant Biology **59:** 651-681

Parida AK, Das AB (2005) Salt tolerance and salinity effects on plants: a review. Ecotoxicology and Environmental Safety **60:** 324-349

Platten JD, Cotsaftis O, Berthomieu P, Bohnert H, Davenport RJ, Fairbairn DJ, Horie T, Leigh RA, Lin H-X, Luan S (2006) Nomenclature for HKT transporters, key determinants of plant salinity tolerance. Trends in Plant Science **11:** 372-374

Ren Z-H, Gao J-P, Li L-G, Cai X-L, Huang W, Chao D-Y, Zhu M-Z, Wang Z-Y, Luan S, Lin H-X (2005) A rice quantitative trait locus for salt tolerance encodes a sodium transporter. Nature genetics **37:** 1141

Rogowsky P, Guidet F, Langridge P, Shepherd K, Koebner R (1991) Isolation and characterization of wheat-rye recombinants involving chromosome arm 1DS of wheat. Theoretical and Applied Genetics **82:** 537-544

Roy S, Chakraborty U (2014) Salt tolerance mechanisms in salt tolerant grasses (STGs) and their prospects in cereal crop improvement. Botanical Studies **55:** 31

Shi H, Quintero FJ, Pardo JM, Zhu J-K (2002) The putative plasma membrane Na^+/H^+ antiporter SOS1 controls long-distance Na^+ transport in plants. The Plant Cell **14:** 465-477

Chapter 5:

General discussion and future outlooks

CHAPTER 5: GENERAL DISCUSSION

5.0 Key findings

This PhD project explored the relationships between solute barrier formation, particularly in exodermal cell layers, tissue ion accumulation, root respiration rates and overall plant biomass production, tested the plant responses in terms of barrier formation following phytohormone treatments, and tested for associations with variation in a key membrane transport mechanism.

The first step in the project was to screen a diverse barley collection to determine if exodermal barriers could be detected, and to evaluate the extent of variation of apoplastic barriers among diverse barley lines (Chapter 2). The results of this screening revealed extensive variation in apoplastic barrier formation within the wild barley accessions tested, specifically variation in suberin and lignin deposition, and exodermis formation was observed to be sometimes salt-inducible or constitutive depending on the barley accession.

In this first step barley accessions with the greatest diversity in root solute barriers were identified, which enabled them to be included in more extensive experiments to check trends in ion accumulation, rates of root O_2 consumption, and shoot and root growth (length and biomass) under control and saline conditions (Chapter 2). This revealed that a commercial barley, Barke, lacked an exodermal barrier and had higher root Na^+ accumulation and higher rates of root O_2 consumption (energy expenditure) compared to the diverse wild barley accessions tested. One wild barley, HID138, had notably prominant apoplastic barrier deposition, particularly low Na^+ accumulation and a lower rate of root O_2 consumption (energy expenditure). HID138 also retained more K^+ in the roots compared to Barke. These observations prompted the development of a hypothesis that there could be a relationship between the deposition of exodermal barriers and the amount of ion accumulation and energy

expenditure in barley. However, other factors may also contribute to the observed differences in root Na^+ and K^+ accumulation and rate of root O_2 consumption because the barely accessions tested are genetically diverse and likely to differ in many mechanisms that could influence ion accumulation and respiration characteristics.

To limit the impact of genetic differences influencing the various characteristics of interest within the barley accessions the deposition of exodermal barriers and their effect on the ion accumulation and rate of root O_2 consumption were investigated in RILs (HEB13) developed from a cross between Barke and HID138 (Maurer et al., 2015) (Chapter 3). The ion accumulation and biomass data recorded for the selected HEB13 lines were within range of values recorded for their parents, Barke and HID138, indicating the likelihood of heritability in relation to the factors influencing the characteristics tested within the population. In addition, HEB13s which had a mostly Barke genetic background, such as HEB13-68, developed a noticeable exodermis similar to HID138 whereas Barke did not develop an exodermis in the conditions tested. This reveals that the genetic loci required to successfully form an exodermis can be introduced into commercial lines from the wild lines used in the population, and that this is heritable in subsequent generations. There were no obvious correlations observed between the deposition of root solute barriers and root ion accumulation in the HEB13 material tested. Since our analysis was based on qualitative data rather than quantitative data, further work is required to confirm this observation.

The role of phytohormones in regulating suberisation in the roots of barley was of interest because in Arabidopsis previous studies demonstrated that phytohormone treatments influenced trends in suberin deposition. ABA treatment enhanced root suberisation in all of the barley material tested, similar to what was observed in Arabidopsis (Barberon et al., 2016). However, in ACC-treated plants there was no obvious difference relative to the control plants, whereas in Arabidopsis ACC treatment reduced suberin deposition. Possibly the ACC

treatment used was insufficient to cause a change, and/or the barley has a different response to ACC relative to Arabidopsis. To further test these alternative approaches could be used, such as modifying the concentration of ethylene or its precursor to check whether degradation of suberin deposition occurs in barley in conditions differing from the conditions tested in this study.

The root-to-shoot Na^+ transport regulation through the Na^+ transporter HKT1;5 plays a key role in the differences in ion accumulation in the shoots and roots of many cereal species, including barley (Houston et al. 2020). This prompted a sub-aim to investigate the expression of *HvHKT1;5* in the barley population and check for possible sequence variation between the wild barley accessions (Chapter 4). this analysis revealed that *HvHKT1;5* was not expressed in the one-week-old seedling material tested, indicating that HvHKT1;5 is not a key factor influencing differences in ion accumulation in both root and shoot at this stage of plant development (Figure 5 and Figure S9 Chapter 2). The *HvHKT1;5* sequence comparison analysis revealed that there was allelic variation in *HvHKT1;5* in the barley accessions tested, and these allelic differences might impact the functionality of the protein and salinity tolerance of the barleys at a later developmental stage. Hypothetically plants might manage adaptation to salinity by coordinating changes in both key membrane transport steps and ion transport mechanisms in a cell and tissue specific manor. It would be interesting to test whether plant roots alter the regulation of mechanisms such as HKT1;5 differently depending on whether or not they deploy additional apoplasmic barriers when experiencing changes in soil salinity.

5.1 Could the deposition of additional root apoplastic barriers be beneficial for barley plants?

Five factors were identified that could be key in influencing whether or not having an additional root barrier would be beneficial for barley plants in unfavourable growing conditions:

(1) Exodermal barriers can be inducible or constitutive, and it might be more useful to have inducible barriers in some conditions and constitutive barriers in other conditions. The PCA analysis (Figure S10, Chapter 2) used to assess associations between different characteristics in the barley material tested indicated that having a constitutively strong exodermal barrier might be useful for preventing Na^+ influx and K^+ loss in the root under saline conditions. However, deposition of this barrier was also associated with reduced biomass in HID138. Deposition of an exodermal barrier is likely to be unnecessary in optimal growth conditions. but it may be crucial for providing extra protection against water loss, K^+ leakage, Na^+ influx, radial oxygen loss and pathogen attack under some stressful conditions (Zimmermann and Steudle, 1998; Taleisnik et al., 1999; Kotula et al., 2009c; Krishnamurthy et al., 2011).

(2) The quantity and combination of suberin and lignin associated with apoplastic barriers can vary depending on the environment, in different barley lines and at different stages of root development. For example, in some lines such as in HID069 and HID357, the fluorescence signal for suberin was higher in saline conditions compared to signal detected in the roots grown in control conditions (Figure 2, Chapter 2). An increase in suberin deposition in the cell wall could be part of the strategy that HID069 and HID357 use to adapt to salt stress.

Our PCA plot illustrated that HID003 tended to have higher biomass but low root K^+ whereas HID138 had the opposite (Figure S10, Chapter 2). HID138 and HID003 deposited both exodermal lignin and suberin but the amount of these material in HID003 appeared to be less compared to HID138 based on the intensity of the staining (Figure 2 and 3, Chapter 2), and the

difference in the amount of these cell wall materials could have been associated with the differences in biomass (Figure 4, Chapter 2) and root K^+ retention (Figure 5, Chapter 2). In addition, HID003 could also have different composition of suberin compared to HID138. There are two types of suberin; aromatic and aliphatic suberin, in which the latter has been reported to contribute to hydrophobic characteristics of suberin due to its low permeability to water (Zimmermann et al., 2000; Hose et al., 2001). Some of the barley accessions, such as HID138, could potentially have different proportions of aliphatic suberin compared to other accessions, such as HID003, and this could have influenced potential differences in water and solute permeability. The amount and composition of the aliphatic suberin monomers such as ω-hydroxy acids (ω-OH-acids) and α,ω-dicarboxylic acids (α,ω-diacids), alcohol and fatty acids might be different between HID003, HID138 and the other accessions tested. These differences in the amount and composition of the suberin monomers could affect the micro-structure of the suberin and how well the monomers impregnate the cell wall pores, thus influencing how tight and effective the barrier is (Schreiber et al., 2005b; Ranathunge and Schreiber, 2011; Kreszies et al., 2018).

In a previous study, the quantity of aliphatic suberin was, on average, six times higher in rice exodermis than corn exodermis; and 35-fold higher in rice endodermis compared to maize endodermis (Schreiber et al., 2005b). The substantial difference in the amounts of suberin in rice relative to maize was reported to be linked to significantly lower water transport into the roots in rice compared to maize (Schreiber et al., 2005b). In the barley cultivar "Golf" the proportion of aromatic suberin was higher compared to the proportion of aliphatic suberin, and the composition of suberin monomers varied in different root zones; these differences in suberin monomer characteristics could influence the effectiveness of the solute barriers (Ranathunge et al., 2017).

(3) Cell wall materials can be either reversible or irreversible. For example, suberin deposition is reversible whereas lignin deposition is irreversible (Barberon et al., 2016). Therefore, having suberin deposited in the exodermal layer is likely to give plants more flexibility to adapt to changing conditions. This flexibility may be important for ensuring that the uptake of water and nutrients into the exodermal cells is not excessively disrupted when plants experience a change from stressful conditions to optimal growth conditions. Lignin deposition is permanent, which presumably means that depositing lignin permanently reduces free apoplastic flux of water and solutes to the roots and possibly reduces root growth (Zhao and Dixon, 2011; Pfister et al., 2014).

(4) The location and specific pattern of root barrier deposition varies. Lignin deposition was noticeably only found in the anticlinal walls, but not in the tangential walls within the barley material tested (Chapter 2). Irreversible lignin was sometimes deposited in both anticlinal and tangential walls, and this may be a disadvantage for growth under optimal conditions. Suberin deposition sometimes covered the entire cell wall area, forming a structure called suberin lamellae that can reduce the direct uptake of water and solutes into the cells. In HID003, some exodermal cells were only suberized in the anticlinal walls but not in the tangential walls (see Figure S4, Chapter 2 for more detail), while in HID138, the entire exodermal cells were suberized (Figure 2, Chapter 2). The unsuberised tangential walls could be the potential key sites where most of the direct uptake of nutrients and water into the cells can occur through membrane transporters such as aquaporins and ion transport proteins. It is possible that non-suberised exodermal cells at the tangential walls could have similar functions as endodermal passage cells. There is less information available in the literature about exodermal passage cells relative to the information about endodermal passage cells (Liu et al., 2019).

One interesting pattern identified was the U-shaped suberin deposition in both endodermal and exodermal as illustrated in Figure S3 and pictured in Figure S4, Chapter 2. The suberin deposition in the anticlinal and the outer tangential walls was thicker than in the inner tangential walls. The thicker outer tangential walls could possibly restrict direct uptake of water and solutes into the cells. It is possible that there might be greater density of plasmodesmata networks in the heavily suberised outer tangential wall of endodermal and exodermal cells to facilitate the transport of water and solutes from neighbouring cells through symplastic pathways, but this remains to be tested in barley. In Arabidopsis there was large network of plasmodesmata in the heavily suberised endodermal cells (Barberon et al., 2016). At the sites where there were less suberised inner tangential walls of exodermal cells, water and solutes would have more options to move across the cell membrane into the intercellular spaces and travel across the cortex cells apoplastically, symplastically or in transcellular fashion. It would be interesting to test whether there was less plasmodesmatal networks in the less suberised tangential walls than the heavily suberised tangential walls.

(5) The effect of depositing significant amounts of exodermal lignin and suberin might be a reduction in the membrane surface area accessible for water and nutrient absorption (Kamula et al., 1994; Enstone et al., 2002). In HID138 significant exodermal lignin was deposited in anticlinal walls, and suberin covered the entire surface of exodermal cells and this may restrict the direct uptake of water, ions and other nutrients, reducing surface absorption to the epidermis or non-suberized exodermal cells. This may be compensated for by the development of root hairs to increase the absorption surface. Root hair development is highly regulated by salt stress (Wang et al., 2008). Therefore, it would be interesting to test the effect of salt stress on root hair development in the material used in this study. Another factor influencing water and nutrient movement is increased efficiency in cell-to-cell transport of water and nutrients. This can be achieved by a number of cell membrane transporters, such as aquaporins. For example,

Kreszies et al. (2019b) reported that a wild barley accession had higher overall expression of aquaporin genes in the roots compared to the commercial cultivar, Scarlett, and they suggested that this accounted for greater water permeability through cell-to-cell transport. Future work on root solute barriers and their effects on ion accumulation will need to factor in morphological differences such as root hairs; and variation in membrane transport activity, such as aquaporin regulation, to better understand how these characteristics are coordinated with changes in cell wall material associated with apoplastic barriers.

5.2 The effect of phytohomones on root suberisation in barley

There are many factors that contribute to the development of root solute barriers. For example, a previous study on Arabidopsis identified two phytohormones; ABA and ethylene as major regulators for endodermal suberisation (Barberon et al., 2016). These hormones have an antagonistic effect on suberisation, in which ABA was shown to enhance suberisation while ethylene triggered degradation of suberisation (Barberon et al., 2016). This indicates that suberisation is a flexible and reversible process that is dependent on environmental cues or signals in plants. As expected, each barley accession tested enhanced suberin deposition in response to ABA treatment (Chapter 2), indicating that similar regulatory processes exist in barley and to Arabidopsis. Maybe ABA-triggered signalling leading to suberin deposition is part of conserved root cell gene functions (Kajala et al., 2020). Intriguingly, ACC-treated plants did not show obvious differences in suberin deposition relative to control plants, indicating that some of the mechanisms for regulating changes in diffusion barriers might be different in barley compared to Arabidopsis. There appeared to be a reduction in the abundance of endodermal passage cells in ABA-treated barley accession HID138, similar to what has been described previously in Arabidopsis (see Chapter 2) (Andersen et al., 2018), but as the approach was qualitative rather than quantitative an alternative approach is needed to follow up and test whether there was an influence of the ABA treatment on passage cell number in the barley

material tested. In this study observations of suberin deposition were only made in a transverse orientation at maturation zones due to limitations in development of high-throughput microscopy sampling methods. Future work is needed to investigate other sections of the roots to determine the extent to which suberin deposition varies along the length of the roots.

5.3 Is signalling from shoots important in root barrier development?

Roots and shoots respond to changes in the environment by transmitting signals that can lead to cascades of responses including root suberisation. Hypothetically it is possible that in addition to signals originating in roots there could be signals originating in the shoots which could influence suberin deposition in the roots (Figure 1).

Relevant plant signalling cascades could involve phytohormones, such as ABA. Previous studies have reported that ABA signals from the shoot caused changes in root morphology and growth such as root length and lateral root development (McAdam et al., 2016; Xie et al., 2020). For example, a recent study reported that exogenous application of 2 µM ABA to Arabidopsis shoots caused a significant increase in basipetal auxin transport, which lead to 18% longer primary roots compared to the controls (Xie et al., 2020). In our saline conditions we observed that many lines, such as HID003, HID138 and HID357, had relatively longer roots compared to their root lengths when grown in the control conditions (Figure 4, Chapter 2). Another study by McAdam et al. (2016) reported that shoot-derived ABA could suppress the formation of lateral roots in *Pisum sativum*. The emergence of lateral roots from the pericycle cells can break the endodermal and exodermal apoplastic barrier, which could lead to apoplastic leakage of the external solution into the roots (Peterson and Moon, 1993). Therefore, the suppression of lateral root formation could help prevent this type of leakage. These two previous studies indicate that, in addition to root ABA, there might be a possibility that shoot-derived ABA can also influence root anatomical changes for example in root suberisation by increasing the level of total ABA in the root. The level of ABA in plants is increased in response

to environmental factors such as salt stress (Barberon et al., 2016). Differences in the ABA level might contribute to differences in the amount of suberin deposition in the cell walls and influence exodermal development. It is possible that HID138 received a different magnitude of signal from the shoot or root relative to Barke or the other lines, and this could have led to a phenotypic change in the root such as the enhanced suberisation and induced exodermal barrier (Chapter 2), but testing this hypothesis would require measurement of ABA signalling in this material. In Chapter 2, when Barke was treated with 40mM NaCl, there was no obvious exodermal suberin detected. However, Barke treated with 5µM ABA had noticeable fluorescence in the anticlinal walls of outer cortical cells contrary to what was observed under 40mM NaCl (Figure 7, Chapter 2). This finding indicates that there might have been differences in internal signalling that led to differences in suberin deposition.

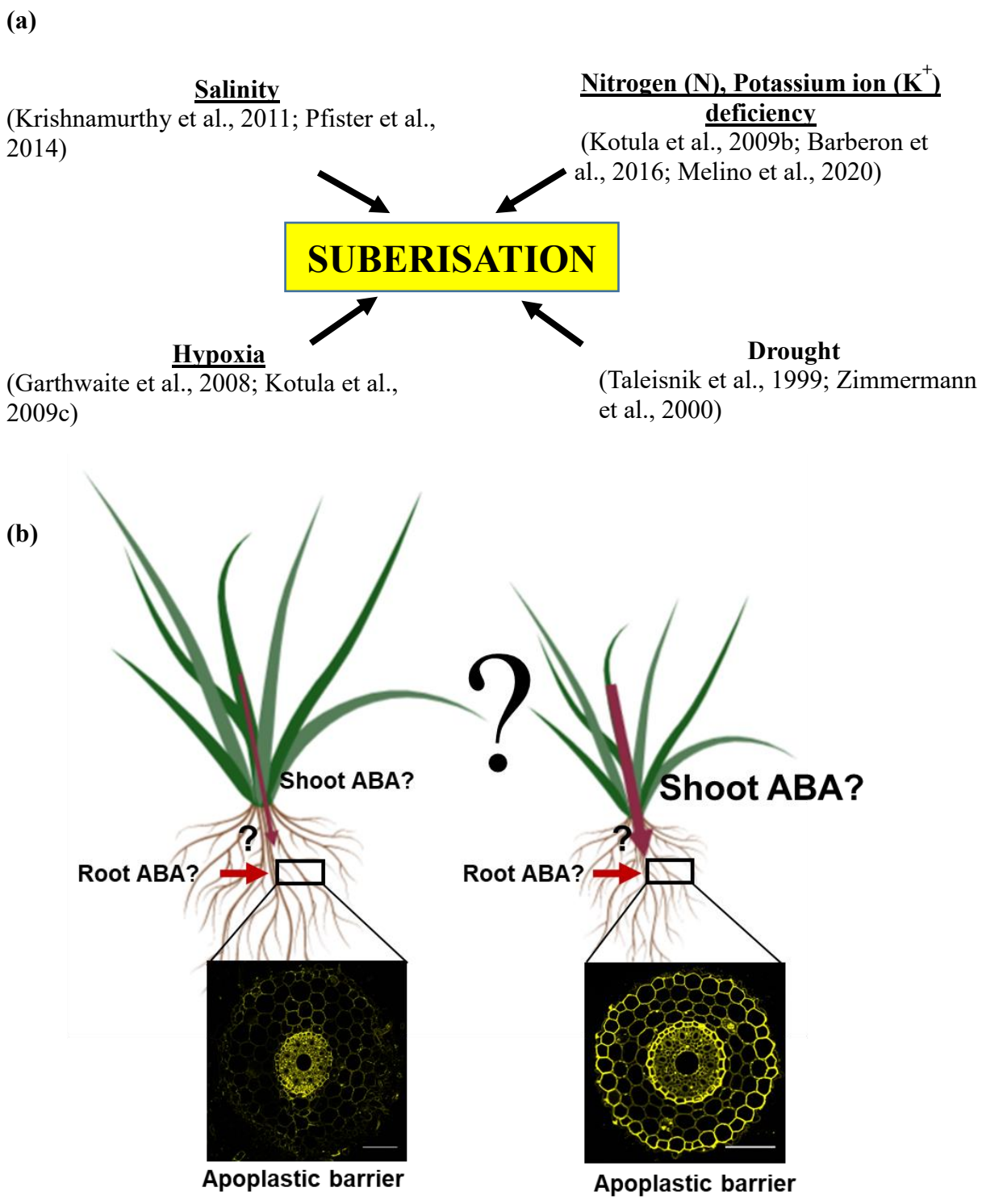

FIGURE 1 Known and hypothetical factors influencing root apoplastic barrier deposition. (a) Known factors that influence the deposition of suberisation in the root. (b) Illustration showing the hypothetical effect of different levels of signal from both root and shoot that could lead to differences in suberin deposition in the roots. Image was created with BioRender.

5.4 Is there any correlation between trends in membrane transport regulation and solute barrier development?

The tissue ion analysis of Barke and selected HID lines revealed that one line, HID069, had particularly low leaf Na^+:K^+ ratios compared to the other lines (Figure S9, Chapter 2). The variation in ion accumulation led to investigate whether there might be any involvement of a major membrane transporter, HvHKT1;5, which is known to influence Na^+ and K^+ accumulation in barley (Houston et al. 2020). In Chapter 4 we revealed that *HvHKT1;5* was not expressed in the roots of any of the barley lines at the developmental stage, one-week-old seedlings, selected here for all experiments. This indicates that HvHKT1;5 was not a factor contributing to the variation in ion accumulation observed. Further research at a later stage of plant development and/or with higher salt concentrations may be required to explore whether or not there is any correlation between HvHKT1;5 function, ion accumulation, and root barriers deposition in this material.

Our HKT1;5 SNP analysis (Chapter 4) revealed that Barke contains a non-functional version of HvHKT1;5 similar to Morex (Houston et al., 2020). Both Barke and Morex have a proline at position 189, whereas the seven selected HID lines all have a leucine at position 189 (Chapter 4). Plants with the HvHKT1;5 (P189) version have been shown to be defective in Na^+ retrieval from the xylem, which leads to higher Na^+ accumulation in the leaf (Houston et al., 2020). Interestingly, a previous study reported that Barke is tolerant to salinity to a similar extent to wild barley accessions (Saade et al., 2016). It is possible that Barke utilises other transport proteins to regulate Na^+ influx into the shoot and/or adapts other mechanisms to tolerate high leaf Na^+ accumulation, such as compartmentalising Na^+ into vacuoles using vacuolar membrane transporters (Munns and Tester, 2008). For example, overexpression of vacuolar *NHX1* in Arabidopsis increased its salt tolerance compared to wild-type (Apse et al., 1999). There is also controversy regarding whether HvHKT1;5 has positive or negative impacts

on salt tolerance (Huang et al., 2020). When HvHKT1;5 from Golden Promise and HmHKT1;5 from *Hordeum marinum* were expressed in rice they both led to greater Na^+ uptake and greater salt sensitivity (Huang et al. 2020). The authors observed that in heterologous systems HmHKT1;5 transported less Na^+ than HvHKT1;5.

Barke, which lacks an exodermal barrier, had higher root O_2 consumption (respiration) than wild barley accessions (Chapter 2). It is possible that Barke prioritised use of energy to efflux Na^+ out of the root using active membrane transporters rather than expending energy on extensive cell wall modification. The constant efflux of Na^+ would require more energy in the form of ATP, which may lead to higher overall energy consumption in roots relying on pumping out salt compared to the use of energy in wild barley accessions to create barrier for limiting salt influx. Salt Overly Sensitive 1 (SOS1) is one of the many transport proteins that are involved in extruding root Na^+ back to the soil (Shi et al., 2002; Olías et al., 2009). Previously Shi et al. (2002) reported that *SOS1* was expressed in the plasma membrane of Arabidopsis epidermal cells in the root tips. Due to the lack of large vacuoles in Arabidopsis for Na^+ compartmentalisation, it is probably important that Na^+ is effluxed back into the soil (Shi et al., 2002). The O_2 consumption is higher in the apical region in roots relative to the other regions of the root (Berry and Brock, 1946; Armstrong et al., 2000). Preliminary finding for rate of O_2 consumption at different root regions shows that root region containing the root tips had higher O_2 consumption compared to the basal region (Appendix 6). It would be interesting to explore whether higher respiration is consistently observed wherever there is higher ion flux in plant roots.

In the present study Barke had more seminal roots compared to the wild barley accessions tested (Appendix 7). However, a correlation analysis did not show significant correlation between the number of seminal roots and the rate of O_2 consumption (Appendix 8). The results of the O_2 experiment are therefore not determined by how many seminal root plant

has. The energy from respiration is also needed for maintenance of biomass (Munns and Gilliham, 2015). Therefore, the bigger the biomass, the higher O_2 demand is. Thus, root biomass differences in the barley tested is likely to influence O_2 consumption. For example, Barke had bigger root biomass compared to HID138, and this different in biomass could possibly confounded the interpretation of the rates of O_2 consumption measured. To minimise the effect of biomass variation within the samples, the O_2 consumption of each sample was standardised to biomass. We identified accessions that differed in their root respiration. In future studies this material could be used to map which genetic loci are associated with differences in root respiration.

5.5 Future outlooks

The was notable phenotypic variation in the barley material used in this project to explore root apoplastic barrier deposition, tissue ion content, membrane transport mechanisms, root respiration and links between hormone treatments and root barrier deposition. This variation could be used in future studies to address key knowledge gaps. Key focus points for future studies include:

1) Testing quantitative approaches for measuring suberin and lignin: It is possible that more quantitative measurement of suberin and lignin in the roots could be achieved by using methods such as gas chromatography-mass spectrometry (GC-MS) or Fourier Transform Mid-Infrared Spectroscopy (FTIR) (Lopes et al., 2000; Franke and Schreiber, 2007). Quantitative approaches are needed to detect changes in lignin and suberin deposition to the resolution required to accurately compare genotypes of interest. One key limitation is that it would be difficult to differentiate the spatial amount of the cell wall material in distinct cell layers, but whole tissue analysis would be possible. In this study we established root staining methods that were useful for narrowing down key genotypes of interest, but they were limited because they were

qualitative, we lacked a suitable high-throughput and quantitative method for detecting spatial deposition in distinct cell layers.

2) Vertical sectioning of the roots for suberin deposition would be useful, particularly for assessing passage cell number in different barley lines and in response to different treatments. In future research root segments could be treated with ClearSee reagent and treated with a compatible suberin stain such as Nile red (Ursache et al., 2018). This would enable a larger observation area of suberin deposition in the root, and potentially enable counting of passage cell number in roots.

3) Barley might have a homolog similar to the Arabidopsis *SUBERMAN* gene. It would be interesting to explore if there is a SUBERMAN-like gene in barley and identify the localisation of expression in the root using in-situ PCR. Suberin related genes can be amplified using labelled nucleotides directly within plant tissues (Athman et al., 2014). SUBERMAN is a MYB transcription factor that regulates the establishment of endodermal suberin in Arabidopsis. *SUBERMAN* is expressed in pericycle cells in Arabidopsis and controls endodermal suberin deposition (Cohen et al., 2020). By identifying if *SUBERMAN* homologs exist in barley, it may be possible to link expression with root morphology measurements to enable selection of barley lines based on expression rather than the need for root microscopy measurements in the future. Other possible suberin gene that can also be targeted in barley is *HvHORST* (Melino et al., 2020).

4) Measuring root and shoot O_2 consumption in the selected HEB13s lines. This data could help future assessments of the cost-effectiveness of exodermal barriers. There are HEB13 lines which have mostly Barke chromatin, but still form an exodermis, so they must have the loci from their HID138 parent that enables them to form an exodermis. Testing of the respiration in roots of material that is near isogenic but

differs in root apoplastic barrier deposition could help in the assessment of the relationships between energy use and apoplastic barrier deposition.

5) Measuring net fluxes of Na^+ and K^+ at the maturation zones between key accessions that differ in root apoplastic barriers using Micro-electrode Ion Efflux Estimation (MIFE) technique (University of Tasmania, Hobart) (Newman, 2001; Bose et al., 2015). The material tested in this study has sufficient genetic variation to enable future studies to select material that is near isogenic but differs in root apoplastic barriers. Testing of root ion flux in this type of material could help reveal relationships between barrier formation and ion flux trends in barley.

5.6 Closing remarks

Endodermal barriers play a crucial role in vascular plants and exodermal barriers could also provide a fitness advantage by providing extra protection against uncontrolled flux in roots. Uncontrolled flux is likely to be problematic when plants experience various abiotic stresses such as salinity, drought, hypoxia and nutrient-deficient soils, and biotic stress such as pathogen invasion. This study provides new insight into the diversity of apoplastic barrier traits in barley, particularly the variation in exodermal layer deposition, which could be useful in the future as a possible source of energy efficient mechanisms for improving environmental stress tolerance. Characterisation of the root barrier traits in the diverse barley accessions sets up new opportunities to explore the relationships between these barriers and other traits associated with solute transport to further increase our understanding of the mechanisms that regulate ion flux and stress tolerance. The data resources generated are also useful for future assessment of the genes and signals influencing the development of endodermal and exodermal layers in cereal crops.

5.7 References

Andersen TG, Naseer S, Ursache R, Wybouw B, Smet W, De Rybel B, Vermeer JE, Geldner N (2018) Diffusible repression of cytokinin signalling produces endodermal symmetry and passage cells. Nature **555:** 529-533

Apse MP, Aharon GS, Snedden WA, Blumwald E (1999) Salt tolerance conferred by overexpression of a vacuolar Na^+/H^+ antiport in Arabidopsis. Science **285:** 1256-1258

Armstrong W, Cousins D, Armstrong J, Turner D, Beckett P (2000) Oxygen distribution in wetland plant roots and permeability barriers to gas-exchange with the rhizosphere: a microelectrode and modelling study with *Phragmites australis*. Annals of Botany **86:** 687-703

Athman A, Tanz SK, Conn VM, Jordans C, Mayo GM, Ng WW, Burton RA, Conn SJ, Gilliham M (2014) Protocol: a fast and simple *in situ* PCR method for localising gene expression in plant tissue. Plant methods **10:** 29

Barberon M, Vermeer JEM, De Bellis D, Wang P, Naseer S, Andersen TG, Humbel BM, Nawrath C, Takano J, Salt DE, Geldner N (2016) Adaptation of root function by nutrient-induced plasticity of endodermal differentiation. Cell **164:** 447-459

Berry LJ, Brock MJ (1946) Polar distribution of respiratory rate in the onion root tip. Plant Physiology **21:** 542

Bose J, Rodrigo-Moreno A, Lai D, Xie Y, Shen W, Shabala S (2015) Rapid regulation of the plasma membrane H^+-ATPase activity is essential to salinity tolerance in two halophyte species, *Atriplex lentiformis* and *Chenopodium quinoa*. Annals of Botany **115:** 481-494

Cohen H, Fedyuk V, Wang C, Wu S, Aharoni A (2020) SUBERMAN regulates developmental suberization of the Arabidopsis root endodermis. The Plant Journal **102:** 431-447

Enstone DE, Peterson CA, Ma FS (2002) Root endodermis and exodermis: Structure, function, and responses to the environment. Journal of Plant Growth Regulation **21:** 335-351

Franke R, Schreiber L (2007) Suberin—a biopolyester forming apoplastic plant interfaces. Current Opinion in Plant Biology **10:** 252-259

Garthwaite AJ, Armstrong W, Colmer TD (2008) Assessment of O_2 diffusivity across the barrier to radial O_2 loss in adventitious roots of *Hordeum marinum*. New Phytologist **179:** 405-416

Hose E, Clarkson D, Steudle E, Schreiber L, Hartung W (2001) The exodermis: a variable apoplastic barrier. Journal of Experimental Botany **52:** 2245-2264

Houston K, Qiu J, Wege S, Hrmova M, Oakey H, Qu Y, Smith P, Situmorang A, Macaulay M, Flis P (2020) Barley sodium content is regulated by natural variants of the Na^+ transporter *HvHKT1; 5*. Communications Biology **3:** 1-9

Huang L, Kuang L, Wu L, Shen Q, Han Y, Jiang L, Wu D, Zhang G (2020) The HKT transporter HvHKT1; 5 negatively regulates salt tolerance. Plant Physiology **182:** 584-596

Kajala K, Shaar-Moshe L, Mason GA, Gouran M, Rodriguez-Medina J, Kawa D, Pauluzzi G, Reynoso M, Canto-Pastor A, Lau V (2020) Innovation, conservation and repurposing of gene function in plant root cell type development. BioRxiv

Kamula S, Peterson C, Mayfield C (1994) The plasmalemma surface area exposed to the soil solution is markedly reduced by maturation of the exodermis and death of the epidermis in onion roots. Plant, Cell & Environment **17:** 1183-1193

Kotula L, Ranathunge K, Schreiber L, Steudle E (2009b) Functional and chemical comparison of apoplastic barriers to radial oxygen loss in roots of rice (*Oryza sativa* L.) grown in aerated or deoxygenated solution. Journal of Experimental Botany **60:** 2155-2167

Kotula L, Ranathunge K, Steudle E (2009c) Apoplastic barriers effectively block oxygen permeability across outer cell layers of rice roots under deoxygenated conditions: roles of apoplastic pores and of respiration. New Phytologist **184:** 909-917

Kreszies T, Eggels S, Kreszies V, Osthoff A, Shellakkutti N, Baldauf JA, Zeisler-Diehl VV, Hochholdinger F, Ranathunge K, Schreiber L (2019b) Seminal roots of wild and cultivated barley differentially respond to osmotic stress in gene expression, suberization, and hydraulic conductivity. Plant, Cell & Environment

Kreszies T, Schreiber L, Ranathunge K (2018) Suberized transport barriers in *Arabidopsis*, barley and rice roots: From the model plant to crop species. Journal of Plant Physiology **227:** 75-83

Krishnamurthy P, Ranathunge K, Nayak S, Schreiber L, Mathew MK (2011) Root apoplastic barriers block Na^+ transport to shoots in rice (*Oryza sativa L.*). Journal of Experimental Botany **62:** 4215-4228

Liu G, Stirnemann M, Gübeli C, Egloff S, Courty P-E, Aubry S, Vandenbussche M, Morel P, Reinhardt D, Martinoia E (2019) Strigolactones play an important role in shaping exodermal morphology via a KAI2-dependent pathway. iScience **17:** 144-154

Lopes MH, Neto CP, Barros A, Rutledge D, Delgadillo I, Gil A (2000) Quantitation of aliphatic suberin in *Quercus suber* L. cork by FTIR spectroscopy and solid-state ^{13}C-NMR spectroscopy. Biopolymers: Original Research on Biomolecules **57:** 344-351

Maurer A, Draba V, Jiang Y, Schnaithmann F, Sharma R, Schumann E, Kilian B, Reif JC, Pillen K (2015) Modelling the genetic architecture of flowering time control in barley through nested association mapping. Bmc Genomics **16**

McAdam SA, Brodribb TJ, Ross JJ (2016) Shoot-derived abscisic acid promotes root growth. Plant, Cell & Environment **39:** 652-659

Melino V, Plett D, Bendre P, Thomsen H, Zeisler-Diehl V, Schreiber L, Kronzucker H (2020) Nitrogen depletion enhances endodermal suberization without restricting transporter-mediated root NO_3^- influx. Journal of Plant Physiology**:** 153334

Munns R, Gilliham M (2015) Salinity tolerance of crops–what is the cost? New Phytologist **208:** 668-673

Munns R, Tester M (2008) Mechanisms of salinity tolerance. Annual Review of Plant Biology **59:** 651-681

Newman I (2001) Ion transport in roots: measurement of fluxes using ion-selective microelectrodes to characterize transporter function. Plant, Cell & Environment **24:** 1-14

Olías R, Eljakaoui Z, Pardo JM, Belver A (2009) The Na^+/H^+ exchanger SOS1 controls extrusion and distribution of Na+ in tomato plants under salinity conditions. Plant Signaling & Behavior **4:** 973-976

Peterson CA, Moon GJ (1993) The effect of lateral root outgrowth on the structure and permeability of the onion root exodermis. Botanica Acta **106:** 411-418

Pfister A, Barberon M, Alassimone J, Kalmbach L, Lee Y, Vermeer JEM, Yamazaki M, Li GW, Maurel C, Takano J, Kamiya T, Salt DE, Roppolo D, Geldner N (2014) A receptor-like kinase mutant with absent endodermal diffusion barrier displays selective nutrient homeostasis defects. Elife **3**

Ranathunge K, Kim YX, Wassmann F, Kreszies T, Zeisler V, Schreiber L (2017) The composite water and solute transport of barley (Hordeum vulgare) roots: effect of suberized barriers. Annals of Botany **119:** 629-643

Ranathunge K, Schreiber L (2011) Water and solute permeabilities of *Arabidopsis* roots in relation to the amount and composition of aliphatic suberin. Journal of Experimental Botany **62:** 1961-1974

Saade S, Maurer A, Shahid M, Oakey H, Schmockel SM, Negrao S, Pillen K, Tester M (2016) Yield-related salinity tolerance traits identified in a nested association mapping (NAM) population of wild barley. Scientific Reports **6**

Schreiber L, Franke R, Hartmann KD, Ranathunge K, Steudle E (2005b) The chemical composition of suberin in apoplastic barriers affects radial hydraulic conductivity differently in the roots of rice (*Oryza sativa L.* cv. IR64) and corn (*Zea mays L.* cv. Helix). Journal of Experimental Botany **56:** 1427-1436

Shi H, Quintero FJ, Pardo JM, Zhu J-K (2002) The putative plasma membrane Na^+/H^+ antiporter SOS1 controls long-distance Na^+ transport in plants. The Plant Cell **14:** 465-477

Taleisnik E, Peyrano G, Cordoba A, Arias C (1999) Water retention capacity in root segments differing in the degree of exodermis development. Annals of Botany **83:** 19-27

Ursache R, Andersen TG, Marhavý P, Geldner N (2018) A protocol for combining fluorescent proteins with histological stains for diverse cell wall components. The Plant Journal **93:** 399-412

Wang Y, Zhang W, Li K, Sun F, Han C, Wang Y, Li X (2008) Salt-induced plasticity of root hair development is caused by ion disequilibrium in *Arabidopsis thaliana*. Journal of Plant Research **121:** 87-96

Xie Q, Essemine J, Pang X, Chen H, Cai W (2020) Exogenous application of abscisic acid to shoots promotes primary root cell division and elongation. Plant Science **292:** 110385

Zhao Q, Dixon RA (2011) Transcriptional networks for lignin biosynthesis: more complex than we thought? Trends in Plant Science **16:** 227-233

Zimmermann HM, Hartmann K, Schreiber L, Steudle E (2000) Chemical composition of apoplastic transport barriers in relation to radial hydraulic conductivity of corn roots (*Zea mays L.*). Planta **210:** 302-311

Zimmermann HM, Steudle E (1998) Apoplastic transport across young maize roots: effect of the exodermis. Planta **206:** 7-19

Appendices

APPENDIX 1 The origin of 25 wild barley accessions (HID accessions) used in this project and their shattering characteristic.

25 barley accessions	Origin	Shattering
HID003	Iraq	Less shattering
HID004	Iraq	Highly shattering
HID055	Turkey	Highly shattering
HID062	Turkey	Highly shattering
HID065	Turkey	Highly shattering
HID069	Turkey	Highly shattering
HID080	Turkey	Highly shattering
HID099	Syria	Highly shattering
HID101	Syria	Highly shattering
HID102	Syria	Highly shattering
HID109	Syria	Highly shattering
HID114	Lebanon	Highly shattering
HID138	Iran	Highly shattering
HID140	Iraq	Highly shattering
HID144	Iran	Highly shattering
HID219	Afghanistan	Highly shattering
HID249	Iran	Highly shattering
HID270	Iran	Highly shattering
HID294	Iran	Highly shattering
HID295	Iran	Highly shattering
HID357	Turkey	Highly shattering
HID358	Turkey	Highly shattering
HID359	Israel	Highly shattering
HID380	Tibet, China	Highly shattering
HID386	Israel	Highly shattering

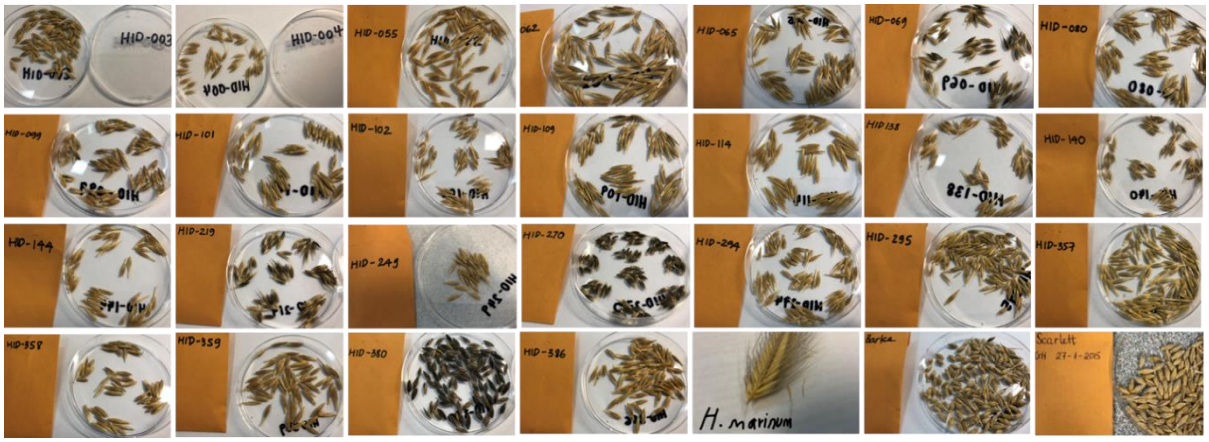

APPENDIX 2 Diversity in the seed from 28 barley collection that have been screened in this project. Twenty-five of the barley accessions are wild barley accessions, also identified as Hordeum Identity (HID) accessions. The 25 wild barley and a commercial barley line, Barke are the parent panel for the HEB25 Nested Association Mapping population (Maurer et al., 2015). *Hordeum marinum* at the third bottom left is included as a positive control, as it is previously known to induce an exodermis under abiotic stress (Kotula et al., 2014). Another commercial barley line, Scarlett is also included as it was reported previously to lack an exodermis under conditions of osmotic stress (Kreszies et al., 2019a).

APPENDIX 3 Subsets of HEB13s used in this project and parents. HEB13s is a progeny population that was developed from the cross between Barke and HID138. HEB13s are part of the HEB25 Nested Association Mapping population developed by Maurer et al. (2015) to increase the genetic diversity in the subsequent progenies also known as recombinant inbred lines (RILs) (see Introduction in Chapter 3 for more detail information). There are a total of 57 HEB13s lines. In this project, subsets of the HEB13s were chosen as they had the biggest difference in existing shoot ion data obtained from Meng et al. (2017). They were replanted in the paper towel system with a treatment of 40mM NaCl for 7d (see Figure 1 Chapter 2). The tissue ion accumulation and root spatial lignin and suberin deposition were investigated.

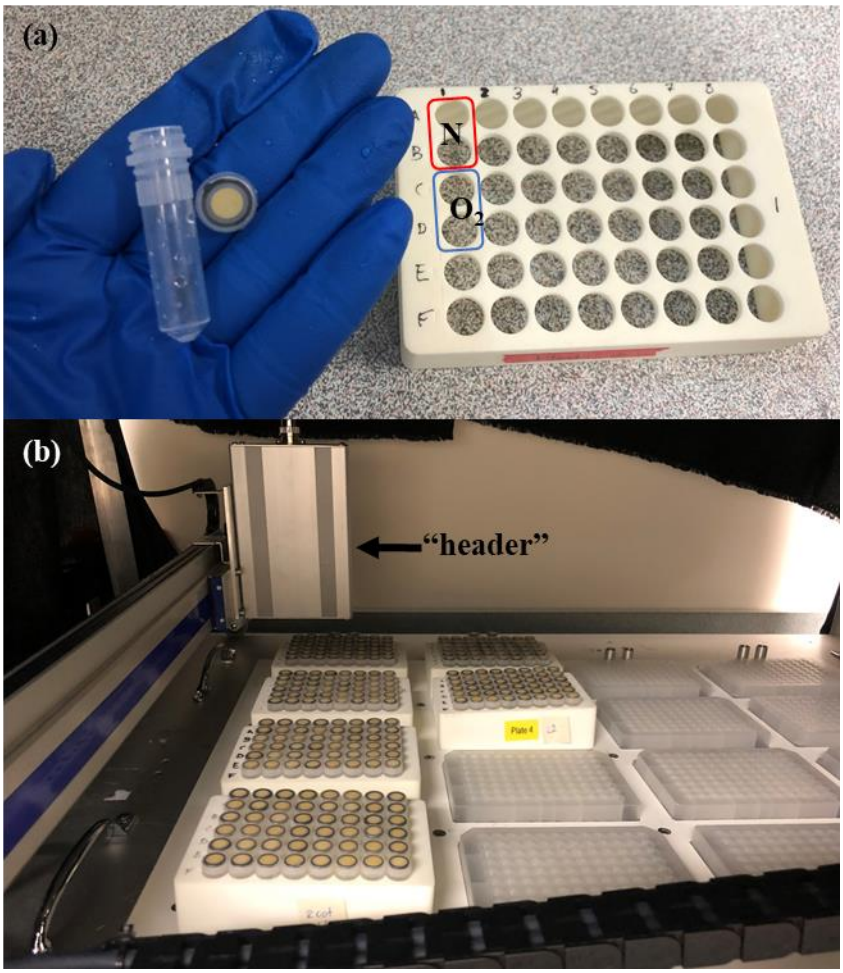

APPENDIX 4 Q2 machine for respiration measurements. (a) Tube with O_2-sensor cap and the tube's rack. The first two columns (A1 and B1) were reserved for tubes containing 100% nitrogen gas and the next two columns (C1 and D1) were reserved for tubes containing ambient air. These four tubes were used as standard for measuring the O_2 consumption. (b) The arrangement of the rack inside the machine. The arrow shows the header that detects the amount of O_2 in the tube by scanning the O_2-sensor cap. The measurement was taken overnight in the dark (see Figure S1, Chapter 2).

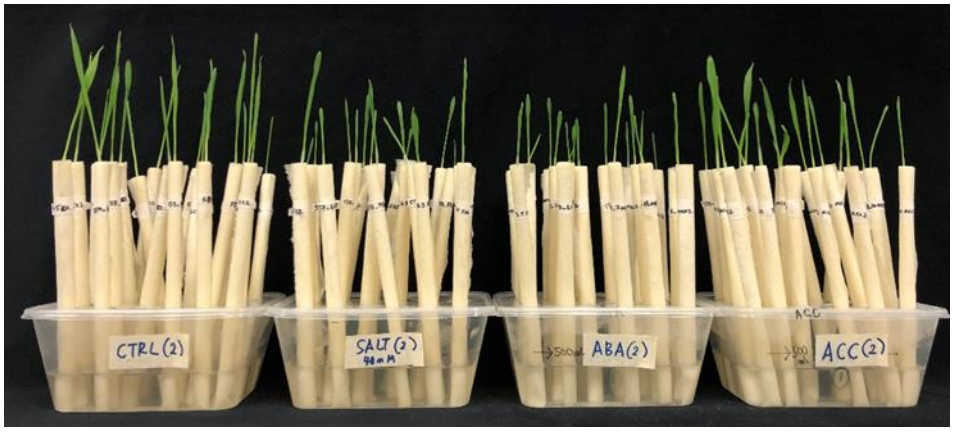

APPENDIX 5 Image of 7d old barley seedlings in hormone experiment. From left; control, 40mM NaCl, 5µM ABA and 100µM ACC, an ethylene precursor, grown in paper towel inside a transparent box (see Figure 1 Chapter 2).

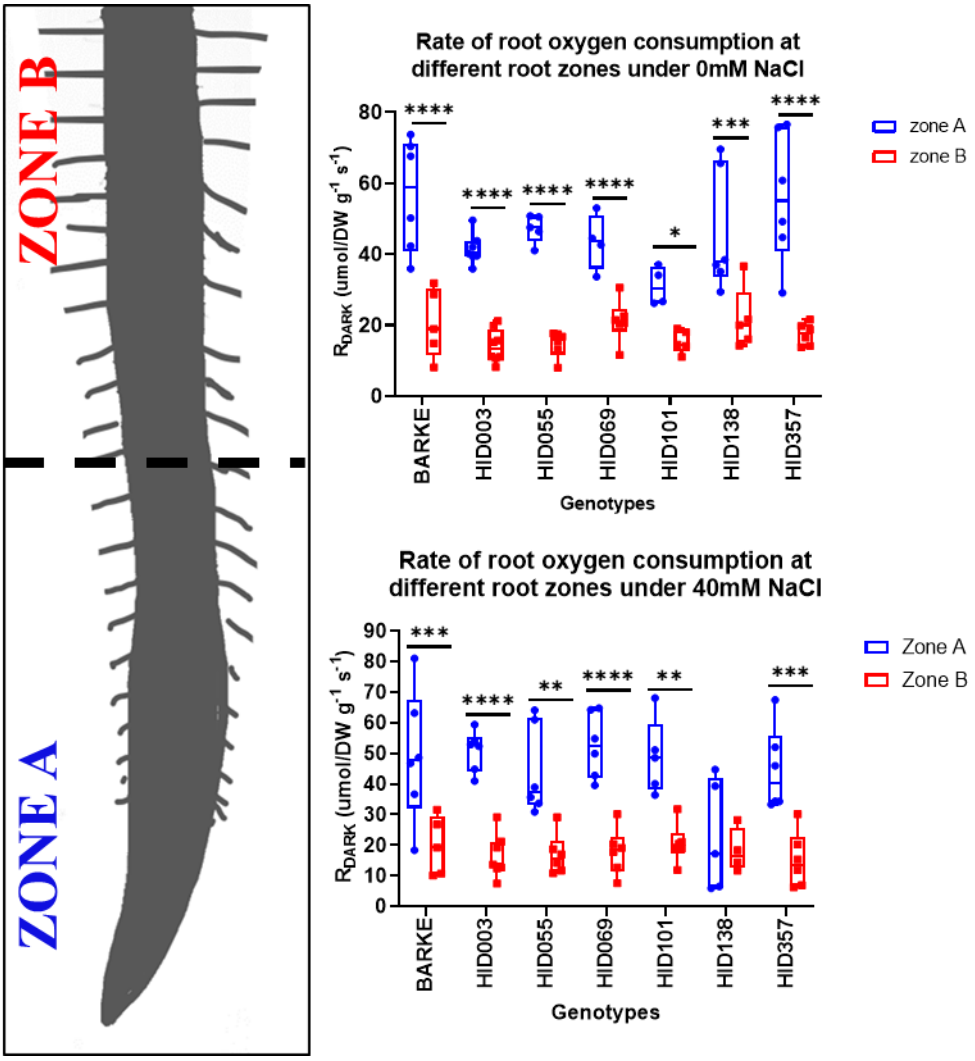

APPENDIX 6 Root O_2 consumption in different root zones. The longest seminal root was harvested and divided in two sections; zone A (apical, elongation, maturation regions) and zone B (maturation, basal region). The O_2 consumption was measured using Q2 meter as described in Chapter 2. The data is an individual replicates (n = 6). The O_2 consumption in each genotypes was compared between the zones using Sidak's comparison test. The significant difference $p<0.05$, $p<0.01$, $p<0.001$ and $p<0.0001$ indicated by (*), (**), (***) and (****) respectively.

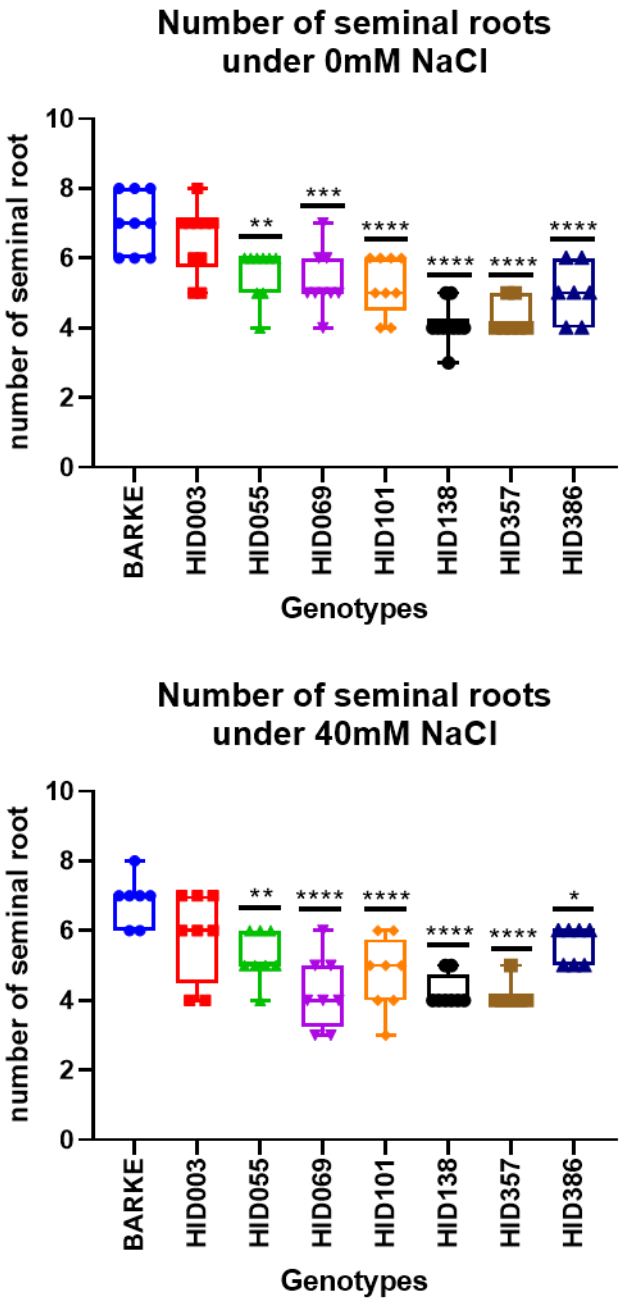

APPENDIX 7 Total number of seminal roots of 7 d old barley seedlings. (a) Number of seminal roots under 0mM NaCl and (b) 40mM NaCl. Data represent individual biological replicates (n = 7-10). Each HID accession was compared with the elite cultivar (Barke) using one-way ANOVA with Dunnet's multiple comparison test. ANOVA significant difference $p<0.05$, $p<0.01$, $p<0.001$ and $p<0.0001$ indicated by (*), (**), (***) and (****), respectively.

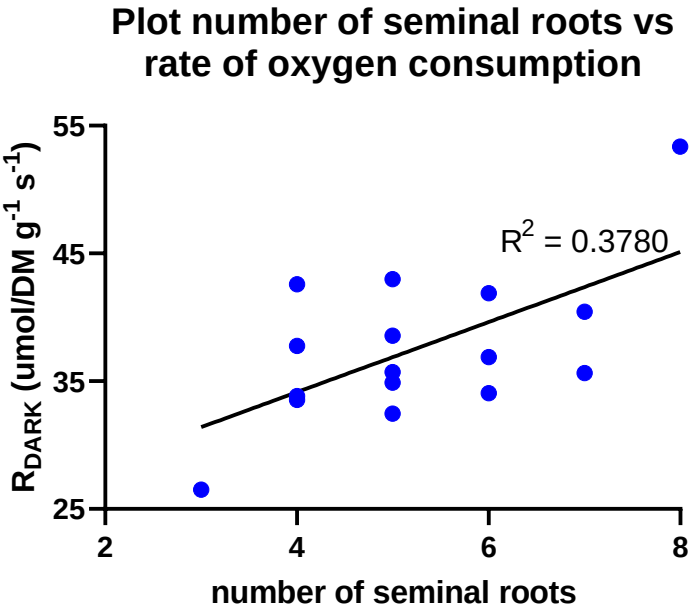

APPENDIX 8 Correlation plot of the number of seminal root (mean) with the rate of O_2 consumption (mean) of 7 d old barley seedlings in both control and saline conditions.

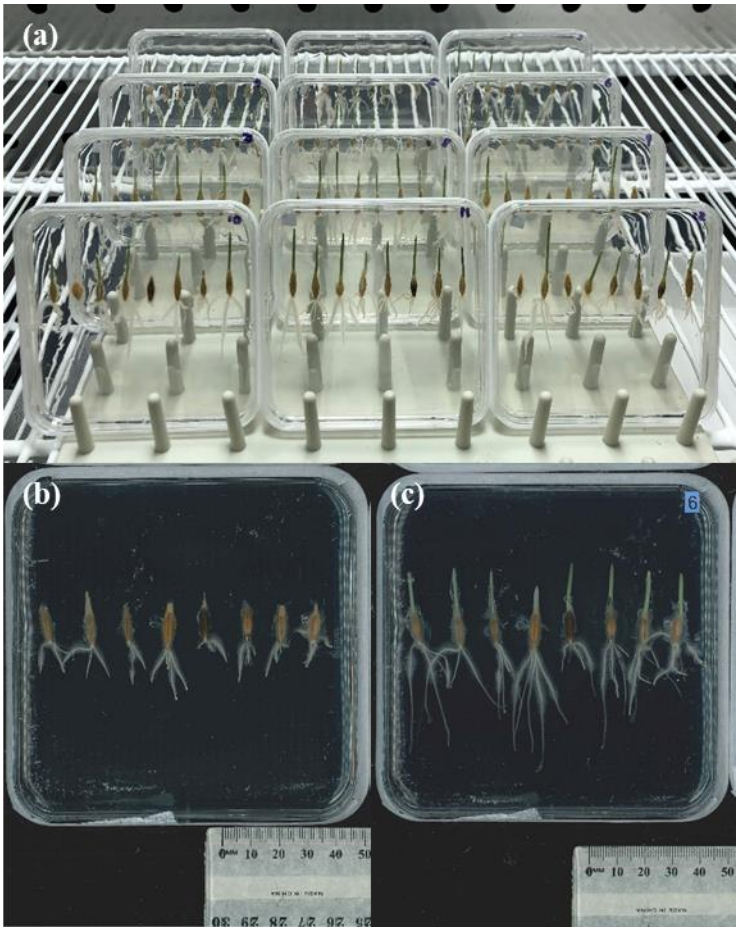

APPENDIX 9 Plant growth in half MS agar with 40mM NaCl. Seed was first germinated on moist filter paper overnight in dark places before it was replanted on agar. (a) The image of growth set up on half M/S media taken at day 3 inside a growth room under (12 h : 12 h, night : dark) with the temperature 22^{o}C : 15^{o}C. Seedling growth at (b) day 1 and (c) day 3 on media. The images of the seedling growth was taken for every 24 hours and the length of the longest root was measured using ImageJ. The result of the growth rate measured is reported in Figure S6 Chapter 2.

```
HID386      MGSLHVSGSTTTQHSRVLRAYQLLFFHVHPFWLQLLYFVSISFFGCVLLRALPMKTSMPT     60
HID069      MGSLHVSGSTTTQHSRVQRAYQLLFFHVHPFWPQLLYFVSISFFGFVMLRALPMKTSMPT     60
HID101      MGSLHVSGSTTTQHSRVQRAYQLLFFHVHPFWPQLLYFVSISFFGFVMLRALPMKTSMPT     60
HID357      MGSLHVSGSTTTQHSRVQRAYQLLFFHVHPFWPQLLYFVSISFFGFVMLRALPMKTSMPT     60
HID138      MGSLHVSGSTTTQHSRVQRAYQLLFFHVHPFWPQLLYFVSISFFGFVMLRALPMKTSMPT     60
HID055      MGSLHVSGSTTTQHSRVQRAYQLLFFHVHPFWPQLLYFVSISFFGFVMLRALPMKTSMPT     60
BARKE       MGSLHVSGSTTTQHSRVQRAYQLLFFHVHPFWPQLLYFVSISFFGFVMLRALPMKTNMPT     60
HID003      MGSLHVSGSTTTQHSRVQRAYQLLFFHVHPFWPQLLYFVSISFFGFVMLRALPMKTNMPT     60
            ***************** ************** ************ *:********.***

HID386      DLDLIFTSVSATTVSSMQAVEMESFSSPQLLLLTLLMLLGGEVFTSMLGMYFTYVKSKKK    120
HID069      DLDLIFTSVSATTVSSMQAVEMESFSNPQLLLLTLLMLLGGEVFTSMLGMYFTYVKSKKK    120
HID101      DLDLIFTSVSATTVSSMQAVEMESFSNPQLLLLTLLMLLGGEVFTSMLGMYFTYVKSKKK    120
HID357      DLDLIFTSVSATTVSSMQAVEMESFSNPQLLLLTLLMLLGGEVFTSMLGMYFTYVKSKKK    120
HID138      DLDLIFTSVSATTVSSMQAVEMESFSNPQLLLLTLLMLLGGEVFTSMLGMYFTYVKSKKK    120
HID055      DLDLIFTSVSATTVSSMQAVEMESFSNPQLLLLTLLMLLGGEVFTSILGMYFTYVKSKKK    120
BARKE       DLDLIFTSVSATTVSSMQAVEMESFSNPQLLLLTLLMLLGGEVFTSMLGMYFTYVKSKKK    120
HID003      DLDLIFTSVSATTVSSMQAVEMESFSNPQLLLLTLLMLLGGEVFTSMLGMYFTYVKSKKK    120
            *************************.******************:*************

HID386      EAQAPHDDGANVKPAPSSLELTAASICMDDGTAQDRIEQGFKDQPHYGRAFLTRLLLFIV    180
HID069      EAQAPHDDGAKVKPAPSSLELTAASICMDDGTAQDRMEQGFKDQPRYGRAFLTRLLLFIV    180
HID101      EAQAPHDDGAKVKPAPSSLELTAASICMDDGTAQDRMEQGFKDQPRYGRAFLTRLLLFIV    180
HID357      EAQAPHDDGAKVKPAPSSLELTAASICMDDGTAQDRMEQGFKDQPRYGRAFLTRLLLFIV    180
HID138      EAQAPHDDGAKVKPAPSSLELTAASICMDDGTAQDRMEQGFKDQPRYGRAFLTRLLLFIV    180
HID055      EAQAPHDDGAKVKPAPSSLELTAASMCMDDGTAQDRMEQGFKDQPRYGRAFLTRLLLFIV    180
BARKE       EAQAPHDDGAKVKPAPSSLELTAASICMDDGTAQDRMEQGFKDQPRYGRAFLTRLLLFIV    180
HID003      EAQAPHDDGAKVKPAPSSLELTAASICMDDGTAQDRMEQGFKDQPRYGRAFLTRLLLFIV    180
            **********:**************:**********:********:**************

HID386      VGYHAVVHLAGYSLMLVYLSVVSGARTVLAGKGISMHTFSVFTVVSTFANCGFMPNNEGM    240
HID069      VGYHAVVHLAGYSLMLVYLSVVSGARTVLAGKGISMHTFSVFTIVSTFANCGFMPNNEGM    240
HID101      VGYHAVVHLAGYSLMLVYLSVVSGARTVLAGKGISMHTFSVFTIVSTFANCGFMPNNEGM    240
HID357      VGYHAVVHLAGYSLMLVYLSVVSGARTVLAGKGISMHTFSVFTIVSTFANCGFMPNNEGM    240
HID138      VGYHAVVHLAGYSLMLVYLSVVSGARTVLAGKGISMHTFSVFTIVSTFANCGFMPNNEGM    240
HID055      VGYHAVVHLAGYSLMLVYLSVVSGARTVLAGKGISMHTFSVFTIVSTFANCGFMPNNEGM    240
BARKE       VGYHAVVHPAGYSLMLVYLSVVSGARTVLAGKGISMHTFSVFTIVSTFANCGFMPNNEGM    240
HID003      VGYHAVVHLAGYSLMLVYLSVVSGARTVLAGKGISMHTFSVFTIVSTFANCGFMPNNEGM    240
            ******** ********************************:*****************

HID386      ASFRSFPGLLLLVMPHVLLGNTLFPVFLRLAIWALQRFTKRPELGELRSIGYDHLLTSRH    300
HID069      ASFRSFPGLLLLVMPHVLLGNTLFPVFLRLAIWALQRFTKRPELGELRSIGYDHLLTSRH    300
HID101      ASFRSFPGLLLLVMPHVLLGNTLFPVFLRLAIWALQRFTKRPELGELRSIGYDHLLTSRH    300
HID357      ASFRSFPGLLLLVMPHVLLGNTLFPVFLRLAIWALQRFTKRPELGELRSIGYDHLLTSRH    300
HID138      ASFRSFPGLLLLVMPHVLLGNTLFPVFLRLAIWALQRFTKRPELGELRSIGYDHLLTSRH    300
HID055      ASFRSFPGLLLLVMPHVLLGNTLFPVFLRLAIWALQRFTKRPELGELRSIGYDHLLTSRH    300
BARKE       ASFRSFPGLLLLVMPHVLLGNTLFPVFLRLAIWALQRFTKRPELGELRSIGYDHLLTSRH    300
HID003      ASFRSFPGLLLLVMPHVLLGNTLFPVFLRLAIWALQRFTKRPELGELRSIGYDHLLTSRH    300
            ************************************************************

HID386      TRFLAFTVAVFVLAQLSLFCAMEWGSDGLRGLTAAQKLVAALFMSVNSRHAGEMVVDLST    360
HID069      TRFLAFTVAVFVLAQLSLFCAMEWGSDGLRGLTAAQKLVAALFMSVNSRHAGEMVVDLST    360
HID101      TRFLAFTVAVFVLAQLSLFCAMEWGSDGLRGLTAAQKLVAALFMSVNSRHAGEMVVDLST    360
HID357      TRFLAFTVAVFVLAQLSLFCAMEWGSDGLRGLTAAQKLVAALFMSVNSRHAGEMVVDLST    360
HID138      TRFLAFTVAVFVLAQLSLFCAMEWGSDGLRGLTAAQKLVAALFMSVNSRHAGEMVVDLST    360
HID055      TRFLAFTVAVFVLAQLSLFCAMEWGSDGLRGLTAAQKLVAALFMSVNSRHAGEMVVDLST    360
BARKE       TRFLAFTVAVFVLAQLSLFCAMEWGSDGLRGLTAAQKLVAALFMSVNSRHAGEMVVDLST    360
HID003      TRFLAFTVAVFVLAQLSLFCAMEWGSDGLRGLTAAQKLVAALFMSVNSRHAGEMVVDLST    360
            ************************************************************

HID386      VSSAVVVVYMVMMYLPPYATFLPVEDSNQQVGTDQKRTSIWQKLLMSPLSCIAIFIVVVC    420
HID069      VSSAVVVVYMVMMYLPPYTTFLPVEDSNQQVGTDQKRTSIWHKLLMSPLSCIAIFIVVVC    420
HID101      VSSAVVVVYMVMMYLPPYTTFLPVEDSNQQVGTDQKRTSIWHKLLMSPLSCIAIFIVVVC    420
HID357      VSSAVVVVYMVMMYLPPYTTFLPVEDSNQQVGTDQKRTSIWHKLLMSPLSCIAIFIVVVC    420
HID138      VSSAVVVVYMVMMYLPPYTTFLPVEDSNQQVGTDQKRTSIWHMLLMSPLSCIAIFIVVVC    420
HID055      VSSAVVVVYMVMMYLPPYTTFLPVEDSNQQVGTDQKRTSIWHKLLMSPLSCIAIFVVVVC    420
BARKE       VSSAVVVVYMVMMYLPPYTTFLPVEDSNQQVGTDQKRTSIWHKLLMSPLSCIAIFVVVVC    420
HID003      VSSAVVVVYMVMMYLPPYTTFLPVEDSNQQVGTDQKRTSIWHKLLMSPLSCIAIFVVVVC    420
            ******************:**********************: ************:****
```

```
HID386      ITERRQISDDPLNFNVINIAVEVISAYGNVGFSTGYSCGRQVTPDGSCRDAWVGFSGKWS    480
HID069      ITERRQISDDPLNFNVINIAVEVISAYGNVGFSTGYSCGRQVTPDGSCRDAWVGFSGKWS    480
HID101      ITERRQISDDPLNFNVINIAVEVISAYGNVGFSTGYSCGRQVTPDGSCRDAWVGFSGKWS    480
HID357      ITERRQISDDPLNFNVINIAVEVISAYGNVGFSTGYSCGRQVTPDGSCRDAWVGFSGKWS    480
HID138      ITERRQISDDPLNFNVISIAVEVISAYGNVGFSTGYSCGRQVTPDGSCRDAWVGFSGKWS    480
HID055      ITERRQISDDPLNFNVISIAVEVISAYGNVGFSTGYSCGRQVTPDGSCRDAWVGFSGKWS    480
BARKE       ITERRQISDDPLNFNVISIAVEVISAYGNVGFSTGYSCGRQVTPDGSCRDAWVGFSGKWS    480
HID003      ITERRQISDDPLNFNVISIAVEVISAYGNVGFSTGYSCGRQVTPDGSCRDAWVGFSGKWS    480
            ****************.****************************************

HID386      REGKLALIAVMFYGRLKKFSMHGGQAWRIV 510
HID069      REGKLALIAVMFYGRLKKFSMHGGQAWRIV 510
HID101      REGKLALIAVMFYGRLKKFSMHGGQAWRIV 510
HID357      REGKLALIAVMFYGRLKKFSMHGGQAWRIV 510
HID138      REGKLALIAVMFYGRLKKFSMHGGQAWRIV 510
HID055      REGKLALIAVMFYGRLKKFSMHGGQAWRIV 510
BARKE       REGKLALIAVMFYGRLKKFSMHGGQAWRIV 510
HID003      REGKLALIAVMFYGRLKKFSMHGGQAWRIV 510
            ****************************
```

APPENDIX 10 Amino acid sequences comparison between the wild barley accessions and the commercial barley Barke in HvHKT1;5. There four common amino acid differences found between these genotypes when referred to Barke (shared the same amino acid sequence similarity with Morex) shown in the bracket.

References

Kotula L, Colmer TD, Nakazono M (2014) Effects of organic acids on the formation of the barrier to radial oxygen loss in roots of *Hordeum marinum*. Functional Plant Biology **41:** 187-202

Kreszies T, Shellakkutti N, Osthoff A, Yu P, Baldauf JA, Zeisler-Diehl VV, Ranathunge K, Hochholdinger F, Schreiber L (2019a) Osmotic stress enhances suberization of apoplastic barriers in barley seminal roots: analysis of chemical, transcriptomic and physiological responses. New Phytologist **221:** 180-194

Maurer A, Draba V, Jiang Y, Schnaithmann F, Sharma R, Schumann E, Kilian B, Reif JC, Pillen K (2015) Modelling the genetic architecture of flowering time control in barley through nested association mapping. Bmc Genomics **16**

Meng R, Saade S, Kurtek S, Berger B, Brien C, Pillen K, Tester M, Sun Y (2017) Growth curve registration for evaluating salinity tolerance in barley. Plant Methods **13**